LUT UNIVERSITY
LUT School of Energy Systems
LUT Mechanical Engineering

Antti Kontio

FATIGUE STRENGTH AND DESIGN RULES OF THE RAIL WELDS IN INDUSTRIAL CRANE RUNWAYS

21.5.2020

Examiner(s): Professor Timo Björk
D. Sc. (Tech.) Juha Peippo
Advisor(s): Professor Timo Björk
M.Sc (Tech.) Antti Ahola
D. Sc. (Tech.) Juha Peippo
M.Sc (Tech.) Kari Siitari

TIIVISTELMÄ

LUT-Yliopisto
LUT School of Energy Systems
LUT Kone

Antti Kontio

Kiskon hitsien väsymislujuus sekä niiden laskentasäännöt teollisuusnosturin radassa

Diplomityö

2020

95 sivua, 66 kuvaa, 14 taulukko ja 16 liitettä

Tarkastajat: Professori Timo Björk
TkT Juha Peippo

Hakusanat: FAT, hitsi, jäännösjännitys, standardi, tilastollinen regressio, väsytyskoe

Työssä tutkitaan kolmen erilaisen hitsausliitoksen väsymislujuutta ja määritetään helposti käytettävät suunnittelusäännöt niiden väsymiseliniän määrittämiseksi. Tutkittavat hitsausliitokset ovat yleisesti käytössä teollisuusnosturien radoissa: kaksi hitsityyppiä liittyvät kiskon jatkamiseen ja kolmas hitsityyppi on katkopienahitsi, jolla kisko kiinnitetään nosturin ratapalkkiin. Erikoispiire tutkittaville hitsausliitoksille on se, että niiden kokema ulkoinen jännitysvaihtelu tapahtuu puristusjännityksen alueella. Hitseille määritetään karakteristinen FAT_c arvo väsytystestauksella ja tulosten tilastollisella käsittelyllä. Elinikätestaus on toteutettu nelipistetaivutuksella. Työssä arvioidaan tutkittavien hitsien jäännösjännitystila jäännösjännitysmittauksilla ja hitsien tutkimisessa vertaillaan eri elinikälaskentamenetelmiä.

Jatkohitsien väsytyskoetulokset osoittavat, että EN13001-3-1 standardin suunnittelusäännöt kiskon jatkohitseille eivät päde jokaiselle nosturiratasovellukselle. Saadut väsytyskoetulokset voidaan skaalata isommalle nosturiratasovellukselle ja tällöin EN13001-3-1 standardissa esitetyt suunnittelusäännöt pätevät. Tämä johtuu siitä, että nykyinen suunnittelusääntö ei ota huomioon hitsin etäisyyttä ratapalkin ja kiskon yhteisestä neutraaliakselista. Tämän vuoksi työssä luotiin uusi ja tarkempi suunnittelusääntö kiskon jatkohitseille. Kiskon jatkohitsien suunnittelusääntöön määritetään hitsausjärjestys hitsin väsymislujuuden kannalta paremman jäännösjännitystilan aikaansaamiseksi. Katkopienahitsien väsytyskoetulokset osoittavat, että nykyisen EN1993-1-9 standardin suunnittelusääntö on konservatiivinen, jos katkohitsi kokee puristusjännitystä. Leikkausjännityksen vaihtelun vaikutusta työssä ei oteta huomioon. Työn tuloksia hyödynnetään Eurocode 3 teräsrakennestandardin kehitystyössä ja eri alojen standardien harmonisoinnissa.

ABSTRACT

LUT University
LUT School of Energy Systems
LUT Mechanical Engineering

Antti Kontio

Fatigue strength and design rules of the rail welds in industrial crane runways

Master's thesis

2020

95 pages, 66 figures, 14 table and 16 appendices

Examiners: Professor Timo Björk
D. Sc. (Tech.) Juha Peippo

Keywords: FAT, fatigue test, regression analysis, residual stress, standard, weld

The work studies fatigue strength of three different weld joints and determines easy-to-use design rules for fatigue life assessment. The joints in this study are commonly used in the industrial crane design: two welds type relates to an extension of a crane rail, and the third type is an intermittent fillet weld that attaches the rail to the load-carrying beam. A unique feature of studied joints is that the experienced external stress range occurs mainly under compressive stresses. The purpose of this study is to determine the characteristic FAT_c value by fatigue testing and statistical analysis of results. Fatigue testing was carried out with four-point bending. In this study, results are validated by measuring residual stresses on the welds and utilizing various fatigue strength assessment methods.

The fatigue test results show that the design rules of the EN13001-3-1 standard for rail connection welds do not apply to every runway application sizes of the crane. The fatigue test results can be scaled to a larger in size runway load-carrying beam, and then the design rules are given in the EN13001-3-1 apply. The difference happens because the current design rules do not consider the distance of the weld to the combined neutral axis of the load-carrying beam and the rail. As a result, a new and more specific design rule for the rail connection welds has been created. In addition, in the design rule for the rail connection welds, the right welding order is defined to achieve a better residual stress state for the welds in terms of fatigue strength. The fatigue test results for intermittent fillet welds show that the design rule of the current EN1993-1-9 standard is conservative if the loading is compressive. The effect of alternating shear stress was not included in the study. The results of this study are utilized for the standard work of the Eurocode 3 steel structure standard, and to further harmonize the different standards.

ACKNOWLEDGEMENTS

This thesis was done for the Konecranes standardization work. The main target of this thesis is to provide more understanding of the welds and what aspects are related to the fatigue strength of the studied welds. I would like to thank Konecranes for their funding of this project.

I would like to thank Juha Peippo and Kari Siitari for finding this interesting topic and how they have provided help, guidance, and advice through this project. In addition, lots of thanks for the guidance of many other colleagues in Konecranes.

I want to thank my advisors Professor Timo Björk and Junior Researcher Antti Ahola from the LUT University for their help and guidance. Additionally, I would like to thank laboratory engineer Matti Koskimäki and laboratory staff for their flexible and productive collaboration during this period of testing.

Finally, special thanks to my wife Elma for the support and encouragement she gave me during this thesis project and my studies.

Antti Kontio

Antti Kontio

Hyvinkää 21.5.2020

TABLE OF CONTENTS

TIIVISTELMÄ
ABSTRACT
ACKNOWLEDGEMENTS
TABLE OF CONTENTS **5**
LIST OF SYMBOLS AND ABBREVIATIONS **8**
1 INTRODUCTION **12**
1.1 Background of the rail connection weld study 13
1.2 Background of the intermittent fillet weld study 16
1.3 Research methods and scope 19
2 FATIGUE STRENGTH ASSESSMENT METHODS **20**
2.1 Fatigue phenomena in the steel structure 20
2.2 Biaxial normal stress and shear stress of the traveling crane 22
2.3 Fatigue strength assessment methods 23
2.3.1 Nominal stress method 23
2.3.1 Effective notch stress method 25
2.3.2 Linear elastic fracture mechanics 26
2.3.3 4R method 27
2.4 S-N curve for structural detail 29
2.4.1 Regression analysis procedure based on IIW recommendations 31
2.4.2 Regression analysis procedure based on Eurocode recommendations 33
3 EXPERIMENTAL TESTING **36**
3.1 Test specimens and studied weld details 36
3.2 Preparing test specimens 38
3.2.2 Hardness measurements from the welds 44
3.3 Residual stress X-ray measurements of the rail connection welds 46
3.3.1 Residual stress measurements results 48
3.4 Laboratory testing and test set up 51
3.5 Test parameters 53
3.5.1 Nominal stress in the testing and calculations 54

3.6 Verification of the fatigue testing system and smaller test specimens compared to the average size of the load-carrying beam 57
3.6.1 HEA340 load-carrying beam measured residual stresses 59
4 RESULTS 61
4.1 Analytical fatigue strength assessment results 61
4.1.1 Nominal stress method 61
4.1.2 Effective notch stress 63
4.1.3 Linear elastic fracture mechanics 64
4.1.4 4R method 67
4.2 Fatigue test results 68
4.3 S-N curves and FAT_c values of the fatigue test results 72
4.4 Scaling test results to real-size runway application 78
4.5 New analytical equations based design rule for the rail connection welds 81
5 DISCUSSION 83
5.1 Further studies 90
6 CONCLUSION 91
LIST OF REFERENCES 94
APPENDIX
Appendix I: Main dimensions of the test set up at LUT University.
Appendix II: ENS-method effective notch radius locations in the studied welds.
Appendix III: Linear elastic fracture mechanics theoretical calculations and comparison to Franc2D analysis result.
Appendix IV: 4R method calculation procedure.
Appendix V: FAT_c value scaling procedure to the typically used crane's runway application profile size.
Appendix VI: Eurocode regression analysis result. The used values of the rail connection weld A3. Nominal stress of the top flange is used.
Appendix VII: IIW recommendations regression analysis and used values of the rail connection weld A3. Nominal stress of the top flange is used.
Appendix VIII: IIW recommendations regression analysis and used values of the rail connection weld A3. Nominal stress of the A3 rail connection weld is used.

Appendix IX:	IIW recommendations regression analysis and used values of the intermittent fillet weld. Nominal stress of intermittent fillet weld is used.
Appendix X:	Eurocode regression analysis result. The used values of the three-side welded rail connection weld A2. Nominal stress of the top flange is used.
Appendix XI:	IIW recommendations regression analysis and used values of the three-side welded rail connection weld A2. Nominal stress of the top flange is used.
Appendix XII:	Material certificates.
Appendix XIII:	HEA160 and HEA340 dimensions.
Appendix XIV:	Test result FAT_c value scaled to the large in size application by using analytical equations.
Appendix XV:	Hardness test (HV5) results.
Appendix XVI:	Relevant strain gauges data of the fatigue test specimens.

LIST OF SYMBOLS AND ABBREVIATIONS

α	Angle between pyramid sides in the HV5 measurement
γ	Safety factor
γ_{Ff}, γ_{Mf}	Fatigue strength safety factors
γ_m	Partial factor for resistances
$\Delta\sigma$	Nominal Stress range
$\Delta\sigma_b$	Bending stress range
$\Delta\sigma_{ENS}$	The effective notch stress range
$\Delta\sigma_{E,2}$	Equivalent constant amplitude normal stress range related to 2 million cycles
$\Delta\sigma_i$	Stress range in the studied area
$\Delta\sigma_k$	Notch stress range value in 4R method
$\Delta\sigma_{k,FEA}$	Notch stress range value from FE-analyse in 4R method
$\Delta\sigma_m$	Membrane stress range
$\Delta\tau$	Shear stress range
$\Delta\tau_{E,2}$	Equivalent constant amplitude shear stress range related to 2 million cycles
η_d	Design value of the possible conversion factor
σ	Maximum or minimum stress
σ_b	Shell bending stress
σ_k	Notch stress in 4R method
σ_m	Membrane stress
σ_{max}	Maximum stress in the stress range
σ_{min}	Minimum stress in the stress range
σ_{nl}	Non-linear stress peak
σ_{res}	Residual stresses
$\sigma_{weld,root}$	Stress in the weld root
σ_x	Global stress component because of global bending
$\sigma_{z,local}$	Local transverse pressure from concentrated wheel load
τ_{xz}	Global shear stress component because of global bending
$\tau_{xz,local}$	Local shear stress

φ	Distribution function of the Gaussian normal distribution probability of exceedance of α = 95%
χ^2	Chi-square for a probability of (1+ β)/2 = 0.875 at n-1 degrees of freedom
A_{profile}	Cross-section of load-carrying beam
A_{rail}	Cross-section of rail
a	Crack size
a_{i}	Initial crack size
a_{w}	Weld throat thickness
b	Variable of the linear curve, fits the constant value
C	Constant of the power-law
C	Fatigue resistance
C_{char}	Characteristic value of fatigue resistance
C_{mean}	Mean value of fatigue resistance
$C_{4\text{R}}$	$10^{20.83}$ (characteristic value, $R_{local,\ ref}$ = 0)
E	Young's modulus
$e_{\text{weld,root}}$	Distance between a neutral axis and a weld root
F	Force
I	Current
$I_{\text{Beam\&rail}}$	Moment of inertia that includes rail and load-carrying beam cross-sections
K	Stress intensity factor
$K_{\text{t,b}}$	Stress concentration factor for bending loading
$K_{\text{t,m}}$	Stress concentration factor for membrane loading
k	Variable of the linear curve, fits slope
k_1	Variable of the linear curve, fits slope
$k_{\text{d,n}}$	Design fractile factor
k_{n}	Characteristic fractile factor
M	Moment
M_{k}(a)	Magnification function for K
m	Curve slope
m	Exponent of the power-law
m_{x}	Mean of the n sample results

m_{4R}	5,85 (R_{local} = 0)
N_{fc}	Calculated number of cycles to failure
$N_{fc,mean}$	Calculated number of cycles to failure mean value
$N_{fc,railconnectionweld}$	Calculated number of cycles to failure with the new design rule for rail connection welds
$N_{f,i}$	Number of cycles to failure
N_{ft}	Number of cycles to failure in fatigue testing
$N_{ft,average\ test}$	Average number of cycles to failure in fatigue testing
n	Number of test specimens
n	Number of test results
R	Stress ratio due to an external load
R_{local}	Local stress ratio at the critical point of the joint where the fatigue failure occurs
R_m	Ultimate strength of the material
r_{true}	Weld toe radius
s_x	Standard deviation of test results
t	Material thickness
t	Value of the two-sided t-distribution (Student's law)
V	Voltage
V_x	Coefficient of variation
v	Poisson’s ratio
W_y	Section modulus
X_d	Design value
X_k	Characteristic value
$Y(a)$	Crack shape factor
A2	Top welded rail connection weld
A3	Three-side welded rail connection weld
Ar	Argon
CO_2	Carbonoxide
ENS	Effective notch stress
ENS_{factor}	Effective notch stress shape factor for nominal stress
FAT	Fatigue strength at two million cycles
FAT_c	Characteristic fatigue strength at two million cycles

FAT_{ENS}	Effective notch stress characteristic fatigue strength at two million cycles
$FAT_{ENS,mean}$	Effective notch stress mean fatigue strength at two million cycles
FAT_m	Mean fatigue strength at two million cycles
FE	Finite element
FEA	Finite element analysis
HAZ	Heat affected zone
HEA	European lightweight wide flange beam
HV5	Vickers hardness measurement with 5 kg weight
IIW	International institute of welding
LEFM	Linear elastic fracture mechanics
MAG	Metal-arc active gas welding
NC	Notch class
Stdv	Standard deviation
S-N	Stress range, Number of cycles (or Wöhler curve)

1 INTRODUCTION

Efficient transporting of bulk material, containers, and even humans requires a safe, smooth, solid, and continuous surface to travel on. To achieve free movement of a body on a surface, two perpendicular directions are controlled independently of each other. When heavy objects are moved in an industry, a common solution is to use a crane, which is installed above a floor lever and called as an overhead crane. Such a crane consists of a hoist, bridge, end carriage, and runway, Figure 1. Free movement of a lifted body in a crane is enabled such that a bridge travels on one direction on a runway, and a hoist travels along a bridge on a perpendicular direction. Runway consists of rails, and load-carrying beams where the rails are mounted to. Therein, rails are essential components to enable smooth transportation of bodies.

This research study is conducted to harmonize the EN13001 crane standard with the upcoming Eurocode 3 version. The work focuses on welds in cranes' runway. A typical runway load-carrying beam size is, for example, HEA300 or bigger depending on the span length between the supporting points and crane's lifting capacity. The customarily used rail size is 30 x 50 (mm).

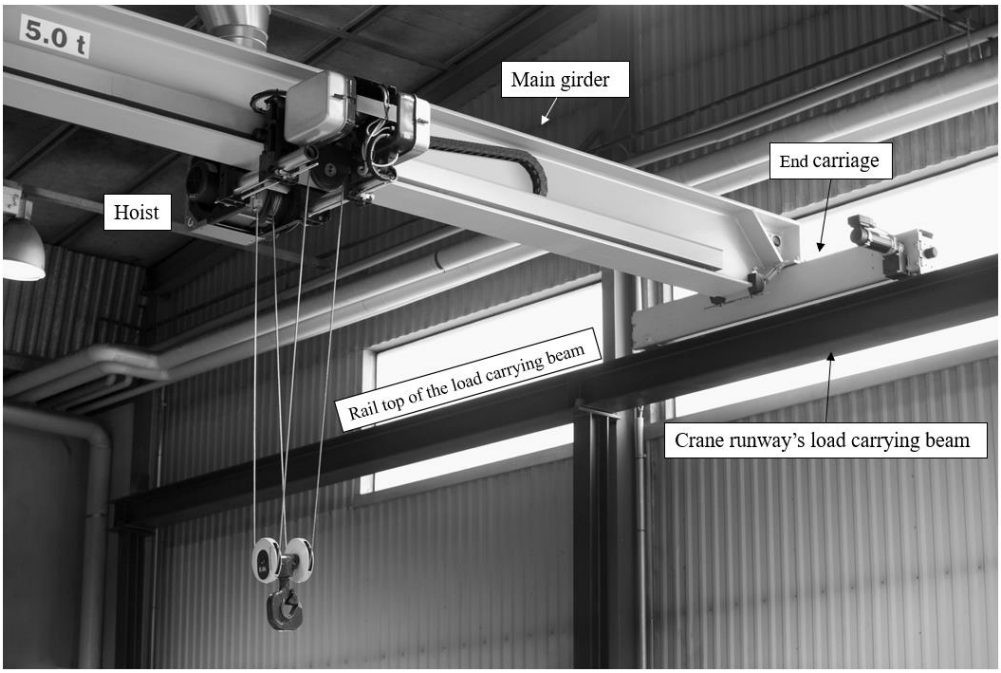

Figure 1. Main components of an overhead crane.

At the moment, the EN1993-1-9 standard fatigue part is missing FAT classes of rail connection welds, and the current EN13001-3-1 standard has the needed design rules for the details. In addition to that, the other studied weld is intermittent fillet welds that are not standardized in the current EN1993-1-9 part when the loading direction is different from the already standardized case. Figure 2 presents the crane runway parts and weld locations. In the design of a crane runway, the rail is included in the cross-section properties with the load-carrying beam.

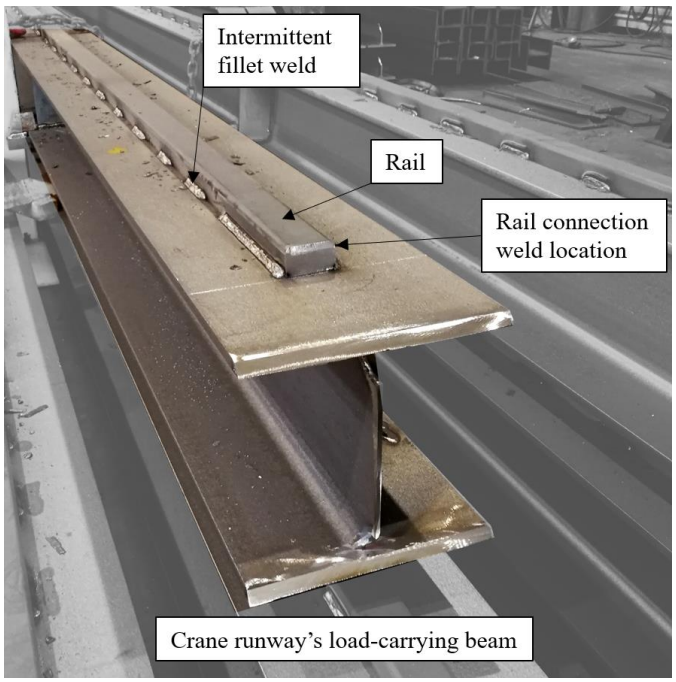

Figure 2. Detailed view of the crane runway.

1.1 Background of the rail connection weld study

The studied rail connection welds are shown in the red square in Figure 3. There are two different studied rail connection welds:

1. Rail is welded from the top surface and, thus, FAT56 (fatigue strength at two million cycles) is valid.
2. Rail is welded from three sides, and then FAT is 71.

There is a note that when there is welded continuous weld next to the connection area, the FAT class will increase by one notch class (NC). These design rules are currently missing from the EN1993-1-9 part. Due to this, structural designers need to apply the different FAT

classes that are presented in Eurocode 3. For the rail connection weld, it is difficult and time-consuming to determine the stresses in the weld without using FE-analysis. The nominal stress of rail connection weld is needed to utilize the current design rules from Eurocode 3.

3.15	m = 3	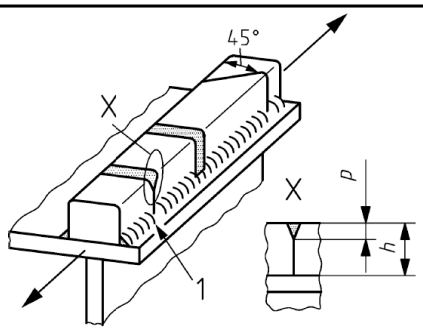 Plate with a rail welded on it, rail joints without butt weld or with partial penetration butt weld, design stress is that calculated in the plate.	Basic conditions: — all welds quality level C or better Special conditions: — continuous welds (1) over the joint on both sides of the rail with at least a length of 3 times h +1 NC
	45	rail joint cut perpendicular or at any other angle, e.g. 45°, p = 0 ,	
	56	single weld on top of the rail, h > p ≥ 0,3 x h	
	71	welds on top and on the two sides of the rail, h > p ≥ 0,2 x h	

Figure 3. In the red square studied rail connection weld details and design rules (EN13001-3-1, 2018, p. 84).

EN1993-1-9 gives only some detailed specifications that could be used in the rail connection welds. Weld toe and weld root need to be calculated separately, as illustrated in Figure 4 and Figure 5. The detail in Figure 4 represents the top layer of the rail connection weld toe. Its FAT class is 112 when the surface is ground evenly with the rail top surface (case 1 in Figure 4).

Detail category	Constructional detail		Description	Requirements
112	size effect for t>25mm: $k_s=(25/t)^{0,2}$	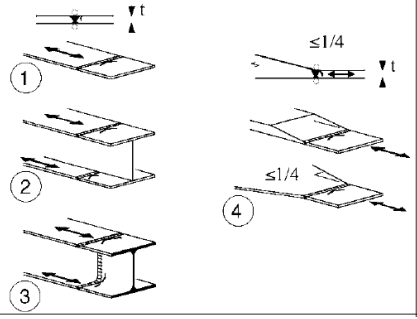	Without backing bar: 1) Transverse splices in plates and flats. 2) Flange and web splices in plate girders before assembly. 3) Full cross-section butt welds of rolled sections without cope holes. 4) Transverse splices in plates or flats tapered in width or in thickness, with a slope ≤ ¼.	- All welds ground flush to plate surface parallel to direction of the arrow. - Weld run-on and run-off pieces to be used and subsequently removed, plate edges to be ground flush in direction of stress. - Welded from both sides; checked by NDT. Detail 3): Applies only to joints of rolled sections, cut and rewelded.

Figure 4. Weld toe details design rule when the weld is grinded evenly (EN1993-1-9, 2005, p. 22).

Figure 5 shows a design rule for the weld root side. The FAT is 36, and it is used if the loading is compressive or tensile. The stress range due to external load must be calculated, referring to the weld area.

36*	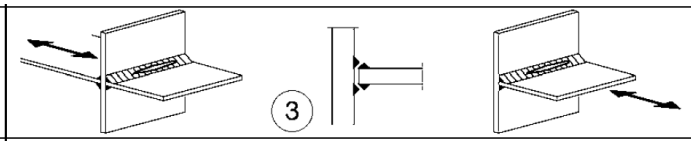	3) Root failure in partial penetration Tee-butt joints or fillet welded joint and effective full penetration in Tee-butt joint.

Figure 5. The FAT class of the weld root side when the loading is the same direction as in the studied situation (EN1993-1-9, 2005, p. 25).

For comparison, in EN13001-3-1 standard design rule for the weld root side and weld toe is presented in Figure 6. In that standard, the FAT class for the weld root side is 45, and for grinded weld toe is 100.

Detail No.	$\Delta\sigma_c$ $\Delta\tau_c$ N/mm^2	Constructional detail	Requirements
3.9	$m = 3$	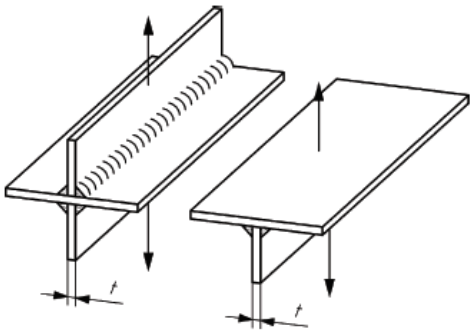 Cross or T-Joint, symmetric double fillet weld	Basic conditions: — continuous weld Special conditions: — automatic welding, no initial points +1 NC — welding with restraint of shrinkage −1 NC
	45	Stress in weld throat	$\sigma_w = F/(2 \times a \times l)$ see Annex C
	71	Quality level B	Stress in the loaded plate at weld toe
	63	Quality level C	

Figure 6. EN13001-3-1 design rule for the fillet weld root side when the loading is perpendicular to the weld (EN13001-3-1, 2018, p. 81).

Figure 7 summarizes the needed FAT classes in the rail connection weld that need to be used in the current situation. Like stated earlier, it is difficult to determine the nominal stress in the weld without using FE-analysis. It is needed to determine the nominal stress of the rail connection weld to use the current FAT values in the fatigue life calculations.

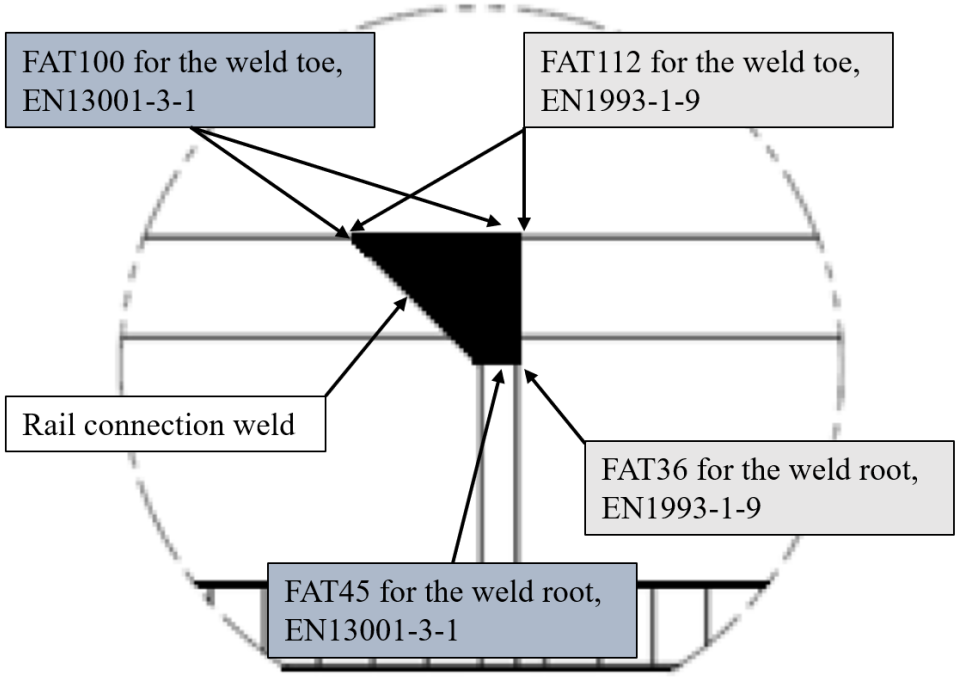

Figure 7. Summary of different FAT classes based on the standard recommendations in the top welded rail connection weld.

Thus, it is shown that there are no clear design rules for the rail connection welds in current Eurocode 3 as in EN13001-3-1 standard. That is why it is recommended to harmonize standards and give an easy to use design rule for the rail connection weld detail.

1.2 Background of the intermittent fillet weld study

In the current EN1993-1-9 standard and International Institute of Welding (IIW) design recommendations give some design rules for the intermittent fillet weld detail. EN1993-1-9 standard gives FAT classes 71 and 80, and the IIW recommendations FAT is between 36 and 80 depending on the loading situation. Design rules for the details are shown in Figure 8 and Figure 9. In both cases, the used stress range $\Delta\sigma$ is parallel to the flange stress. There are no design rules if the load is perpendicular to the intermittent fillet weld.

80	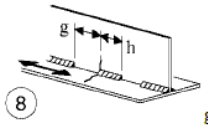	8) Intermittent longitudinal fillet welds.	8) Δσ based on direct stress in flange.
71	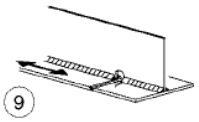	9) Longitudinal butt weld, fillet weld or intermittent weld with a cope hole height not greater than 60 mm. For cope holes with a height > 60 mm see detail 1) in Table 8.4	9) Δσ based on direct stress in flange.

Figure 8. Intermittent fillet weld design rule in the current Eurocode 3 (EN1993-1-9, 2005, p. 21).

IIW recommendations design rule is based on the ratio between normal stress in the flange and shear stress in the web values. It is based on the fact that the shear forces in the web plate of the load-carrying beam are effective and therefore affecting parallel to the flange plate.

No.	Structural Detail	Description (St. = steel; Al. = aluminium)	FAT St.	FAT Al.	Requirements and remarks
324	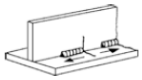	Intermittent longitudinal fillet weld (based on normal stress in flange **σ** and shear stress in web **τ** at weld ends) τ/σ = 0 0.0–0.2 0.2–0.3 0.3–0.4 0.4–0.5 0.5–0.6 0.6–0.7 >0.7	 80 71 63 56 50 45 40 36	 32 28 25 22 20 18 16 14	Analysis based on normal stress in flange and shear stress in web at weld ends Representation by formula: Steel: FAT = 80 · (1 - Δτ/Δσ) but not lower than 36 Alum.: FAT = 32 · (1 - Δτ/Δσ) but not lower than 14
325	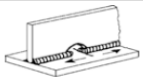	Longitudinal butt weld, fillet weld or intermittent weld with cope holes (based on normal stress in flange **σ** and shear stress in web **τ** at weld ends), cope holes not higher than 40 % of web τ/σ = 0 0.0–0.2 0.2–0.3 0.3–0.4 0.4–0.5 0.5–0.6 >0.6	 71 63 56 50 45 40 36	 28 25 22 20 18 16 14	Analysis based on normal stress in flange and shear stress in web at weld ends Representation by formula: Steel: FAT = 71 · (1 − Δτ/Δσ) but not lower than 36 Alum.: FAT = 28 . (1 − Δτ/Δσ) but not lower than 14

Figure 9. IIW Recommendations for intermittent fillet welds (Hobbacher, 2014, p. 49).

EN1993-1-9 does not have a design rule for intermittent fillet weld when the loading is perpendicular to the fillet weld. The closest possible weld detail is continuous fillet weld, and then the design rule is FAT36, which is presented in Figure 5. Based on the EN1993-1-9 standard pages 17-18, FAT design rules are used for tensile and compressive loading. For the compressive loading, it is possible to reduce the compressive stress by 0.6 factor in calculations, if the detail is non-welded or stress relieved, as shown in Figure 10.

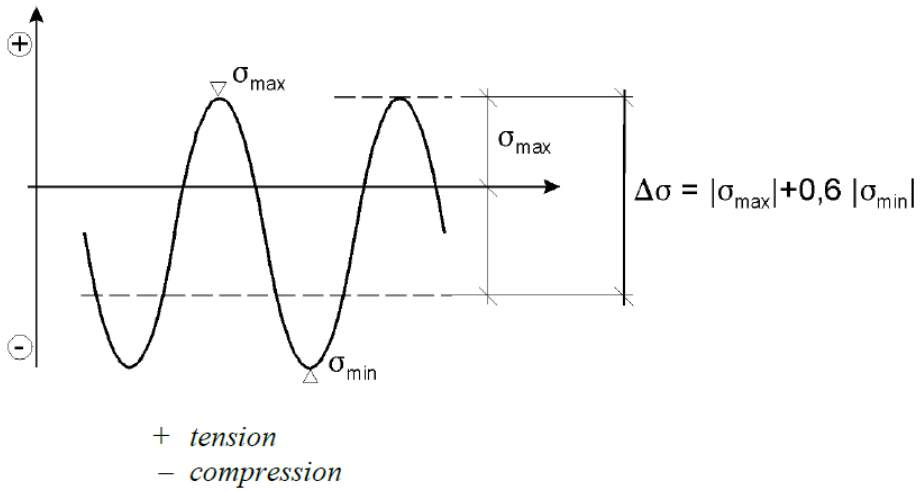

Figure 10. Modified stress range for non-welded or stress relieved details (EN1993-1-9, 2005, p. 18).

Konecranes uses intermittent fillet-welds, Figure 11, in the crane runway design to minimize deformations due to a welding process, as shown. The rail is welded to the top flange of the load-carrying beam. In this situation, bending stress is mostly on the compressive side in the rail welds. The intermittent fillet weld is assumed to have direct contact without any clearance between rail and load-carrying beam. In that case, wheel load forces are going with the surface pressure to the load-carrying beam. If there is a gap between the surfaces of a rail bottom and a top flange, the weld becomes a primary load-carrying element. Therein, wheel forces travel through the weld. In that scenario, there are no clear design rules in Eurocode 3. If the current EN1993-1-9 design rule FAT36 is used, fatigue life estimation is short in Konecranes' runway applications. Konecranes' experience has shown that intermittent fillet welds have better fatigue life in the described loading situation than current design rules calculate. That is why, in this research, intermittent fillet welds are studied under compressive loading.

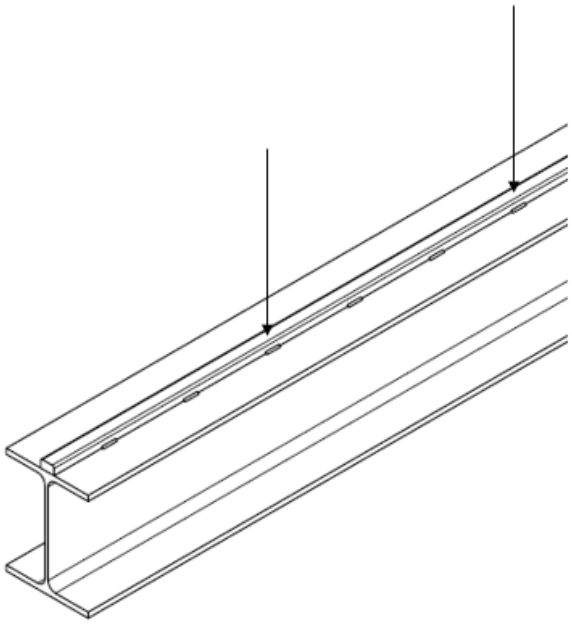

Figure 11. A picture of the crane's runway load-carrying beam and the rail welded by intermittent fillet welds. Two arrows represent the wheel loads from end carriage.

1.3 Research methods and scope

In this study, studied welds fatigue strength is determined by laboratory testing. Widely used fatigue strength assessment methods are used to study the weld details. With analytical calculations, the aim is to get an understanding of how the weld detail needs to be calculated to estimate fatigue strength and see possible advantages and disadvantages of different methods.

Some published relevant articles have conducted similar types of testing for the intermittent fillet weld, such as Euler & Kuhlmann, (2018) fatigue tested continuous fillet weld to connect rail to the load-carrying beam top flange.

Based on fatigue test results and theoretical calculations, the goal is to compare results and create relevant conclusions. If there is a significant difference between test results and theoretical results, arguments, and reasons are presented. In this study, the main objective is to determine the characteristic nominal stress fatigue strength at two million cycles FAT_c based on fatigue testing for the studied welds and different regression analysis of the fatigue test results. The shear stress loading has not been tested on the welds in this study.

2 FATIGUE STRENGTH ASSESSMENT METHODS

2.1 Fatigue phenomena in the steel structure

Fatigue loading can cause the structure to fail and lose its load-carrying capacity in specified time despite the structure static load-carrying capacity is fulfilled. Fatigue loading is varying in respect of load direction, magnitude, or location. Variation can be constant amplitude loading or variable amplitude loading. Constant amplitude loading causes constant stress ranges. Typically fatigue loading is variable amplitude loading. Then stress range varies in respect of time. (Ongelin & Valkonen, 2010, p. 425.) For example, overhead crane causes to the crane's runway load-carrying beam variable amplitude loading.

Welded joints can have small initial cracks that start to propagate under fatigue loading. The initial crack may start to initiate in the base material and then to propagate due to fluctuating load. Crack initiation or propagation is seen when the stress range is occurring. In the welded structure, the critical location in the fatigue strength point of view is the transition between weld and base material. The fatigue performance of the welded connection usually is smaller than the base material fatigue strength. For that reason, welding quality significantly affects the fatigue strength of the whole structure. Structural discontinuity example in the welded structure is shown in Figure 12. (Ongelin & Valkonen, 2010, pp. 426-427)

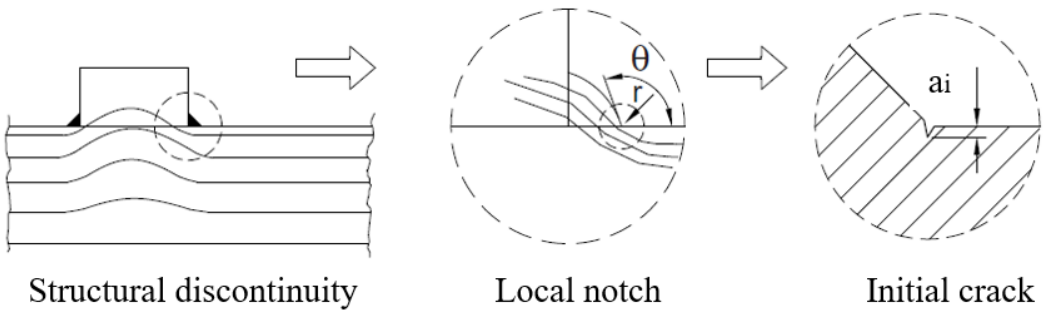

Figure 12. Welded structure different level discontinuities and typical initial crack location (Ongelin & Valkonen, 2010, p. 426).

The number of load cycles to failure depends on the nature of the loading. An underlying assumption is that the tensile stress range causes fatigue failure, not compressive stress. For

example, if part of the stress range is on the compressive side, the fatigue life is longer compared to the situation where the whole stress range is on the tensile side. This assumption is not valid for every case, and it can be used for materials that do not have residual stresses. After welding, there are residual stresses in the weld, and it affects the mean value of the stress range. The magnitude of the stress range $\Delta\sigma$ is the essential factor in the fatigue phenomena. Standards for the welded structures assume that there is tensile residual stress in the weld that is affecting the mean stress. Because of this assumption, the compressive stress is assumed to have the same effect on the fatigue life than the tensile stress in the welded structures. These factors influence the welded structure fatigue strength:

- The magnitude of the stress range
- Low cycle and high cycle fatigue behaviour
- Discontinuities in the structure
- The shape of the weld
- Size of initial crack
- Residual stresses
- Material toughness
- Local boundary condition
- Applied stress ratio
- Corrosion environment

(Ongelin & Valkonen, 2010, pp. 426-435)

It is mentioned earlier that welding causes residual stresses. Residual stresses have a consequential effect on the fatigue performance of the welded joint. High residual tensile stress harms fatigue strength, and accordingly, compressive residual stresses increase fatigue strength. At the weld toes, tensile residual stresses as high as material yield strength can be assumed to be present after welding. At the weld root side, it is challenging to measure residual stresses. There have been carried out simulations for the multi-pass fillet and butt welds. Results have shown compressive residual stresses in the root side, and the magnitude can be the base material yield stress. There are several affecting factors for the final residual stress state, for example, the number of weld passes, inter-pass time, weld penetration, and contact mechanism between the adjoined components: stiffness of the components and the constraints. Despite the simulation results, an unfavorable global residual stress state can be present because of the fabrication and erection of the whole structure. Because of this, high

tensile residual stresses need to be also assumed for the weld root side unless better conditions are proven. (Fricke, 2013, pp. 754-756)

2.2 Biaxial normal stress and shear stress of the traveling crane

Traveling wheel load causes normal biaxial stress and shear stress range, Figure 13. Wheel load causes stress field that includes local stress components: local transverse pressure $\sigma_{z,local}$ from concentrated wheel load, and the local shear stress $\tau_{xz,local}$. In addition to these, there are global stress components σ_x and related shear stress τ_{xz} because of global bending. The crane runway static system effects that all these stress components might not reach their maximum values simultaneously. Stress values $\sigma_{z,local}$ and $\tau_{xz,local}$ are naturally effecting out-of-phase, Figure 13. (Nussbaumer, et al., 2018, p. 216)

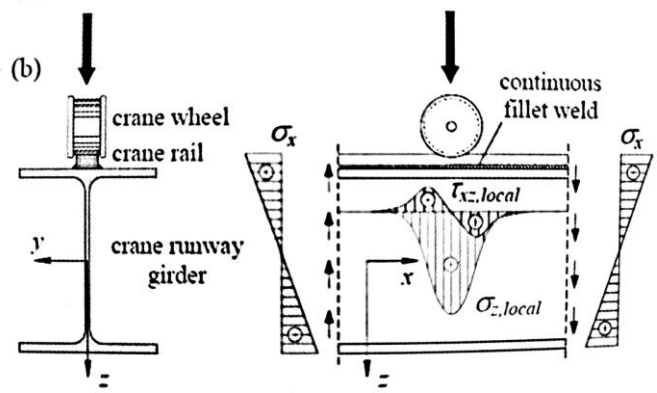

Figure 13. Detail of runway under bending and local stresses due to wheel passage (Nussbaumer, et al., 2018, p. 216).

"Thus, under bending and shear stress range, the fatigue crack is likely propagate vertically, as under local normal stress range, the fatigue crack is likely propagate horizontally. This case is thus complicated to verify and the interaction between these different loadings is not clearly treated in the EN1993-1-9. Instead, for crane runways, the EN1993-6 requires that the verification is made by taking into account both local and global effects together in equation 1. " (Nussbaumer, et al., 2018, pp. 215-217)

$$\left(\frac{\gamma_{Ff} \cdot \Delta\sigma_{E,2}}{\Delta\sigma_c / \gamma_{Mf}}\right)^3 + \left(\frac{\gamma_{Ff} \cdot \Delta\tau_{E,2}}{\Delta\tau_c / \gamma_{Mf}}\right)^5 \leq 1.0 \qquad (1)$$

where,

$\Delta\sigma_{E,2}$	equivalent constant amplitude normal stress range related to 2 million cycles
$\Delta\tau_{E,2}$	equivalent constant amplitude shear stress range related to 2 million cycles
γ_{Ff}, γ_{Mf}	fatigue action effects, respectively fatigue strength safety factors

There are other interaction equations introduced in different reference books, for example, in the EN13001-3-1 standard and the IIW recommendations. Based on the IIW recommendations, the interaction equation power values need to be different. It suggests using elliptical interaction that has the power of two values instead of three in the nominal stress part and two instead of five in the shear stress part (Hobbacher, 2014, p. 94).

2.3 Fatigue strength assessment methods

In this chapter, the main fatigue assessment methods are presented. These methods have been utilized in this study. In addition to these methods, the Hot Spot method is commonly used to calculate the fatigue strength of the structure in many fields of structural engineering. To use the Hot Spot method, the critical point needs to be in the weld toe. Officially, the Hot Spot method cannot calculate weld root fatigue strength. This method is not introduced or utilized in this study.

2.3.1 Nominal stress method

The nominal stress method is generally used in the mechanical or structural engineering areas to evaluate the structural detail fatigue life, for example, in the bridges, cranes, vessels, and many other applications. It is included in the relevant design codes. There can be engineering areas that do not utilize this method. These are primarily automotive and aircraft industries. In those industries, there are extraordinarily high requirements for lightweight design and damage tolerance. (Radaj D, 2006, p. 15)

It is needed to determine the used nominal stress in the studied situation to use the nominal stress method. Nominal stress is calculated stress in the specific area under consideration. In the nominal stress, elastic behaviour is presumed. In simple components, for example, beam, the nominal stress can be calculated by elementary theories of structural details. Nominal

stress takes account of the macro-geometric shape (Figure 14) that increases the stress nearby the component joint, for example, large cut-outs. However, it does not consider the local effects that increase the stress, for example, in Figure 15 weld detail. (Hobbacher, 2014, pp. 15-16)

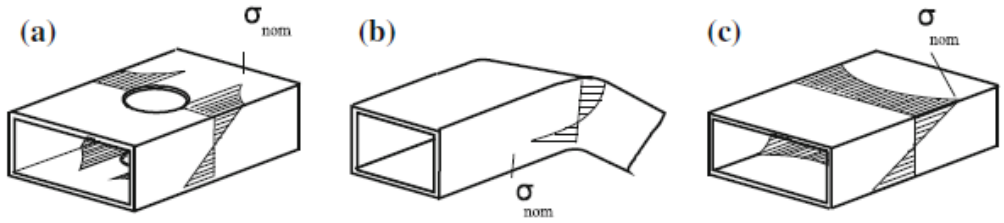

Figure 14. Examples of macro geometric effects. Stress concentrations at (a) cut-outs, (b) curved beams, and (c) wide plates (Hobbacher, 2014, p. 15).

In the EN1993-1-9 standard, the fatigue strength is calculated by the nominal stress method. Nominal stress range can be nominal direct stress $\Delta\sigma$ or nominal shear stress $\Delta\tau$ or combination of both nominal stresses. The number of load cycles to failure N_f for nominal stress ranges can be calculated by equation two, where m is the slope of the fatigue strength curve. In the nominal direct stress situation, m is three, and for nominal shear stress, $\Delta\tau$ m is 5. FAT is the reference value for fatigue strength at 2 million cycles for the structural detail. FAT values are specific for the detail, and value is drawn by testing the detail. (EN1993-1-9, 2005, pp. 12-14) FAT values of structural details are presented in different standards, for example, in EN1993-1-9 & EN13001-3-1 standards and IIW recommendations.

$$N_f = \left(\frac{\text{FAT}}{\Delta\sigma \text{ or } \Delta\tau}\right)^m \cdot 2 \cdot 10^6 \tag{2}$$

The nominal stress method is an easy way to assess the fatigue strength of a structure. Different joint catalogs and standards have the most typical structural details classified. In many cases, fabricated structures are geometrically complex, and this leads to difficulties in determining the nominal stress, or it can be impossible. Load directions and constraints can be different in the studied structure than in the classified detail. This kind of situation causes the nominal stress method to be unsuitable for assessing fatigue strength of studied structural detail. (Poutiainen, 2006, p. 16)

2.3.1 Effective notch stress method

The effective notch stress method (ENS) is a local approach that estimates the total stress at the root of a notch in the studied detail by using a notch that has an effective root radius. In Figure 15, weld detail non-linear stress distribution stress components are presented, where σ_m is membrane stress, σ_b shell bending stress, and σ_{nl} is a non-linear stress peak. ENS takes account of all the stress components that are presented in Figure 15. Linear-elastic material behaviour is assumed in the ENS method.

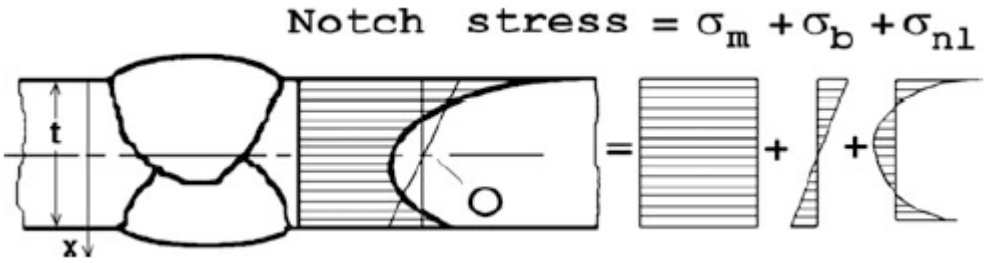

Figure 15. Non-linear stress distribution separated into stress components (Hobbacher, 2014, p. 14).

Finite element analysis (FEA) is used to utilize this method, and instructions for the modeling practices are presented. At the weld toe and weld root side, an effective notch root radius of 1 mm needs to be created. With fictitious rounding, the idea is to take into account the weld shape parameters variation: At the bottom of the rounding, there is a similar stress level, which describes the effective stress acting on average in the area of weld toe or weld root. It takes into account the stress concentration so that the fatigue stress comes approximately correctly described by one value. The radius of 1 mm produces effective local stress correctly. The rounding size is verified and the needed element size around the root radius. This primary method is limited to material thickness $t \geq 5$ mm. There are other instructions on how to do ENS fatigue strength assessment for material thicknesses $t < 5$ mm. One example picture of the rounding locations is shown in Figure 16. This method is used to estimate the fatigue failure in the weld root or weld toe. (Hobbacher, 2014, pp. 27-29)

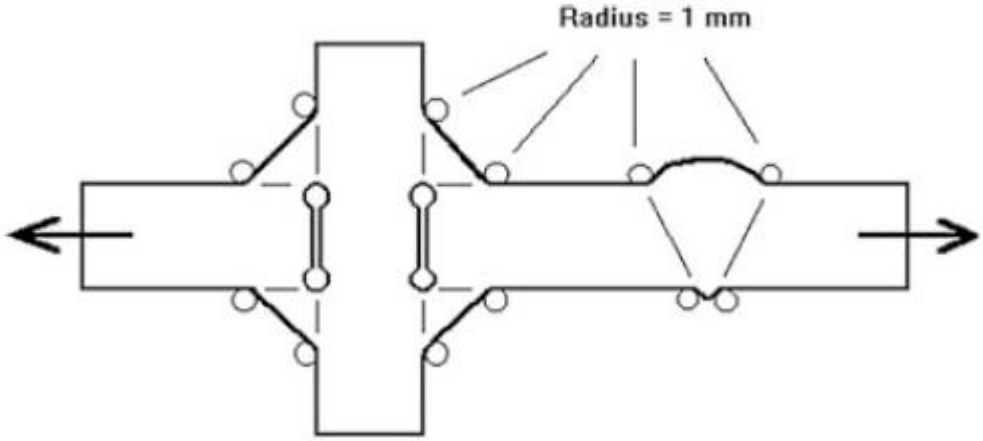

Figure 16. Fictitious roundings of weld toes and roots (Hobbacher, 2014, p. 27).

ENS calculation method is shown in equation three. The effective notch stress range $\Delta\sigma_{ENS}$ is obtained from the FE-model that includes fictitious roundings, and the used stress is maximum principal stress to calculate the fatigue life. For the fatigue assessment single S-N curve is used. For steel, the used comparison FAT_{ENS} is 225 for every ENS structural details when maximum principal stress is used, and the reference cycle is two million cycles. (Hobbacher, 2014, p. 62)

$$N_{fc,\,ENS} = \left(\frac{FAT_{ENS}}{\Delta\sigma_{ENS}}\right)^3 \cdot 2 \cdot 10^6 \tag{3}$$

2.3.2 Linear elastic fracture mechanics

Linear elastic fracture mechanics (LEFM) is practical to estimate the propagation rate of cracks or crack-like imperfections. The underlying assumption is that welded components have initial cracks after welding with a short period of crack initiation. That is why in the welded structure is reasonable to assume that crack propagation is the governing process. Because of this fracture mechanics can be used to assess the fatigue life in the welded structure. The fatigue life can be calculated with integrated Paris-Erdogan power law, equation four. The stress intensity factor is calculated according to equation five.

$$\frac{da}{dN} = C \cdot \Delta K^m \tag{4}$$

$$K = M_k(a) \cdot Y(a) \cdot \Delta\sigma \cdot \sqrt{\pi \cdot a} \quad (5)$$

where,

C	constant of the power-law
m	exponent of the power-law
K	stress intensity factor
$\Delta\sigma$	equivalent stress range
$M_k(a)$	magnification function for K
$Y(a)$	crack shape factor
a	crack size

(Bertil & Dobmann G., 2016, p. 17 & 98)

"K is a measure of the severity of the combination of crack size, geometry, and load. K_{ic} is the particular value, called the fracture toughness, where the material fails." (Dowling, 2013, p. 24). Typically characteristic values for the welded joints are: $C = 5.21 \cdot 10^{-13}$ or $3.00 \cdot 10^{-13}$ and m = 3 (units, Newton and millimetres). (Hobbacher, 2014, p. 75)

LEFM does not use S-N curves, and there is no need to determine nominal stress or other stress components in the method. The effect of the whole stress field is taken into account in the fatigue life estimation. LEFM analysis is often time-consuming compared to the other methods, but it can give a better fatigue life estimation in various cases, mainly if initial cracks are present. (Fricke, 2013, p. 768) If an analytical approach is used, the K variable needs to be calculated separately for bending and tensile.

2.3.3 4R method

Many of the basic stress-based fatigue strength assessment methods have been developed further to consider more welded details and local stresses. However, no method includes all the essential parameters to evaluate, particularly fatigue strength of high-quality welded joints made of high and ultra-high-strength steels. 4R concept includes all the essential parameters: R_m the ultimate strength of the material, R stress ratio due to external load, σ_{res} residual stresses, and r_{true} weld toe radius. All these parameters are needed to determine the local stress ratio R_{local}. The 4R method has been developed in a way that the usual engineering practice can obtain all the needed parameters. Local cyclic behaviour at weld

toe is calculated based on the applied stress range, master curve parameters, and the four parameters. 4R method is based on the modified ENS concept, and fictitious rounding r =1 mm or r_{true} + 1 mm is used in the finite element model at the weld toe. The cyclic stress-strain behaviour of the material at critical weld toe is the basic principle for the 4R method. Fatigue life is calculated with the 4R method using equation six. (Björk, et al., 2018, pp. 1-4)

$$N_{f,4R} = \left(\frac{\sqrt{1 - R_{local}}}{\gamma \cdot \left(K_{t,m} \cdot \Delta\sigma_m + K_{t,b} \cdot \Delta\sigma_b \right)} \right)^{m_{4R}} \cdot C_{4R} \qquad (6)$$

where,

R_{local}	local stress ratio at the critical point of the joint where the fatigue failure occurs
γ	safety factor
$K_{t,m}$	stress concentration factor for membrane loading
$K_{t,b}$	stress concentration factor for bending loading
$\Delta\sigma_m$	membrane stress range
$\Delta\sigma_b$	bending stress range
m_{4R}	5.85 (R_{local} = 0)
C_{4R}	$10^{20.83}$ (characteristic value, $R_{local,\ ref}$ = 0)

The denominator can be replaced with $\Delta\sigma_{k,FEA}$ value from finite element analysis. (Björk, et al., 2018, pp. 1-4)

"The essence of the 4R method is to transform linear elastic notch stress, i.e. effective notch stress, to local cyclic elastic-plastic material behaviour from which the true acting local stress ratio at notch root, R_{local}, can be obtained. The cyclic behaviour in the 4R method is based on well-known material behaviour models, such as the Ramberg-Osgood cyclic material model, Neuber's notch theory and the kinematic hardening rule, also known as Bauschinger's effect." (Björk, et al., 2018, p. 2)

Currently, the 4R method is applicable for welded joints and cut edge details. The current 4R method is not including fatigue strength assessment of weld root and thin-walled

structures. (Björk, et al., 2018, pp. 8-9) However, the consideration of the fatigue strength assessment of the weld root side is under work.

2.4 S-N curve for structural detail

"The welded joints are classified according to their shape, type of weld, type of loading and quality of manufacture. They are then allocated to the detail classes representing the design S-N curves based on the results of relevant fatigue tests. The German designation' notch class' is only correct to the extent that the varying fatigue strength is caused by a varying notch effect. The English designation' detail class' or 'fatigue class' (FAT) is more general." (Radaj D, 2006, p. 15) In this report, the FAT class designation is used mainly instead of notch class.

S-N curves (Stress range, Number of cycles) are used to calculate the fatigue strength of a welded structure according to the EN1993-1-9 standard. Every structural detail has its detailed category, that is the FAT class. Experimental tests obtain the specified category value for the structural detail. All the presented FAT class values in the standard are given as a characteristic value. FAT class indicates the reference fatigue strength in two million load cycles with the corresponding $\Delta\sigma$ nominal stress. Detail category value has a 95% survival probability and a 75% confidence level. It takes account, for example, the standard deviation and the sample size and residual stress effects. (EN1993-1-9, 2005, p. 16.) FAT_c is used to present characteristic value and FAT_m to present mean values in this report. FAT mean value presents a 50% survival probability. To assess the FAT_m value, the FAT_c value needs to be multiplied by 1.37 factor (Radaj D, 2006, pp. 28-29). Allows comparing single test results and FAT_m values to each other. Different detail category values in the EN1993-1-9 standard are presented in Figure 17. All variables are assumed to follow either a Normal or a log-normal distribution (EN1990, 2006, p. 169).

When looking at fatigue test results, every structural detail has its own specific S-N curve slope *m* value that is slightly different from others. Based on several fatigue tests, it has been observed that for nominal stress, *m* value is close to three and for shear stress, the $m = 5$, respectively. Based on this finding, it has been decided to use standard values for *m* in the EN1993-1-9 standard. It allows to simplify test results evaluation and give a general

guideline. If a new structural detail is wanted to add in the standard by fatigue testing, the FAT class needs to be classified by described *m* values. (Kouhi, 2015, p. 140)

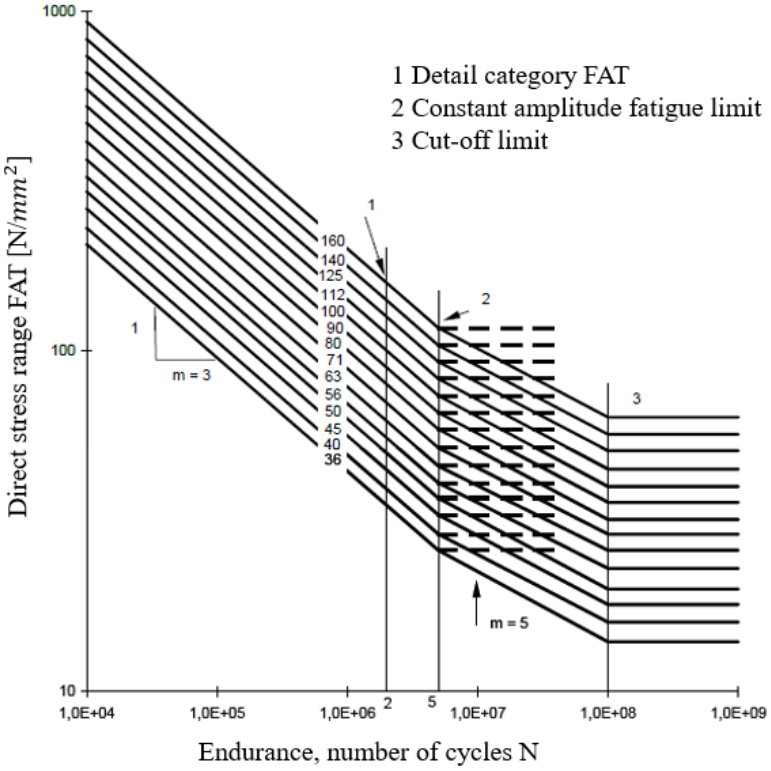

Figure 17. Fatigue strength curves for direct $\Delta\sigma$ stress ranges (EN1993-1-9, 2005, p. 15).

To determine the FAT class of structural detail by testing EN1993-1-9 recommends having more than 10 data points in the statistical analysis. Stress ratio *R* should be constant in the testing. For the derivation of S-N curves, it recommended having two different stress range levels in the testing and test specimens fatigue failure is recommended to be between 50 000 to 1 000 000 cycles. (Hobbacher, 2014, pp. 75-76) The calculation process of linear regression analysis for the detail category based on the test results is presented in chapters 2.4.1 and 2.4.2.

It can be concluded that EN1993-1-9 standard fatigue strength calculation is based on the traditional calculation method. It means that nominal stress is used, and detail category values are drawn by fatigue testing. Test results are analysed and turned into different FAT detail category values by utilizing nominal stress. Technically, the nominal stress method is calculating fatigue strength against experimental values. (Kouhi, 2015, p. 108)

2.4.1 Regression analysis procedure based on IIW recommendations

In the standard based design, characteristic values are used. It includes a safety margin that is applied to the mean values. Characteristic values have a 97.7% survival probability and a 2.3% probability of failure. It has been proved from the fatigue resistance mean value C_{mean} Fatigue resistance C is constant in the equation of the S-N curve with exponent m, equation 7. The slope curve m can be determined accurately from the test data. However, a fixed value of m = 3 can be used for steel and aluminum welded joints if the number of test points is under ten or the data are not evenly enough distributed to determine m accurately. (Hobbacher, 2014, pp. 76-77)

$$N = \frac{C}{\Delta\sigma^m} \tag{7}$$

$$\log N = \log C - m \cdot \log \Delta\sigma$$

$$\rightarrow \log\left(\Delta\sigma_i^{\,m} \cdot N_{f,i}\right) = \log C$$

The equation eight is used to fit the S-N curve to the test data (Rabb, 2013, pp. 74-75). This method is known as the least-square fit procedure.

$$y = -m \cdot x + b \tag{8}$$

where,

$$y = \log\left(N_{f,i}\right),\ x = \log(\Delta\sigma_i)$$

$$b = \frac{\sum_{i=1}^{n} y_i}{n} + m \cdot \frac{\sum_{i=1}^{n} x_i}{n}$$

$$b = \log(C_{mean})$$

where,

$N_{f,i}$	Number of cycles to failure
$\Delta\sigma_i$	Stress range in the studied area

m = 3 fixed value is used in this study. Value m can be calculated separately based on the test data, equation 9:

$$m = \frac{n \cdot \sum_{i=1}^{n} x_i \cdot y_i - \sum_{i=1}^{n} x_i \cdot \sum_{i=1}^{n} y_i}{n \cdot \sum_{i=1}^{n} x_i^2 - (\sum_{i=1}^{n} x_i)^2} \quad (9)$$

FAT_m value can be derived with fatigue resistance C_{mean} value using an equation 10:

$$C_{mean} = FAT_{mean}{}^{m} \cdot 2 \cdot 10^6 \quad (10)$$

Standard deviation Stdv needs to be determined from the test data by equation 11 to calculate the characteristic value:

$$Stdv = \sqrt{\frac{\sum_{i=1}^{n} (\log C_{mean} - \log C_i)^2}{n - 1}} \quad (11)$$

where,

$$\log C_i = \log \Delta\sigma_i{}^{m} \cdot N_{f,i}$$

Finally, characteristic FAT_c value can be calculated by equation 12:

$$\log C_{char} = \log C_{mean} - k \cdot Stdv \quad (12)$$

where,

$$k = 1.645 \cdot \left(1 + \frac{1}{\sqrt{n}}\right)$$

where,

n number of test specimens

IIW recommendations also introduce other regressions analysis method that takes account the probability distribution of the mean corresponds to a Student's law (t-distribution), and the probability distribution of the variance corresponds to a Chi-square law. The main difference between these two IIW regression analysis is the value k calculating formula. This method is presented in the reference book chapter 6.4.1 Statistical Evaluation of Fatigue Test Data. The equation 13 is the general formula for k value that includes a Student's law and a Chi-square law:

$$k_1 = \frac{t_{(p,\,n-1)}}{\sqrt{n}} + \varphi_{(\alpha)}^{-1} \cdot \sqrt{\frac{n-1}{\chi^2_{\left(\frac{1+\beta}{2},\,n-1\right)}}} \qquad (13)$$

where,

t	value of the two-sided t-distribution (Student's law) for p = β = 0.75, or of the one-sided t-distribution for a probability of p = (1+ β)/2 = 0.875 at n-1 degrees of freedom
n	number of test result
φ	distribution function of the Gaussian normal distribution probability of exceedance of α = 95% (superscript -1 indicates inverse function)
χ^2	Chi-square for a probability of (1+ β)/2 = 0.875 at n-1 degrees of freedom

If the variance is fixed from other tests or standard values, no confidence interval must be considered with equation 14:

$$k_1 = \frac{t_{(0.875,n-1)}}{\sqrt{n}} + 1.645 \qquad (14)$$

(Hobbacher, 2014, pp. 129-130)

2.4.2 Regression analysis procedure based on Eurocode recommendations

The EN1990 Eurocode standard introduces two main statistical approaches. The first approach is used to do the statistical determination of a single property. It includes two different methods. The second approach is used to do the statistical determination of resistance models. This part is mainly intended to define procedures for calibrating resistance models and for deriving design values from tests. The referred tests mean that testing is done to reduce uncertainties in parameters used in resistance models. (EN1990, 2006, p. 163 & 175) In this study, the statistical determination of the resistance model is not needed to do because the target is to determine a single property by testing. There are two different methods to determine single property by statistical evaluation:

"Method a) by assessing a characteristic value, which is then divided by a partial factor and possibly multiplied if necessary by an explicit conversion factor.

Method b) by direct determination of the design value, implicitly or explicitly accounting for the conversion of results and the total reliability required. "
(EN1990, 2006, p. 167)

Equations 15 and 16 show how different methods are calculated. The symbols are the same as in the EN1990, and both methods formula correlate to a normal distribution. The single property *X* may represent a resistance of a product or a property contributing to the resistance of a product (EN1990, 2006, p. 171).

Method a):

$$X_k \rightarrow X_d = \eta_d \cdot \frac{X_{k,(n)}}{\gamma_m} = \frac{\eta_d}{\gamma_m} \cdot m_x \{1 - k_n \cdot V_x\} \quad (15)$$

Method b):

$$X_d = \eta_d \cdot m_x \cdot \{1 - k_{d,n} \cdot V_x\} \quad (16)$$

where,

m_x	Mean of the n sample results
$k_{d,n}$	Design fractile factor
k_n	Characteristic fractile factor
V_x	Coefficient of variation of X
γ_m	Partial factor for resistances
η_d	Design value of the possible conversion factor

"In general, EN1990 recommends method (a) with a partial factor taken from the appropriate Eurocode. Method (b) is intended to be applied in special cases", (Gulvanessian, et al., 2002, p. 153). Method (a) is used in this study.

Method (a) includes γ_m partial factor for resistance, and η_d is a possible conversion factor. Based on EN1990 standard:" η_d conversion factor is strongly dependent on the type of test and type of material. The partial factor γ_m should be selected according to the field of

application of the test results." (EN1990, 2006, p. 173) In this study, both factors η_d and γ_m are assumed to be 1.00.

The derivation of a characteristic value from tests using the method (a) should be considered the scatter of test data, statistical uncertainty associated with the number of tests, and prior statistical knowledge. The coefficient of variation V_x can be estimated from the test data using equation 15 if the V_x is unknown. In equation 16, s_x is the standard deviation of test results, and m_x mean of test results. Standard deviation is calculated the same way in the EN1990 standard than in the IIW recommendations, equation 11 and m_x equals to the FAT_m value from equation 10. When V_x is unknown, it is assumed that the V_x value to be not smaller than 0.10. (EN1990, 2006, p. 169 & 171)

$$V_x = \frac{s_x}{m_x} \tag{17}$$

For the method (a), k_n value is needed. In the EN1990, there is a table that includes k_n value based on the number of experiments or numerical test results and is the V_x known or unknown.

Table 1. Values of k_n for the 5% characteristic value. (EN1990, 2006, p. 173)

n	1	2	3	4	5	6	8	10	20	30	∞
V_x known	2.31	2.01	1.89	1.83	1.80	1.77	1.74	1.72	1.68	1.67	1.64
V_x unknown	-	-	3.37	2.63	2.33	2.18	2.00	1.92	1.76	1.73	1.64

3 EXPERIMENTAL TESTING

Fatigue strength of the studied welds is determined by fatigue testing in a laboratory. The welds are also studied using different analytical calculations. The goal is to compare the computational results to the experimental test results. For the two rail connection welds, the target is to give more evidence that the EN13001-3-1 standard design rules are applicable and presented FAT_c values are in line with testing and calculations. An intermittent fillet weld is tested under compressive loading. In addition, residual stress measurements are collected on the rail connection welds areas to determine the residual stress state in the weld. Macroscopic views are taken from the welds to determine the weld shape and weld penetration. Finally, residual stresses from the typically used largely size runway load-carrying beam is measured to see the difference compared to smaller in size fatigue test specimens. These are conducted to gather more data from the welds and testing circumstances and also to validate the fatigue test results. Based on the obtained results, design rules for the studied welds are presented.

3.1 Test specimens and studied weld details

The weld shapes and groove dimensions of the investigated rail connection welds are presented in Figure 18. The smallest possible weld groove shapes and dimensions accepted by the EN13001-3-1 standard have been utilized in this study. The used height of the groove is 9 mm for the top welded rail connection. For the three-side welded rail connection, the weld groove height is 6 mm. Those values are the minimum allowed heights for the design of the studied welds. Those dimensions are desired for testing because nominal stress is the highest possible under allowed groove dimensions in the rail connection welds. Rail parts are machined to get desired dimensions. There is a 2.5 mm clearance between rail and rail connection piece. The clearance is used because, in typical assembly situations, there are always some clearances between the rail pieces to help the assembly phase. Besides, it is wanted to ensure in the laboratory testing that all the trail forces are carried by rail connection weld and assembly fillet welds. The EN13001-3-1 standard does not give instructions related to the clearance size and how it would affect the detail's fatigue life. Obviously, the clearance size will have a more significant role on the welding quality at the weld root side and thus impact on fatigue resistance.

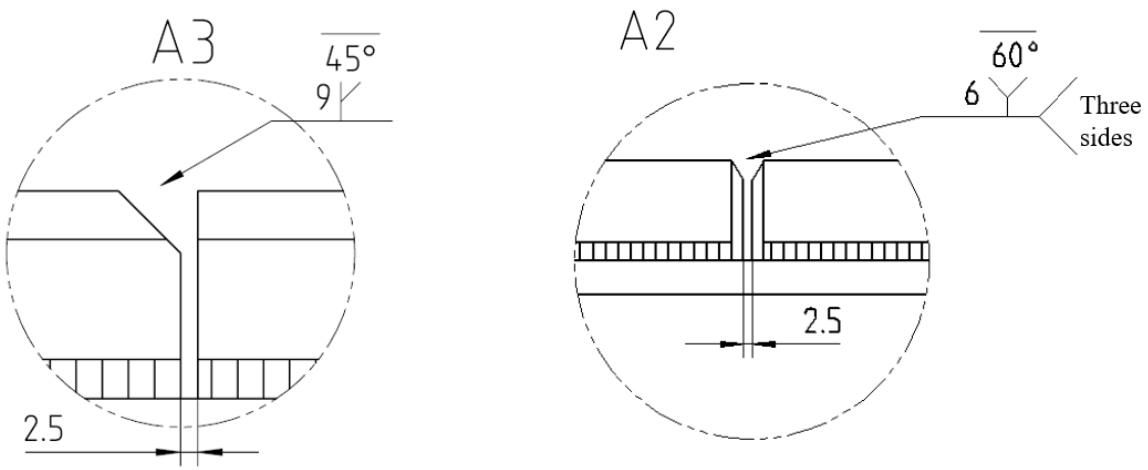

Figure 18. Detail view and main dimensions of studied rail connection welds.

The test specimen span is 3 000 mm, and cylinders distance between each other is 800 mm, measured from the middle of the wheel contact area. The test specimen's main dimensions and welding markings are shown in Figure 19. The red arrows indicate the cylinder forces' location on the test specimen. Intermittent fillet welds length is 50 mm, and designed throat thickness a_w dimension of a fillet weld is 4 mm.

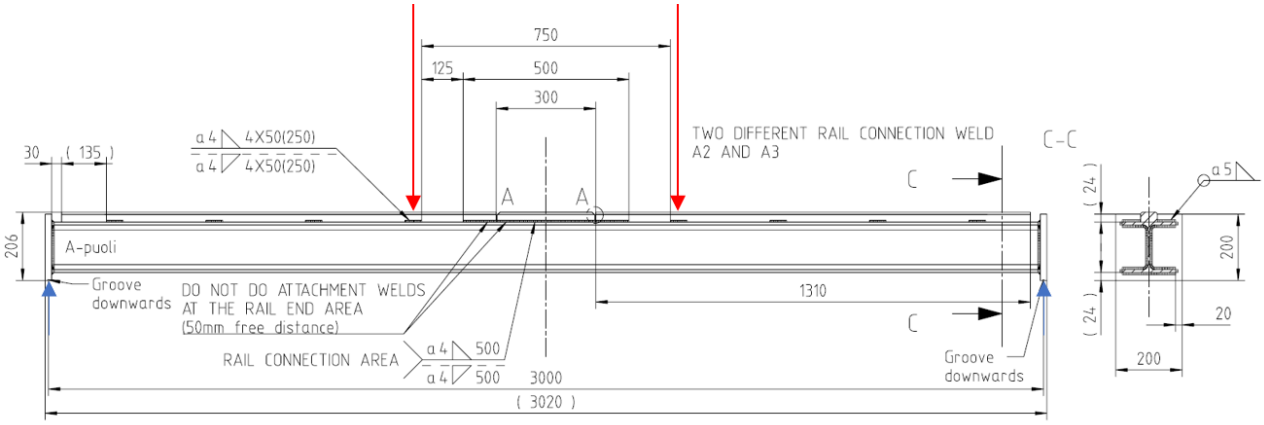

Figure 19. Main dimensions of the test specimen and welding marks.

The contact width of a pusher between cylinder and rail is 30 mm. The pusher applies the forces from the cylinder to the test specimen. The contact area is wider compared to the wheel load applications, but the nominal stress is the same in the intermittent fillet weld in both cases. Based on the standard EN13001-3-1, pages 163-164, sufficient distribution length under concentrated wheel load contact width is 12 mm that is used in the calculations

when used wheel diameter is 70 mm. Figure 20 illustrates how local compressive stress is constant over the intermittent fillet weld.

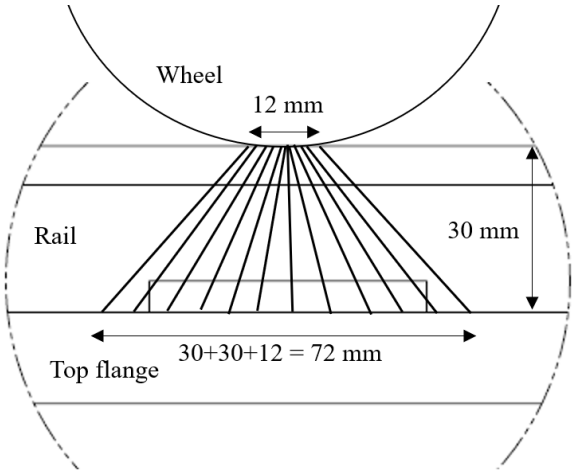

Figure 20. Distribution of the local compressive stress from the wheel in real size application.

The rail height is enough for local compressive stress from wheel load to distribute evenly over the intermittent fillet weld based on the 45° distribution rule. That is why the wider 30 mm contact area can be used in testing and keep the cylinders stable during the fatigue testing.

3.2 Preparing test specimens

Test specimens are manufactured with regular workshop practices. The test specimens are made in a workshop that usually fabricates the Konecranes crane's runways in Finland. Welding order, welding direction, dimensions of the weld throat thickness, and location of the welds have been made the same way in every test specimen. Weld locations are marked for every weld before welding. All the tack welds are placed in the location where the welder needs to stop welding. This way, the welder knows the precise location to stop welding, and tack welds do not affect the quality of the actual welds. The same welder welds all the test specimens. The welder has over 15 years of experience in different types of welding circumstances and welded structures such as nuclear power plants, shipyard, ship repair welding, and pressure vessels.

Test specimens welding order in Figure 21:

1. All the rail pieces are tack welded to the right place

2. Intermittent fillet welds are welded
3. Rail connection welds are welded in turn. The next welding pass is welded when the weld temperature is below 150 °C.
4. Finally, 500 mm assembly fillet weld is welded

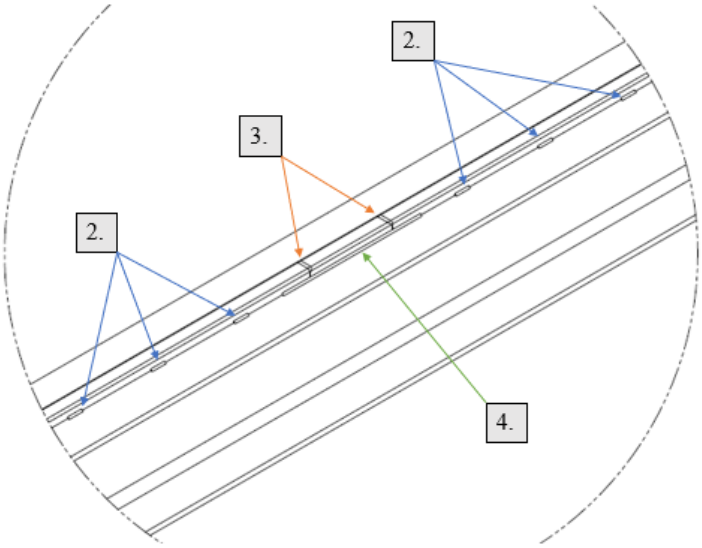

Figure 21. Welding order in the test specimen.

A3 rail connection weld takes three passes to fill the groove. A2 weld needs two passes for the top groove and one pass vertically to full fill grooves from all three sides. Welding torch position is perpendicular to the weld. Welding direction and order are the same for every test specimen. The used mean welding parameters are shown in Table 2.

Table 2. The average welding parameters of the measured values. Measuring is done when the test specimens have been welded.

	A3 top	A2 top	A2 vertical	Intermittent fillet welds	500mm assembly fillet weld
I [A]	210	200	190	230	230
U [V]	27.3	26.1	25.9	27.8	27.8
Wire feed [m/min]	8	8	8	9.5	9.5
Travelling speed [mm/s]	5.92	-	-	5.41	4.87
Heat input [kJ/mm]	0.77	-	-	0.95	1.05

The used welding process is metal-arc active gas welding MAG (136). The used filler material is 1.2 mm flux-cored wire made by Lincoln electric outershield 71E-H, and all the tack welds are made with 1.2 mm metal wire. Shield gas is SK-25 25% Carbonoxide (CO_2) + Argon (Ar), and the flow rate is 18-20 l/min. The rail connection welds are finally grinded with the electrical grinder with the 3M Cubitron II 982C fibre disc and the K40 flap disc. One test specimen after welding is shown in Figure 22.

Figure 22. A2 weld detail test specimen at the welded stage. Grinding is the next phase.

For four (A3) test specimens, there is intentionally made a roughly 1 mm gap between rail and top flange to ensure that the wheel load is going through the intermittent fillet weld without contact between rail and top flange. The gap has been done by placing a 1.2 mm wire between rail and top flange, then the rail pieces are tack welded, and finally, the 1.2 mm wire is removed before final welding. Gap measurement is ongoing in Figure 23, and finished A3 rail connection weld is shown in Figure 24. Note that intermittent weld total length is 60 mm. This length includes the starting and ending of the welding. Pure weld length is 50 mm with the desired a_w dimension.

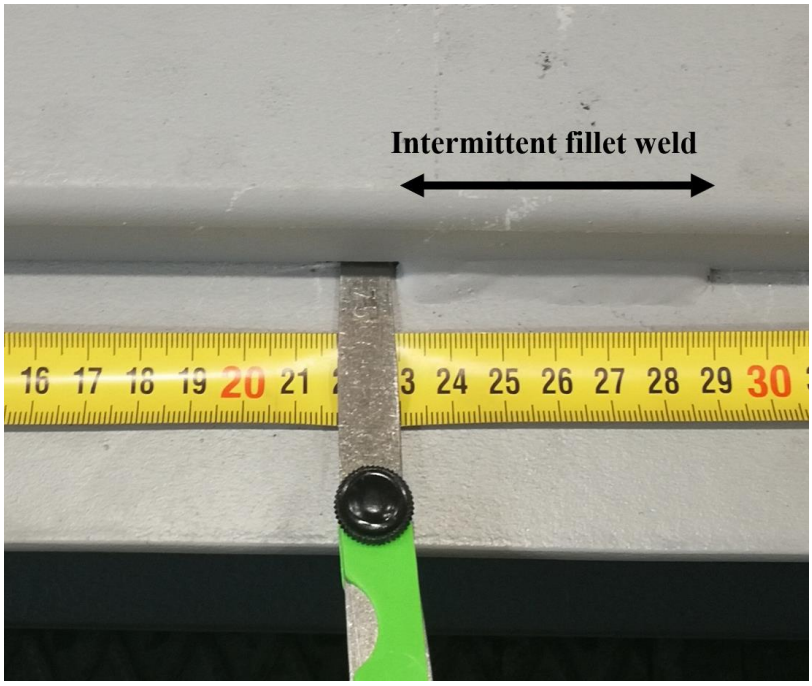

Figure 23. Gap measurements after welding.

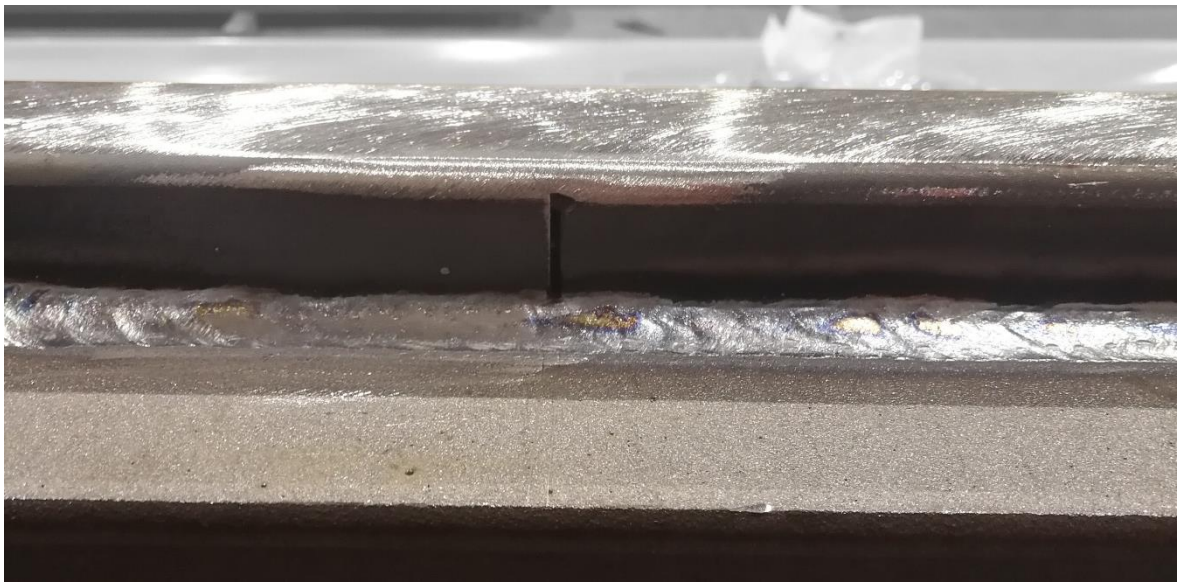

Figure 24. Test specimen after welding and grinding. Rail connection weld detail is A3.

Finally, test specimens are surface treated with workshop primer paint to avoid corrosion. The gap is measured from every test specimen where the gap has been made. Overall the visual inspection shows that the quality of welds is good. Macro pictures of the studied welds after welding are presented in Figure 25, Figure 26, Figure 27, and Figure 28.

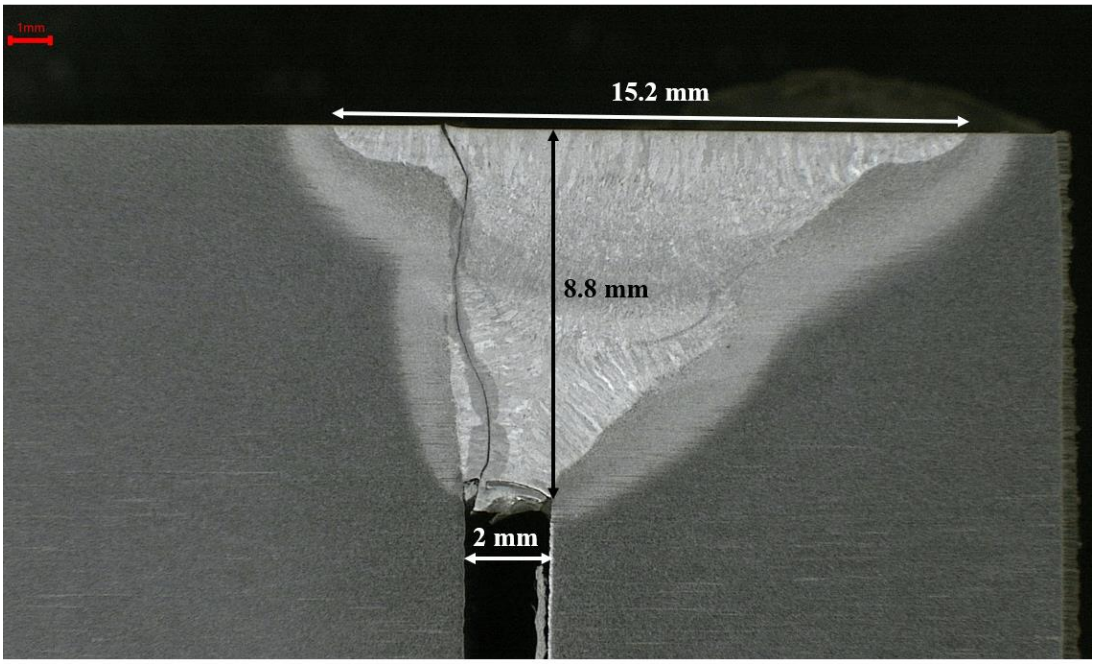

Figure 25. A3 rail connection weld after fatigue test.

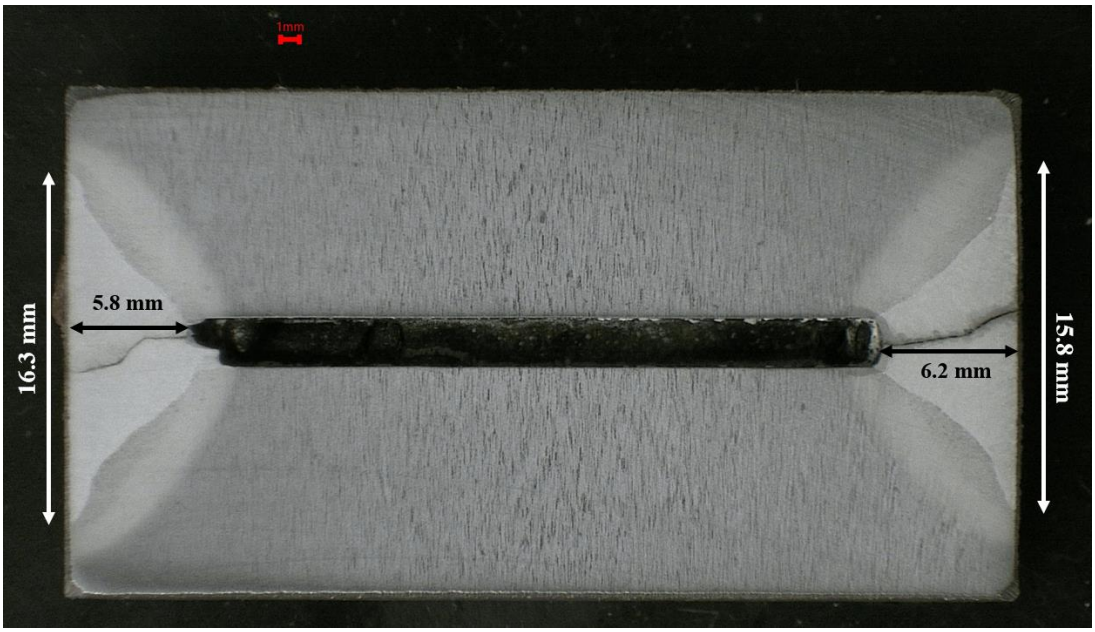

Figure 26. Vertical welds of the A2 rail connection weld after fatigue test.

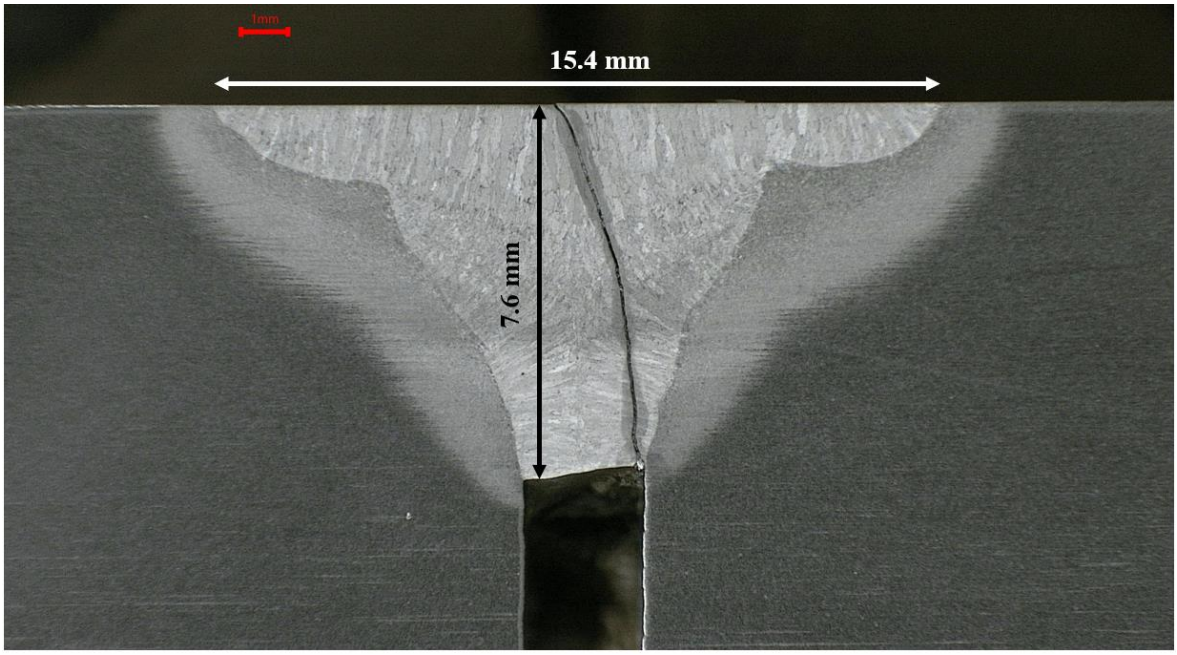

Figure 27. The horizontal weld of the A2 rail connection weld after fatigue test.

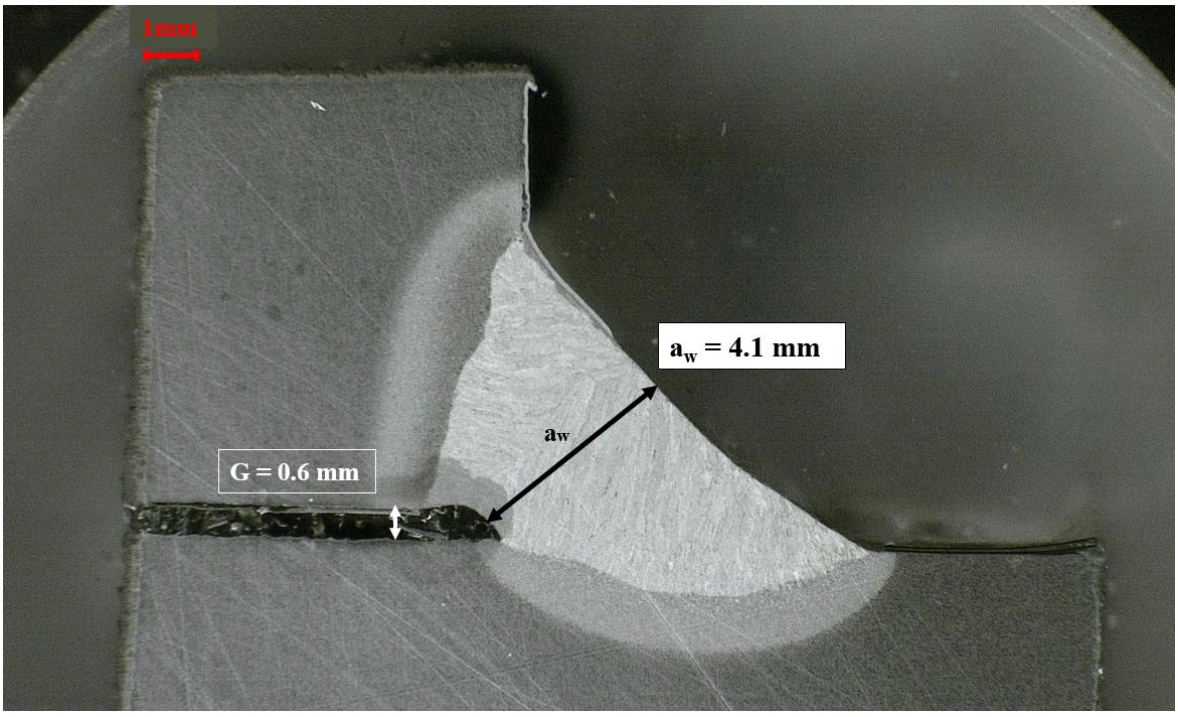

Figure 28. Intermittent fillet weld after 938 000 cycles. The gap is 0.6 mm between rail and the top flange.

The average intermittent fillet weld throat thickness a_w dimension is 4.5 mm based on the macroscopic investigation and measurements with fillet weld gauge. This a_w 4.5 mm value is used in the analytical calculations for the intermittent fillet weld.

3.2.2 Hardness measurements from the welds

Vickers HV5 hardness test method is used to determine the hardness in the studied welds. In the Vickers hardness test, hardness is determined by pressing a square-shaped regular diamond pyramid-shaped to the measuring point with a force *F*, as shown in Figure 29. The angle α between the sides of the pyramid is 136 º. In the HV5 measurement, the measurement is made with 5 kg weight. The tip of the pyramid needs to rest on the material for a fixed time. Finally, the machine measures the diagonals d_1 and d_2 of the depression and, based on that, calculates the Vickers hardness at the measuring point location. (EN6507-1, 2018, pp. 6-8)

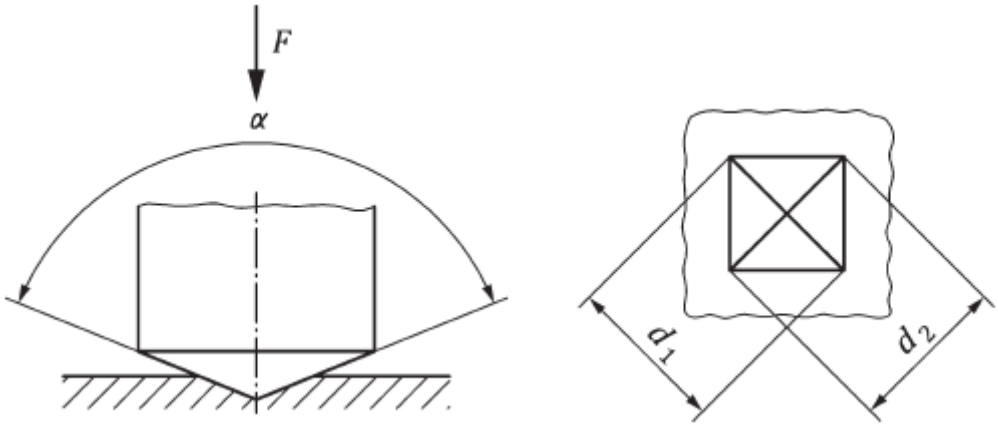

Figure 29. Principle picture of the Vickers hardness measurement (EN6507-1, 2018, p. 7).

" Testing should be carried out to ensure that the highest and the lowest level of hardness of both parent metal and weld metal is determined", (EN9015-1, 2011, p. 1). Two different rows of measurements were performed on each weld joint. The measured areas are the weld top area and the weld root. More than one measurement rows provide comprehensive data to determine the hardness of the weld joint.

Hardness test specimens from the weld area are mechanically cut, and the specimen surface has been carefully polished. Carefully done polishing prevents excess heat from being introduced into the specimen, which could affect hardness results and metallurgical properties in the studied area. Finally, the specimens are carefully cleaned to reveal grain boundaries in macro images. The hardness test is done at room temperature. Test results are presented in Figure 30 and Figure 31.

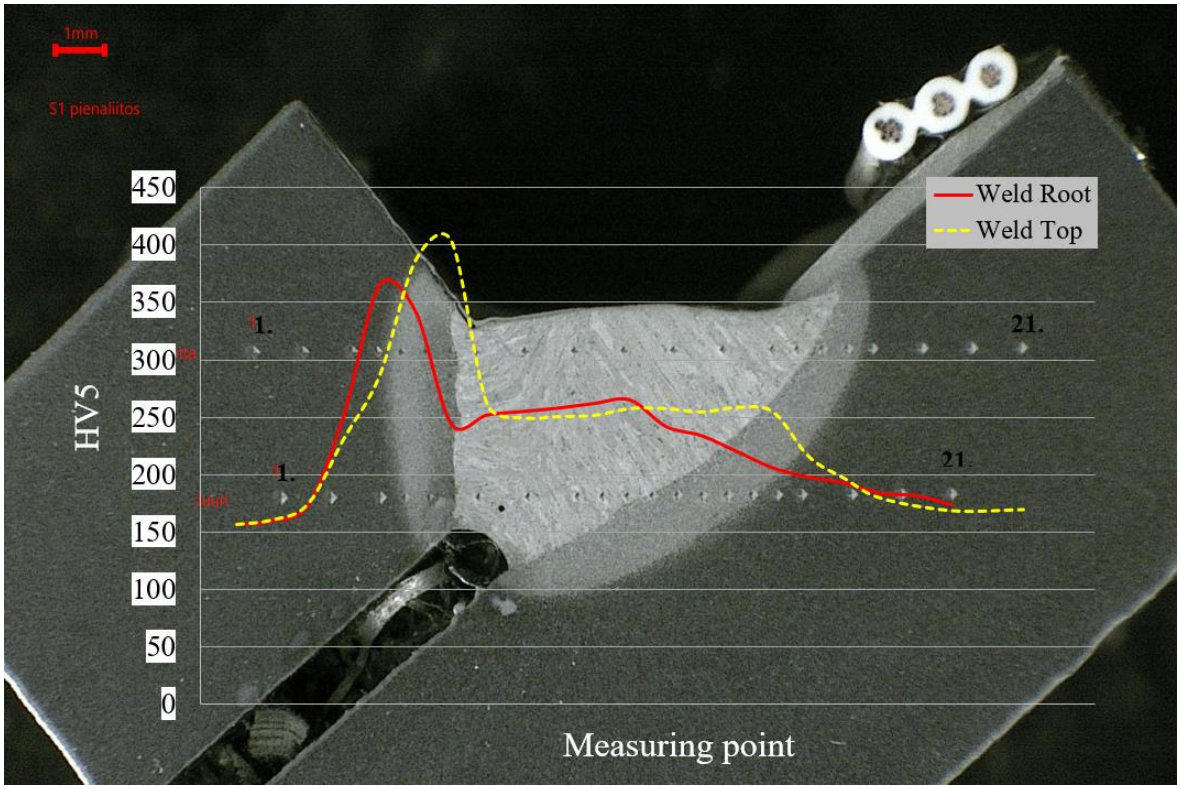

Figure 30. Intermittent fillet weld hardness profile at the weld root and the top of the weld (HV5).

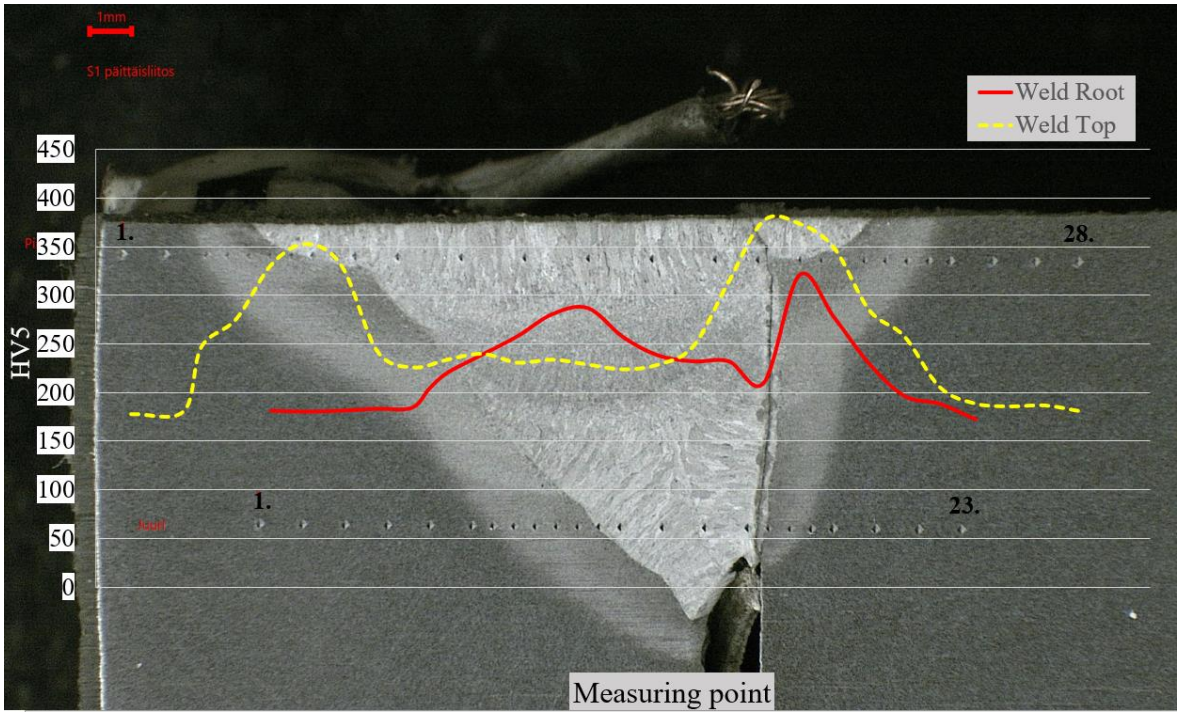

Figure 31. Top welded rail connection weld (A3) hardness profile at the weld root and the top of the weld (HV5).

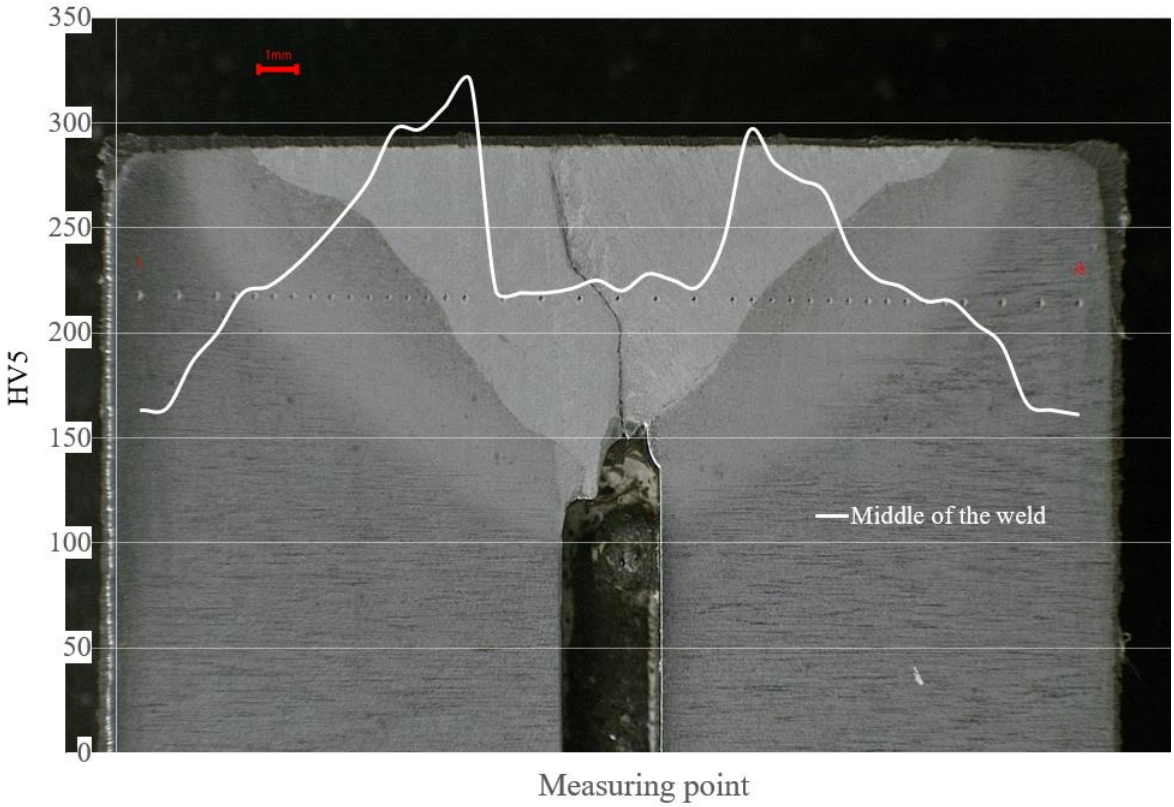

Figure 32. Vertical weld hardness profile (HV5) of the three-side welded rail connection weld (A2). The measurement is done in the middle of the weld.

Exact measuring points location and hardness value are presented in Appendix XV.

3.3 Residual stress X-ray measurements of the rail connection welds

The rail connection weld is measured by the X-ray method to obtain an understanding of the residual stress level in the weld after welding (Figure 33). Measurement is conducted only in the longitudinal direction of the test specimen, not in the perpendicular direction (Figure 33). The measured test specimen is in the welded stage, and it has not been ground before the first measurements.

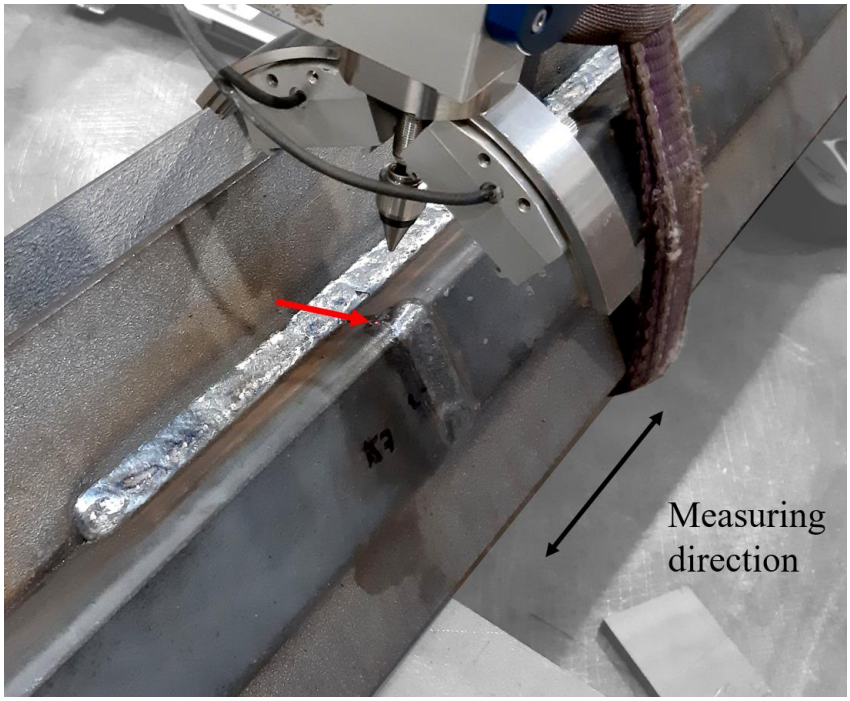

Figure 33. X-ray measurement. The test specimen is measured as-welded stage. The red arrow indicates a measuring point location in the weld root side.

The test specimen is also measured after grinding to see how the grinding effects residual stress level, Figure 34. Rounding of the rail profile is not ground, only top of the rail. In doing so, it allows to find out potential changes of residual stresses due to grinding in the weld root side. X-ray diffraction measures the residual stress on the surface, not through the material. If the ground surface is measured, it does not tell the actual residual stress in the weld, only the outer layer situation. The goal is to estimate the residual stresses in the weld root side because the exact value cannot be measured by X-ray in the studied cases.

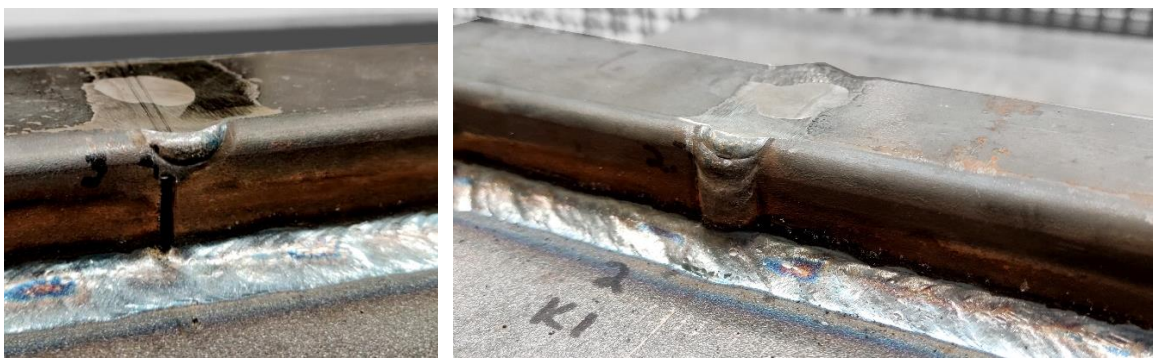

Figure 34. Rail connection welds for residual stress measurements after grinding. Left A3 and right A2 weld detail.

3.3.1 Residual stress measurements results

Residual stress measurements have been taken on both rail connection welds, and two welds of each weld detail A2 and A3 are measured. Every test point is measured twice to double-check that measurements are reliable. Figure 35 shows the primary principal picture of the locations of the measuring points.

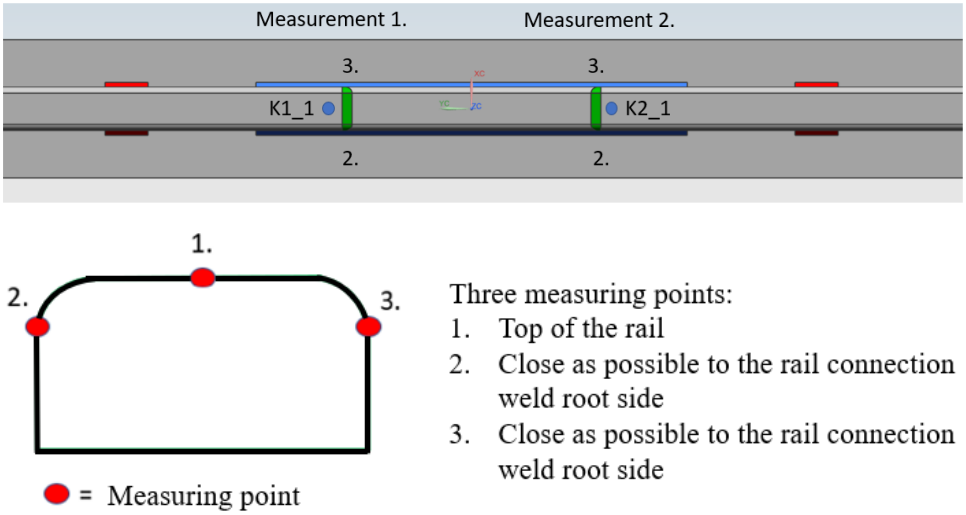

Figure 35. Residual stress point locations of the X-ray measurement.

Measurement points are close to the weld toe, and it has been taken on the outer side of the rail connection welds. In addition to that, residual stresses are measured from the top of the actual weld. This measurement is marked in Figure 36 by W marking, and measuring point locations are shown in Figure 35. All the X-ray measurement results are presented in Figure 36 and Figure 38.

Before grinding		Measurement 1			**Before grinding**		Measurement 2		
Measuring point	Stress MPa	Variation (+/-) MPa	FHMA deg	Variation (+/-)	Measuring point	Stress MPa	Variation (+/-) MPa	FHMA deg	Variation (+/-)
K1_1	-311	29	2.5	0.06	K1_1	-309	31	2.5	0.07
K1_2	-320	74	2.6	0.06	K1_2	-333	77	2.6	0.06
K1_3	-107	75	2.5	0.06	K1_3	-101	75	2.5	0.05
K2_1	-435	37	3.0	0.05	K2_1	-446	28	3.0	0.05
K2_2	-332	14	2.4	0.04	K2_2	-325	13	2.4	0.04
K2_3	-117	33	2.1	0.03	K2_3	-131	30	2.1	0.03
K1_W	-327	19	2.3	0.03	K1_W	-327	19	2.3	0.03
K2_W	-401	55	2.4	0.03	K2_W	-382	4	2.4	0.05

After grinding		Measurement 1			**After grinding**		Measurement 2		
Measuring point	Stress MPa	Variation (+/-) MPa	FHMA deg	Variation (+/-)	Measuring point	Stress MPa	Variation (+/-) MPa	FHMA deg	Variation (+/-)
K1_1	-158.8	42	2.5	0.02	K1_1	-162	40	2.2	0.02
K1_2	-236	136	2.6	0.10	K1_2	-255	127	2.6	0.10
K1_3	-221	78	2.5	0.06	K1_3	-230	91	2.5	0.07
K2_1	-159	42	3.0	0.04	K2_1	-162	42	2.5	0.04
K2_2	-260	26	2.4	0.10	K2_2	-257	25	2.4	0.09
K2_3	-156	10	2.1	0.04	K2_3	-162	15	2.1	0.03
K1_W	-226	28	2.3	0.03	K1_W	-222	24	2.6	0.03
K2_W	-201	10	2.4	0.04	K2_W	-196	12	2.8	0.04

Figure 36. Residual stress measurements result before and after grinding of top welded rail connection weld (A3) detail.

Figure 37 summarizes the residual stress measurements by using the mean results of the measuring point location in the top welded rail connection weld. There are comparison curves before and after grinding.

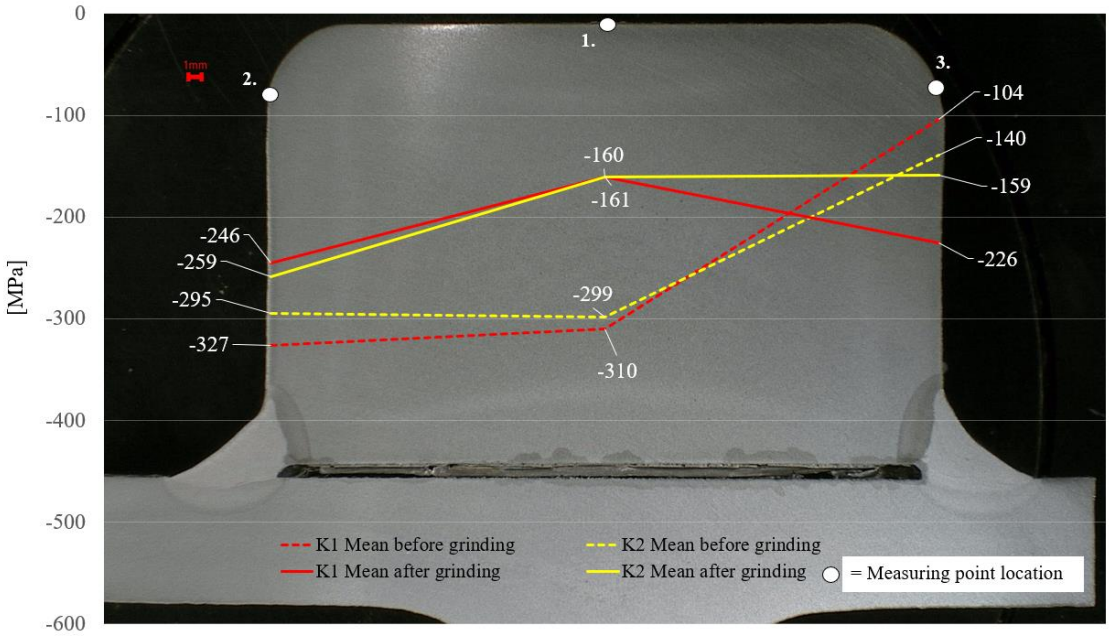

Figure 37. Residual stress measurements mean values after and before grinding of top welded rail connection weld (A3). The direction of measurement is longitudinal to the load-carrying beam.

Figure 38 and Figure 39 shows the three-side welded rail connection weld residual stress measurement results.

Before grinding		Measurement 1			**Before grinding**		Measurement 2		
Measuring point	Stress MPa	Variation (+/-) MPa	FHMA deg	Variation (+/-)	Measuring point	Stress MPa	Variation (+/-) MPa	FHMA deg	Variation (+/-)
K1_1	-382	8	3.1	0.03	K1_1	-373	8	3.1	0.03
K1_2	-243	88	2.4	0.14	K1_2	-260	82	2.4	0.11
K1_3	-164	57	2.1	0.03	K1_3	-161	58	2.1	0.03
K2_1	-476	11	3.3	0.04	K2_1	-471	10	3.3	0.04
K2_2	-193	14	2.3	0.05	K2_2	-188	15	2.3	0.05
K2_3	-369	35	2.5	0.06	K2_3	-368	34	2.5	0.07
K1_W	-197	32	2.3	0.03	K1_H	-188	32	2.3	0.04
K2_W	-169	37	2.2	0.05	K2_H	-177	36	2.2	0.04
After grinding		Measurement 1			**After grinding**		Measurement 2		
Measuring point	Stress MPa	Variation (+/-) MPa	FHMA deg	Variation (+/-)	Measuring point	Stress MPa	Variation (+/-) MPa	FHMA deg	Variation (+/-)
K1_1	68	25	2.5	0.02	K1_1	56	23	2.5	0.02
K1_2	-183	41	2.6	0.13	K1_2	-182	47	2.6	0.13
K1_3	-100	36	2.2	0.09	K1_3	-113	26	2.1	0.07
K2_1	295	19	2.4	0.02	K2_1	295	19	2.4	0.02
K2_2	-264	63	2.3	0.08	K2_2	-254	61	2.3	0.08
K2_3	-365	21	2.6	0.04	K2_3	-361	16	2.6	0.02
K1_W	93	13	2.7	0.01	K1_W	94	15	2.7	0.01
K2_W	238	26	2.6	0.01	K2_W	238	24	2.6	0.02

Figure 38. Residual stress measurements result before and after grinding of the three-side welded rail connection weld (A2) detail.

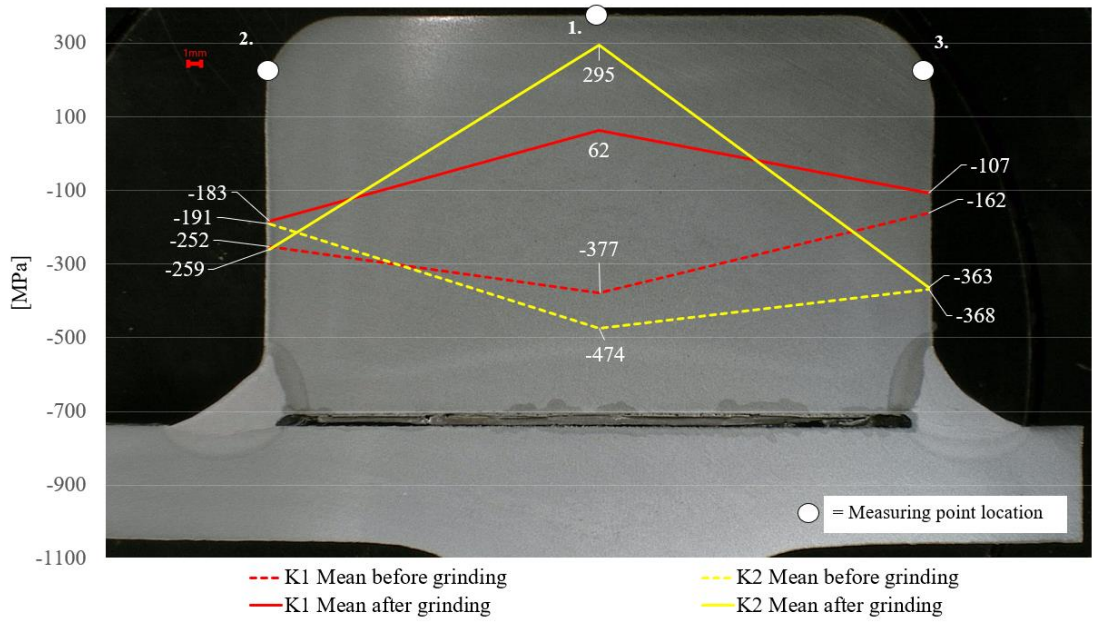

Figure 39. Residual stress measurements mean values after and before grinding of the three-side welded rail connection weld (A2). The direction of measurement is longitudinal to the load-carrying beam.

3.4 Laboratory testing and test set up

Studied welds are tested in the laboratory of Steel Structures at LUT University. The test setup is built in a way that testing time for every test specimen is reasonable, and rail connection welds and intermittent fillet welds can be tested at the same time. Permanent four-point bending is used (Figure 40) to achieve desired aspects in the testing. The test set up main dimensions are presented in appendix I. Testing is done at room temperature.

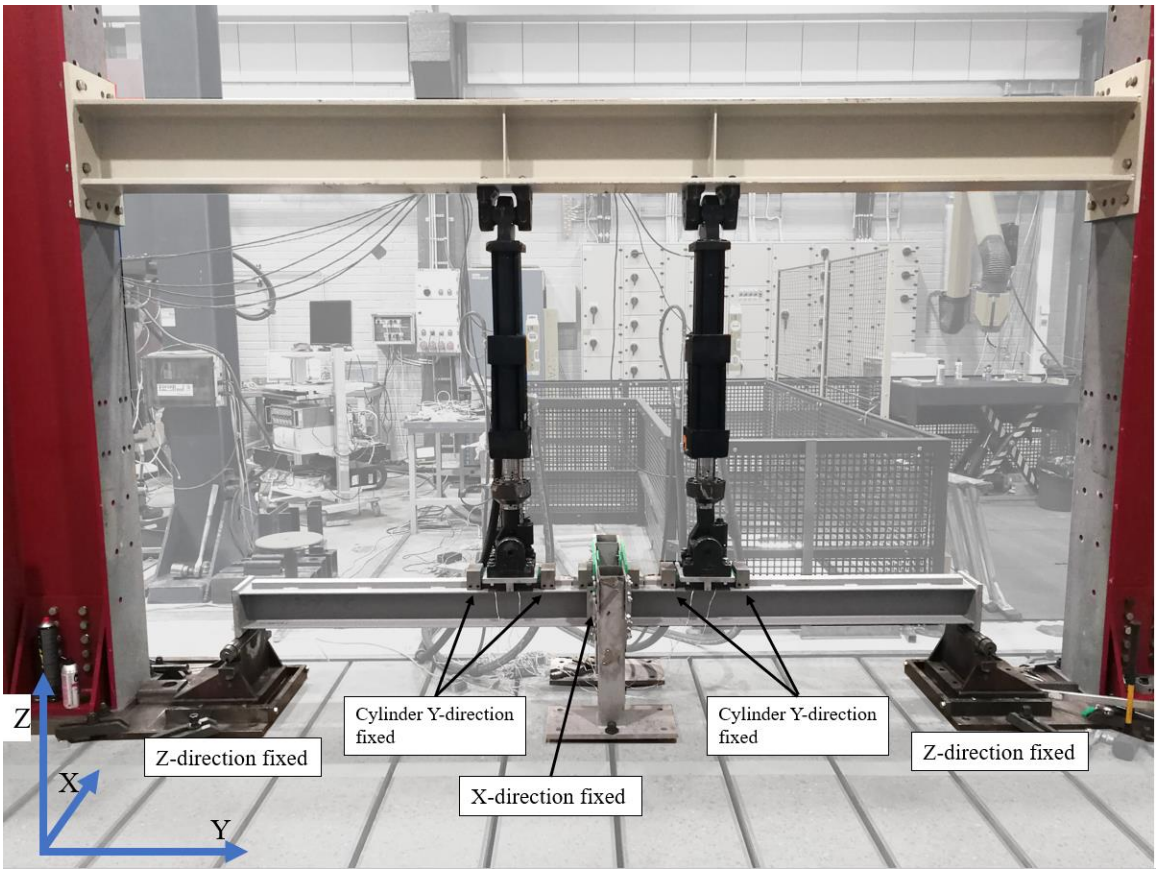

Figure 40. The test set up at LUT University.

Test specimens are scaled-down compared to typical runway application to increase the stress level in the rail connection weld and thus decrease testing time. The used rail profile size is 30 x 50 (mm), which is common in many runway applications, but the load-carrying beam usually is bigger than used in testing. In this test, the load-carrying beam is HEA160. It is usually used, for example, the HEA340 beam under the test loads in crane's runway. HEA160 is used for smaller capacity cranes. HEA refers to a European lightweight wide flange beam. HEA160 and HEA340 dimensions and material certificates are presented in Appendix XII and XIII. Both materials, HEA160, and rail are made from S355J2. Cylinders

are force-controlled, one cylinder is master, and the second is a slave. Most of the test specimens are tested by 66 kN/cylinder force. Other applied forces are 60 kN/cylinder and 75 kN/cylinder.

Studied rail connection welds are located between the two cylinders, where the bending moment of the beam is constant. That is why the nominal stress is the same for both rail connection welds, and it is possible to test two rail connection welds at the same time in one test specimen. In this situation, shear stress of the beam is zero between the cylinders. Test specimen welds are designed in a way that intermittent fillet welds are under the cylinders' wheel contact. In that case, the wheel load goes through the intermittent fillet weld. The situation is the same as in Figure 20, but the contact width is 30 mm instead of 12 mm.

In this research, the traveling wheel load is not used for the intermittent fillet welds and rail connection welds. Traveling wheel load will cause shear stress change in the weld. Now, this is not to be tested, and shear stress is close to zero in the wheel contact area. It is assumed that the interaction equation (1) between nominal and shear stress is working as is presented in the EN1993-1-9 standard.

The interaction equation (1) considers the effect of the shear stresses on the fatigue capacity of the joint separately, and that is why the shear stress change is not to be tested by a traveling wheel. It is assumed that shear stress design details in the Eurocode 3 are valid in these studied situations. This decision also reduces testing time and costs, and test results are more comfortable to analyse, and results are reliable when the loading is uniaxial.

Figure 41 shows all the supporting structures that keep the test specimen and cylinders are in the right place during testing. Between metal parts, there are oiled plastic plates to minimize friction. In Figure 40, two mounting parts that are under test specimen end plates can rotate and move freely on the floor. These arrangements allow the test specimen to behave as it should be in the four-point bending. Strain gauges are utilized in the test specimens, and those values take into account the friction between the moving parts.

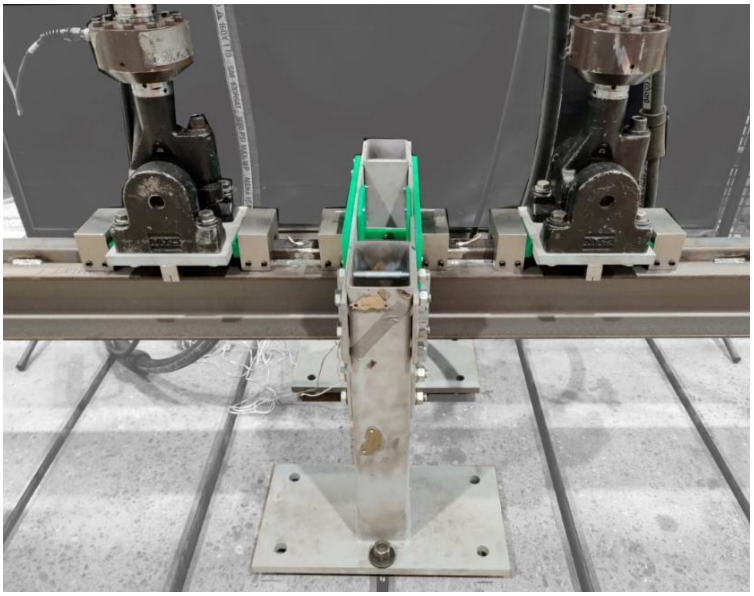

Figure 41. Supporting parts to keep the cylinders and test specimen is in place during the testing.

Figure 42. The test set up and test specimens at LUT University.

3.5 Test parameters

Test specimens are tested by three different loading levels. Most of the test results are tested with 66 kN/cylinder force, and the second loading case is 75 kN/cylinder also, test specimens

are tested by 60 kN/cylinder force. These values are used because they are common maximum values for the wheel loads that are accepted in the industrial crane's runway applications. Therefore, the intermittent fillet welds are tested close to actual loadings. Different load cases also obtain test results from different nominal stress ranges and give additional reliability to the final FAT_c value, which is derived from the fatigue test results. In the test, the applied stress level is higher than it is generally accepted in the runway load-carrying beams in order to reduce the testing time.

In Figure 18, weld shapes of the studied rail connection welds were presented. FAT56 (A3) is the main tested rail connection weld. The target is to get 16 test points for the FAT56 rail connection weld. This number of test points enables to do regression analysis for the test results. FAT71 (A2) rail connection weld is tested to get 10 test points. The goal is to determine if the test results are in line with the EN13001-3-1 design rule. Intermittent fillet welds are tested at the same time when testing rail connection welds and test results are reported. The run-out limit for the studied welds is set in this study to be 500 000 cycles. Some welds, especially intermittent fillet weld, were tested longer. Failure in the studied welds had happened when the crack was propagated through the weld ligament. In order to estimate the time of the failure in the specific number of the cycles, strain gauges in the studied welds and laboratory staff observations are used. Laboratory staff observations are needed because the fatigue crack may grow through the stain gauge before the final fracture happens in the rail connection weld.

3.5.1 Nominal stress in the testing and calculations

In the testing, there were used strain gauges in different locations to determine the failure stage of the studied welds, to ensure that loading is correct for every test specimen and to calibrate the FE-model. There were strain gauges in 12 different locations on the test specimen. A minimum number of strain gauges is three in one test specimen. Based on the strain gauge values, there is under 5% difference between finite element (FE) model results. All the strain gauge locations are shown in Figure 45.

The used nominal stress is verified in the testing. Strain gauge values are measured in the fatigue testing and then compared to the FE-model values. Strain gauges were used in different areas of the test specimen to calibrate the FE-model. Strain gauge locations are

shown in Figure 45. Results show that the FE-model is similar to the testing situation, and strain gauges give the same values as the FE-model. Constraints are the same in the FE-model as in the testing, loading is located at the same position and the wheel contact width. In the FE-model constraints are modeled middle of the test specimen assembly groove. FE-model consists of 3D ten nodes tetra elements, and mesh size is increased in the studied areas to give accurate values. The used material properties are Poisson's ratio ν = 0.3 and Young's modulus E = 207 GPa. An exampling picture of the test specimen FE-model is presented in Figure 43.

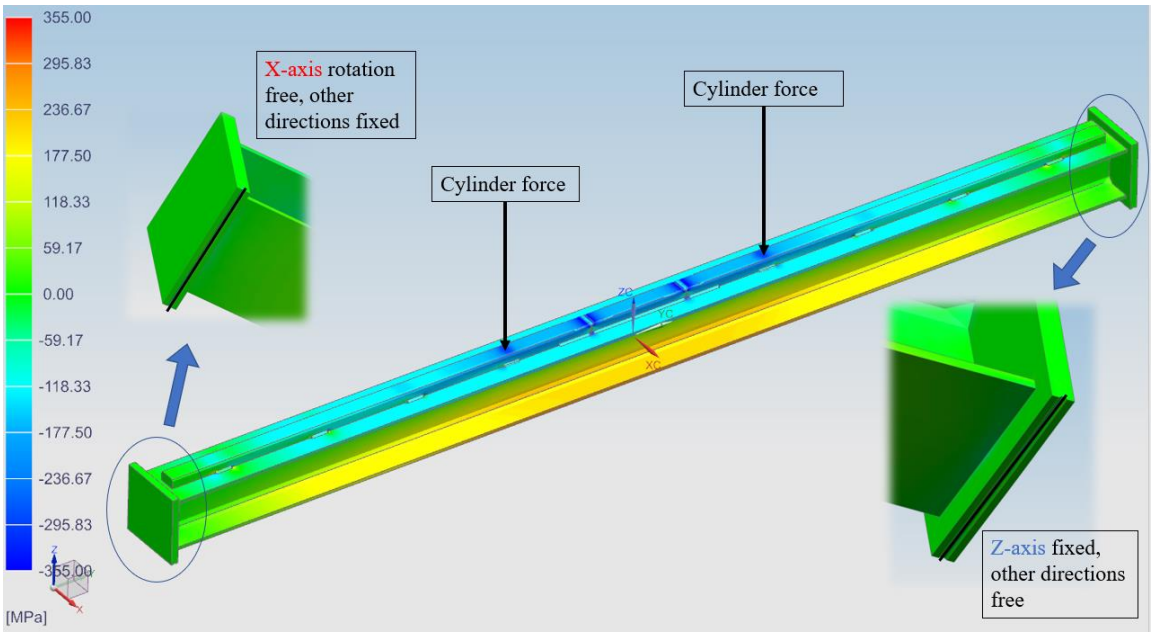

Figure 43. Test specimen FE-model. The used load in the picture is 66 kN/cylinder.

Rail connection weld A3 nominal stress is calculated by using the FE-model. The total sum of the forces in the nominal direction that is going through the weld is used. Finally, that value is divided by the cross-section of the weld (equation 18).

$$\sigma_{\text{top welded rail connection weld}} = \frac{\text{SUM(Fnominal)}}{9\ \text{mm} \cdot 50\ \text{mm}} \tag{18}$$

Illustration picture of how the glue forces are read is shown in Figure 44.

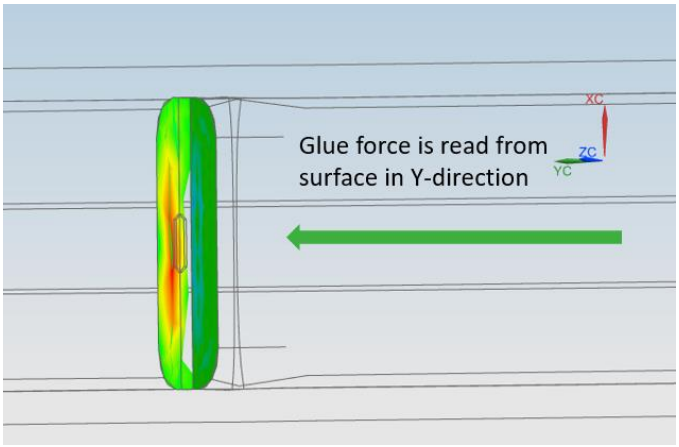

Figure 44. The glue force sum is determined from FE-model.

The affecting nominal stresses in the test are presented in Table 3. Most of the intermittent fillet welds a_w throat thicknesses are approximately 4.5 mm, and that value is used in the calculations. The value is derived from the visual inspection after welding and measuring test specimens.

In Figure 45, the numbered circles show the different areas where the nominal stress is read. Those values are presented in Table 3, and the presented nominal stress values are taken from the calibrated FE-model. Red circles indicate the strain gauge locations in the test specimen.

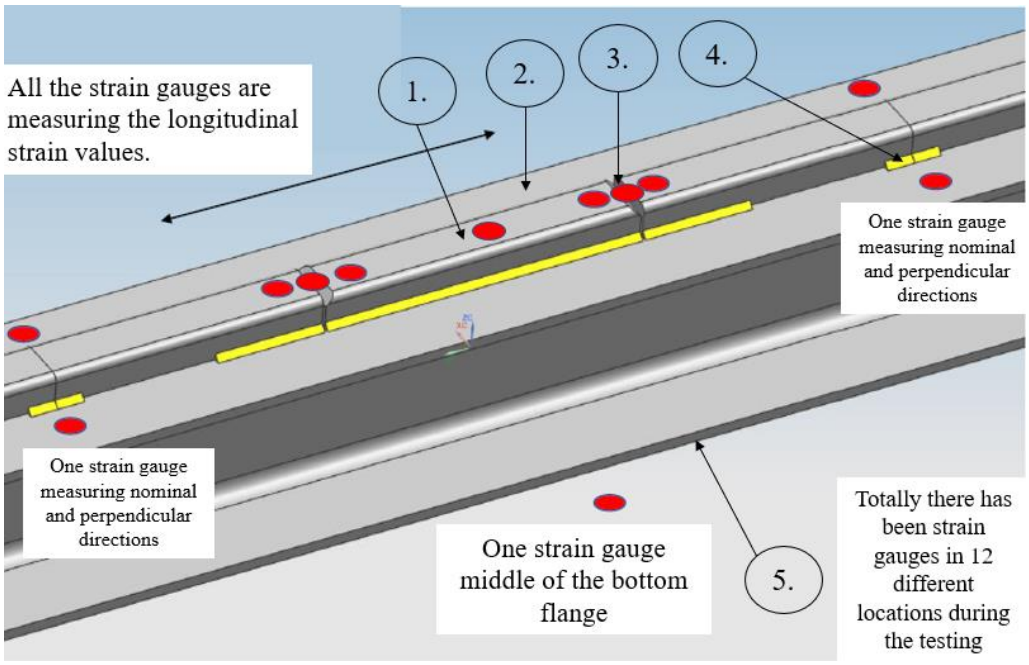

Figure 45. Strain gauge locations in the fatigue testing and nominal stress areas that are used in the calculations.

Table 3. Nominal stress levels when testing rail connection welds with different load cases. The circled number indicates the studied area location in Figure 45.

Loading case	Nominal stress in the area [MPa] based on the calibrated FE-model					
	Bottom flange ⑤	Top flange ②	Top of the rail connection part, ①	Top welded rail connection weld (A3) ③	Intermittent fillet weld when the gap is 1mm and a_w = 4 mm ④	Intermittent fillet weld when the gap is 1mm and a_w = 4.5mm ④
Cylinder force 60kN/unit	257	-139	-220	-380	-150	-133
Cylinder force 66kN/unit	283	-153	-242	-418	-165	-147
Cylinder force 75 kN/unit	322	-174	-275	-474	-188	-167

The nominal stress of rail connection weld is later used when the test results are scaled to the bigger load-carrying beams.

3.6 Verification of the fatigue testing system and smaller test specimens compared to the average size of the load-carrying beam

HEA340 beam is typically used in the crane's runway applications. In the fatigue testing rail connection, welds FAT class is tested with the HEA160 beam. Because there is a definite size difference in the load-carrying beam size, it will affect to the residual stresses in the weld (Figure 46). As presented previously in the theory part, residual stresses have a role in weld fatigue strength. That is why the HEA340 beam is welded with a 30 x 50 (mm) rail. Both materials are S355, and the same welding procedure is used than welding test specimens for fatigue testing. Residual stresses are measured in two different stages to see the difference in the residual stresses during and after welding and compared to HEA160 beam:

1. Residual stresses are measured before welding 500 mm assembly fillet welds
2. Residual stresses are measured as-welded stage after the 500 mm assembly fillet welds are welded

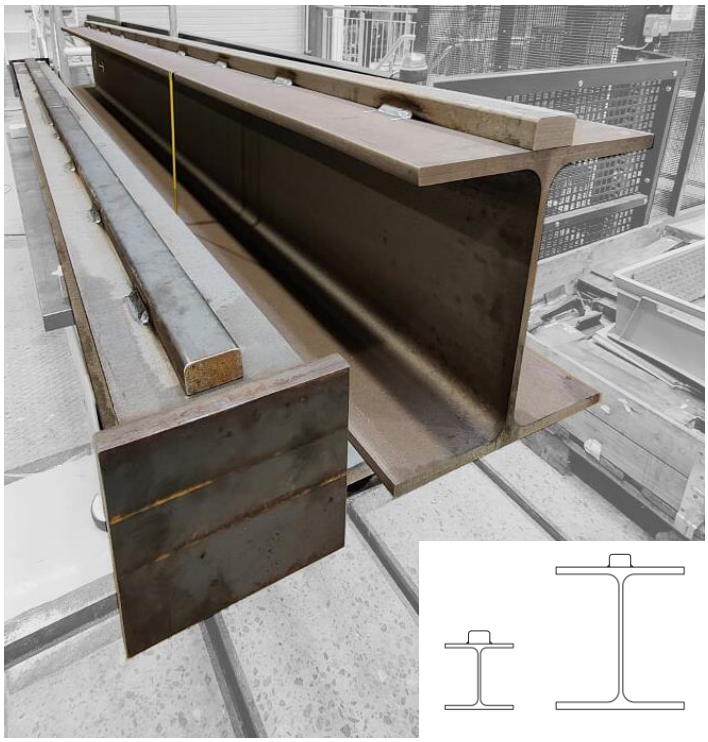

Figure 46. HEA160 with rail compared to HEA340 with rail fatigue test specimen.

Shield gas flow rate was 15 l/min, and the used shield gas is Mison 8, which includes Ar + 8% CO_2 + 0.03% NO. The used welding process is (MAG) 135, and filler material was 1.2 mm ESAB OK AristoRod 12.50 metal wire. Used welding parameters are presented in Table 4. Welding order is the same as fatigue test specimens, and the next welding pass in the rail connection weld is welded when the interpass temperature is under 150 °C. Welding is performed at room temperature.

Table 4. Welding parameters when welding the HEA340 test specimen.

	A3 top	Intermittent fillet welds	500 mm assembly fillet welds
I [A]	270 - 290	280 - 300	280 - 300
U [V]	26.6	27.9	27.9
Wire feed [m/min]	8.0	8.8	8.8

Intermittent fillet welds a_w throat thickness is 5.0 mm average, and the 500 mm assembly fillet welds a_w values are between 5.0-5.5 mm. Visual inspection shows that welds' quality is excellent. HEA340 test specimen after welding is shown in Figure 47.

Figure 47. HEA340 and top welded rail connection weld (A3) after welding and intermittent fillet weld.

3.6.1 HEA340 load-carrying beam measured residual stresses

The residual stress measurement results of HEA340 test specimen top welded rail connection weld (A3) are shown in Figure 48 and Figure 49.

Before 500 mm fillet welds		Measurement 1			**Before 500 mm fillet welds**		Measurement 2		
Measuring point	Stress MPa	Variation (+/-) MPa	FHMA deg	Variation (+/-)	Measuring point	Stress MPa	Variation (+/-) MPa	FHMA deg	Variation (+/-)
K1_1	161	22	2.6	0.02	K1_1	160	23	2.6	0.02
K1_2	-54	29	2.1	0.02	K1_2	-49	31	2.1	0.02
K1_3	38	12	2.3	0.04	K1_3	24	12	2.3	0.04
K2_1	175	11	2.0	0.03	K2_1	180	14	2.0	0.02
K2_2	19	28	2.1	0.02	K2_2	7	25	2.1	0.02
K2_3	5	15	2.3	0.05	K2_3	5	8	2.3	0.05
K1_W	196	37	1.7	0.05	K1_W	191	26	1.7	0.05
K2_W	173	33	1.8	0.03	K2_W	184	31	1.8	0.04
After welding 500 mm fillet welds		Measurement 1			**After welding 500 mm fillet welds**		Measurement 2		
Measuring point	Stress MPa	Variation (+/-) MPa	FHMA deg	Variation (+/-)	Measuring point	Stress MPa	Variation (+/-) MPa	FHMA deg	Variation (+/-)
K1_1	82	27	2.2	0.04	K1_1	83	29	2.2	0.03
K1_2	64	40	2.1	0.05	K1_2	70	38	2.1	0.04
K1_3	-160	31	2.4	0.04	K1_3	-158	33	2.3	0.04
K2_1	153	43	2.1	0.04	K2_1	151	41	2.1	0.04
K2_2	-5	77	2.2	0.04	K2_2	-20	78	2.2	0.04
K2_3	-3	36	2.1	0.04	K2_3	-6	29	2.2	0.04
K1_W	209	67	1.9	0.06	K1_W	217	64	1.8	0.07
K2_W	205	74	1.7	0.06	K2_W	213	73	1.7	0.07

Figure 48. Residual stress measurements result before and after welding 500 mm assembly fillet welds in the top welded rail connection weld of the HEA340 test specimen.

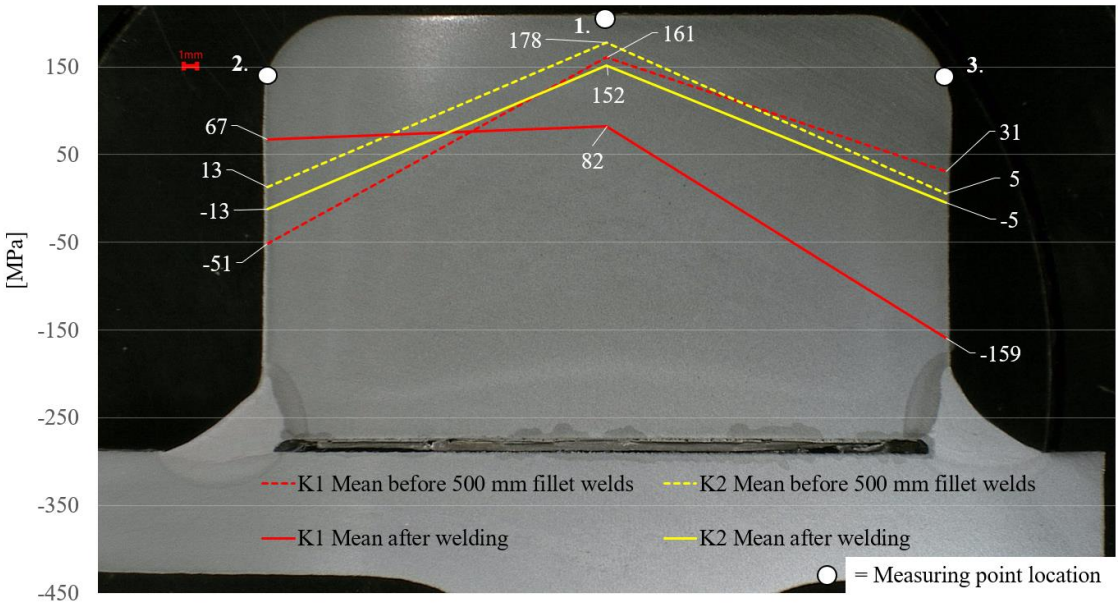

Figure 49. Residual stress measurements mean values before and after welding 500 mm assembly fillet welds in the top welded rail connection weld of the HEA340 test specimen. The direction of measurement is longitudinal to the load-carrying beam.

4 RESULTS

4.1 Analytical fatigue strength assessment results

4.1.1 Nominal stress method

The nominal stress method is utilized to determine the fatigue strength with equation 2. Table 5 summarizes the results with different load cases. There are characteristics and mean fatigue life estimations for each studied case. The used nominal stresses of the top flange are based on the calibrated FE-model. Intermittent fillet weld nominal stress has been obtained by using 4.5 mm throat thickness and 50 mm weld length for the load-carrying cross-section of the weld. The FAT_c values are taken from the EN13001-3-1 and the EN1993-1-9 standards. FAT_m value has been obtained by multiplying the FAT_c value with a 1.37 factor. There are presented FAT classes with and without the special conditions for the rail connection welds in Table 5.

Table 5. Fatigue life estimations of nominal stress method under testing loadings, (xx=FAT class without special conditions // yy= FAT class when special conditions are applied).

Studied area	$\Delta\sigma$ [MPa]	FAT_c [MPa]	N_{fc} [cycles]	FAT_m [MPa]	$N_{fc,mean}$ [cycles]
Intermittent fillet weld, a_w = 4.5 mm. (60kN/cylinder loading)	weld 133	36	39 663	49	100 015
Intermittent fillet weld, a_w = 4.5 mm. (66kN/cylinder loading)	weld 147	36	29 376	49	74 074
Intermittent fillet weld, a_w = 4.5 mm. (75kN/cylinder loading)	weld 167	36	20 035	49	50 521
Intermittent fillet weld, (a_w = 4.5 mm). (60kN/cylinder loading)	weld 133	45	77 466	61	192 959

Table 5. Fatigue life estimations of nominal stress method under testing loadings, (xx=FAT class without special conditions // yy= FAT class when special conditions are applied).

Studied area	$\Delta\sigma$ [MPa]	FAT_c [MPa]	N_{fc} [cycles]	FAT_m [MPa]	$N_{fc,mean}$ [cycles]
Intermittent fillet weld, a_w = 4.5 mm. (66kN/cylinder loading)	weld 147	45	57 374	61	142 912
Intermittent fillet weld, a_w = 4.5 mm. (75kN/cylinder loading)	weld 167	45	39 131	61	97 470
Rail connection weld, A3. Based on the EN13001-3-1 standard (60kN/cylinder loading)	top flange 139	56 // 63	130 783 // 186 212	77 // 86	339 983 // 474 676
Rail connection weld, A3. Based on the EN13001-3-1 standard (66kN/cylinder loading)	top flange 153	56 // 63	98 066 // 139 630	77 // 86	254 934 // 355 182
Rail connection weld, A3. Based on the EN13001-3-1 standard (75kN/cylinder loading)	top flange 174	56 // 63	66 672 // 94 930	77 // 86	173 322 & 241 478
Rail connection weld, A2. Based on the EN13001-3-1 standard (60kN/cylinder loading)	top flange 139	71 // 80	266 539 // 381 290	97 // 110	679 674 // 991 205
Rail connection weld, A2. Based on the EN13001-3-1 standard (75kN/cylinder loading)	top flange 174	71 // 80	135 881 // 194 380	97 // 110	346 495 // 505 313

4.1.2 Effective notch stress

FE-model is used to determine the ENS factors. In the model, one megapascal load is applied in the rail. After analyzing the FE-model, the max principal stress is read from the weld root side. The calculated nominal stress in different loading conditions is then multiplied by this factor to get effective notch stress value in the weld root side.

The FE-model is made based on the IIW recommendations. A 1 mm radius circle is applied to the weld root side and then a 2 mm radius circle around that to help get needed size elements around the rounding. In the FE-model, it is used 0.05 mm element size, and the size is also determined to the radius edge. The used element is an eight-node 2D plane stress element. Used material properties are Poisson's ratio $\nu = 0.3$ and young's modulus $E = 207$ GPa. The same modeling practices and material properties are used in every FE-model. One example FE-model is shown in Figure 50.

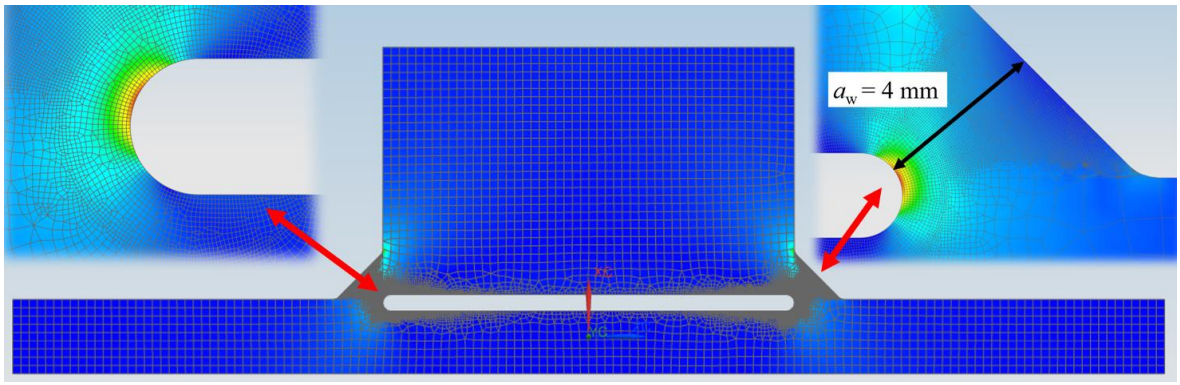

Figure 50. Used FE-model to determine the ENS factor for the intermittent fillet weld.

ENS fatigue life estimations are presented in Table 6. The same 1.37 factor can be used in the ENS calculations to have FAT_m mean values that have a 50% survival probability.

Table 6. ENS-calculation method fatigue life estimations. Table 3 nominal stress values are utilized. A3 rail connection weld dimensions are shown in Figure 18.

Studied area	$\Delta\sigma_{ENS}$ [MPa], $ENS_{factor} \cdot \Delta\sigma = \Delta\sigma_{ENS}$	FAT [MPa]	N_{fc} [cycles]	FAT_m [MPa]	$N_{fc,mean}$ [cycles]
Intermittent fillet weld, a_w = 4 mm. (60kN/cylinder)	4.23 · 150 = 635	225	88 973	308	228 224
Intermittent fillet weld, a_w = 4 mm. (66kN/cylinder)	4.23 · 165 = 698	225	66 990	308	171 837
Intermittent fillet weld, a_w = 4 mm. (75kN/cylinder)	4.23 · 188 = 795	225	45 339	308	116 300
Rail connection weld, A3. (60kN/cylinder)	4.28 · 380 = 1 626	225	5 299	308	13 593
Rail connection weld, A3. (66kN/cylinder)	4.28 · 418 = 1 789	225	3 979	308	10 206
Rail connection weld, A3. (75kN/cylinder)	4.28 · 474 = 2 029	225	2 727	308	6 996

ENS-method effective notch radius locations and values in the studied welds are presented in Appendix II.

4.1.3 Linear elastic fracture mechanics

Linear elastic fracture mechanics analysis is carried out Franc2D software for A3 rail connection weld and intermittent fillet weld. The used software is Franc2D version 4, and the actual 2D-model is done with CASCA pre-processor software. For the three-side welded rail connection, weld A2 Franc2D software is not suitable because the A2 weld detail cannot be studied within 2D dimensions.

Franc2D software is utilized to get fracture propagation time and to see if it is possible to get good results from this analysis method in these studied cases. Used values in the analysis are, $C = 3.00 \cdot 10^{-13}$ (units, Newton and millimetres) and $m = 3$. In the Franc2D, the crack increment is set to be 0.2 amount of crack growth at each step, J-integral is on, and intern theory SIG-THEFT max is on. The same parameters are used for the top-welded rail connection weld A3 and intermittent fillet weld, and the used analysis type is the plane strain method. In the calculation, the used reference loading is 100 MPa. For A3 rail connection weld, the used constraints are on the left side in XY, and Y direction is fixed, and the bottom-line Y direction is fixed. Intermittent fillet weld left side X-direction is fixed, and bottom Y-direction is fixed. In addition to that, the situation is calculated by using an analytical approach to confirm that K1 values are in line with Franc2D results (Appendix III). Franc2D models for the rail connection weld A3 and intermittent fillet weld are shown in Figure 51.

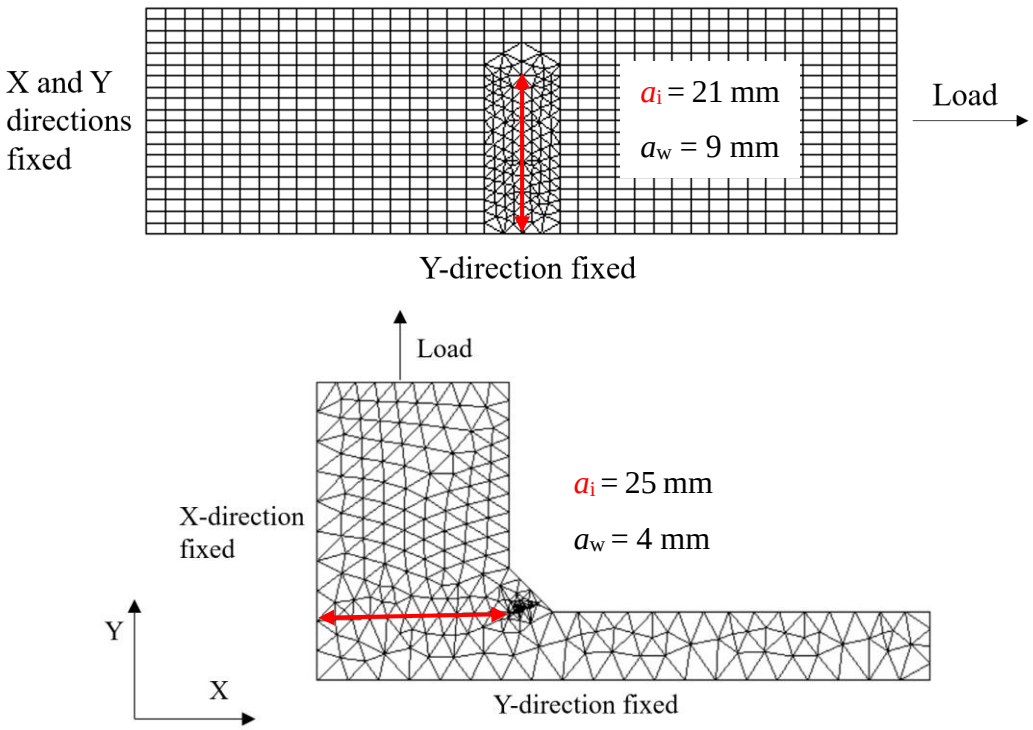

Figure 51. Franc2D cross-section models representing principles of A3 rail connection weld and intermittent fillet weld.

Crack propagation results from the Franc2D analysis are shown in Table 7. The FAT_m class is derived from equation 19, and the N_{fc} value is got from the Franc2D analysis:

$$FAT_m = \sqrt[m]{\frac{N_{fc}}{2 \cdot 10^6}} \cdot \Delta\sigma \quad (19)$$

Table 7. Franc2D linear elastic fracture mechanics method results.

Studied case	N_{fc} [Cycles]	FAT_c based on the result and $\Delta\sigma$ = 100 MPa
A3 rail connection weld	9 125	16
Intermittent weld	27 711	24

In Figure 52, indicates the strain value change in the weld during fatigue testing. Area (1) presents the crack initiation phase, and Area (2) is the crack propagation phase. Delta curve is the difference between max and min strain values of the strain gauge. The strain gauge is located top of the rail connection weld.

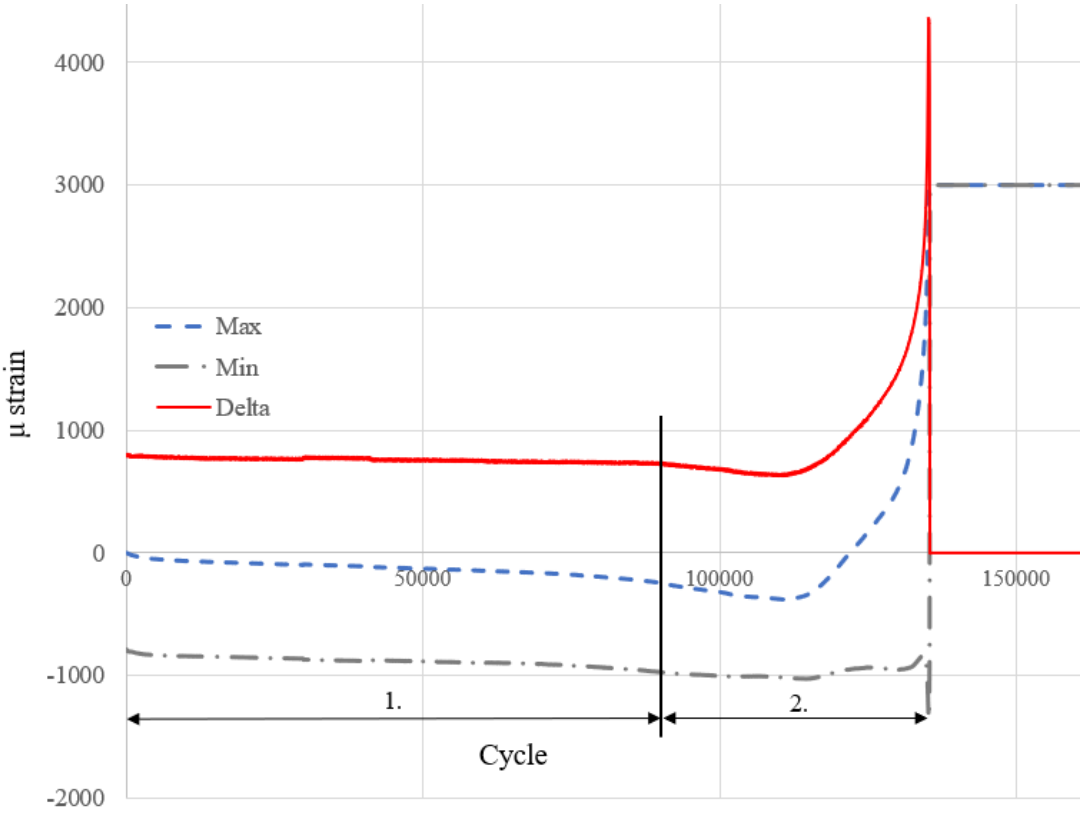

Figure 52. Strain gauge values at the top of the rail connection weld. The test specimen number is A3-9G, and the strain gauge number is 4.

4.1.4 4R method

Maximum points σ and ε are calculated by Ramberg-Osgood material behaviour in the first load cycle. In the plastic regime, local maximum stress is different and maximum stress can be obtained in that region by using Neuber's notch theory. σ_{res} sets the initial starting point in the Ramberg-Osgood material curve. (Björk, et al., 2018, p. 3.) To solve equation 20, numerical solver or other mathematical methods need to be used because closed-form solution is not possible to derive.

$$\frac{\sigma}{E}+\left(\frac{\sigma}{H}\right)^{\frac{1}{n}}=\frac{(\sigma_k+\sigma_{res})^2}{\sigma \cdot E} \tag{20}$$

where,

E	Young's modulus
H	$1.65 \cdot R_m$
n	0.15
σ	Maximum (σ_{max}) or minimum stress (σ_{min})
σ_k	Notch stress
σ_{res}	Residual stresses

The right stress symbol (-) needs to be added to the final σ result, if the loading is compressive in the studied area, like in this study. When unloading occurs, the material behaves based on the kinematic hardening rule, also known as Bauschinger's effect. Ramberg-Osgood material model and Neuber's rule are used to change from a monotonic curve to cyclic curve (Björk, et al., 2018, p. 3.) The $\Delta\sigma$ value can be calculated according to equation 21, but a closed-form solution cannot be derived, and the numerical solver needs to be used.

$$\frac{\Delta\sigma}{E}+2\cdot\left(\frac{\Delta\sigma}{2\cdot H}\right)^{\frac{1}{n}}=\frac{{\Delta\sigma_k}^2}{\Delta\sigma\cdot E} \tag{21}$$

Then σ_{max} or σ_{min} can be calculated by equation 22.

$$\sigma_{min}=\sigma_{max}-\Delta\sigma \tag{22}$$

Finally, R_{local} can be calculated by equation 23.

$$R_{local} = \frac{\sigma_{min}}{\sigma_{max}} \tag{23}$$

These values are utilized to calculate the 4R method fatigue life in the studied situations based on equation 6 in the theory part. Results are shown in Table 8 and detailed calculations in Appendix IV.

Table 8. 4R method results of the top welded (A3) rail connection weld.

Studied case, rail connection weld (A3)	N_{fc} [cycles]
Cylinder force of 60 kN	117 515
Cylinder force of 66 kN	83 001
Cylinder force of 75 kN	75 959

4.2 Fatigue test results

In the testing, the failure occurs when the crack grew through the weld, resulting in lost load-carrying capacity. In Figure 53 left side is a fatigue failure in the top welded rail connection weld and in the assembly fillet weld that is longitudinal to the rail. In the testing, fatigue failure appears firstly in the assembly fillet weld (1.), before the rail connection weld (2.). Three-side welded rail connection weld (A2) fatigue failure is shown on the right side in Figure 53, and the fatigue cracks propagated around the rail connection weld before it merged.

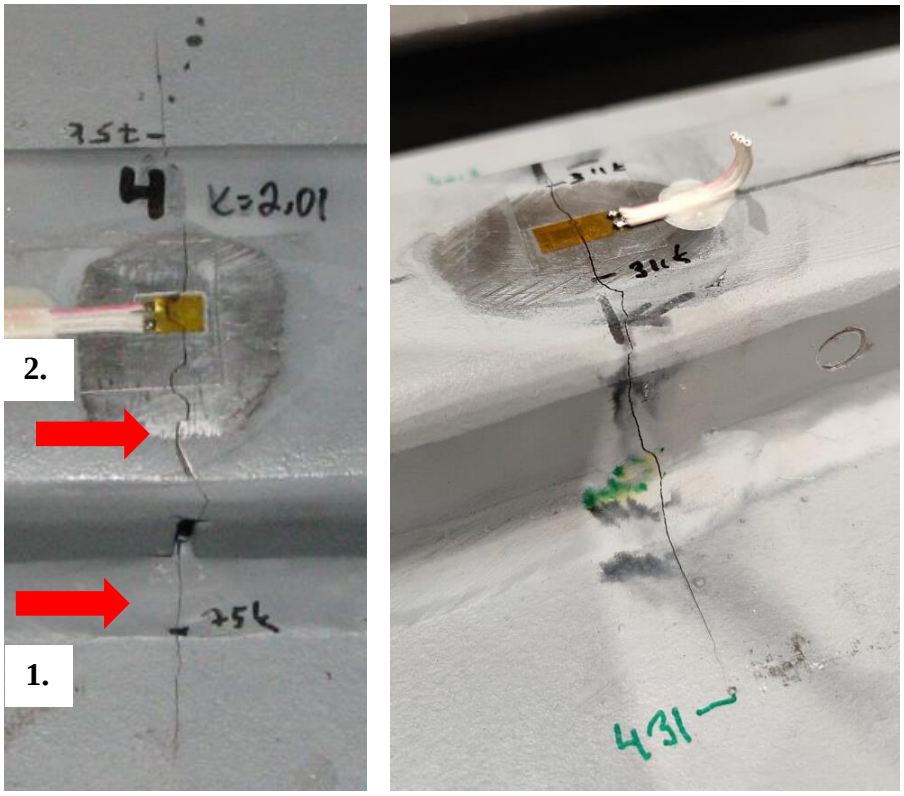

Figure 53. Left is a fatigue failure in the A3 weld after 209 000 cycles in the A3-9G test specimen. On the right side is a fatigue failure of the A2 weld detail.

Test results from the fatigue testing are presented in Table 9. Appendix XVI includes all the strain gauges data of the fatigue test specimens.

Table 9. Test matrix of the top welded rail connection weld (A3) test results. Marking G means that there is a gap between rail and the top flange in the test specimen. The fatigue life estimation values are characteristic.

								Fatigue testing results		
Type of joint	Test piece code	Testing order	Cylinder force [N]	a-dimension, avarage measured	Nominal stress intermittent fillet weld F/A [Mpa]	Top flange nominal stress (FE-model) [Mpa]	Cycles to failure based on the EN13001 standard	Cycles to failure, rail weld 1	Cycles to failure, rail weld 2	Test stopped
A3										
	A3-2	1	60 000	5	120	-138	133 646	221 194	254 110	550 158
	A3-6	7	75 000	4.6	163	-174	66443	143 769	140 596	174 934
	A3-7	6	66 000	4.4	150	-153	98066	211 865	242 648	301 645
	A3-9 G	3	66 000	4.5	146	-153	98066	138 482	161 552	904 856
	A3-11	8	75 000	4.1	182	-174	66443	104 901	110 357	205 911
	A3-16 G	2	66 000	3.9	169	-153	98066	188 278	100 856	938 440
	A3-17 G	4	66 000	4	165	-153	98066	105 357	138 907	605 182
	A3-18 G	5	66 000	4.2	157	-153	98066	107 686	108 301	500 008

In Figure 54, test points are plotted according to the fatigue life estimation based on the EN13001-3-1 design rules of rail connection weld detail with FAT56 and FAT63 in the logarithmic scale. Figure 54 shows how the test results are scattered compared to the design rule. There are two comparison lines: the grey line number of cycles to failure in fatigue testing N_{ft} is multiplied by three, and the second grey line N_{ft} is divided by three. This rule is presented in Radaj, Sonsino and Fricke, 2016, book page 28. Between the two grey lines, the survival probability level is 95 %. The x-axis is the fatigue test result, and the y-axis value is the calculated fatigue life based on the EN13001-3-1 standard.

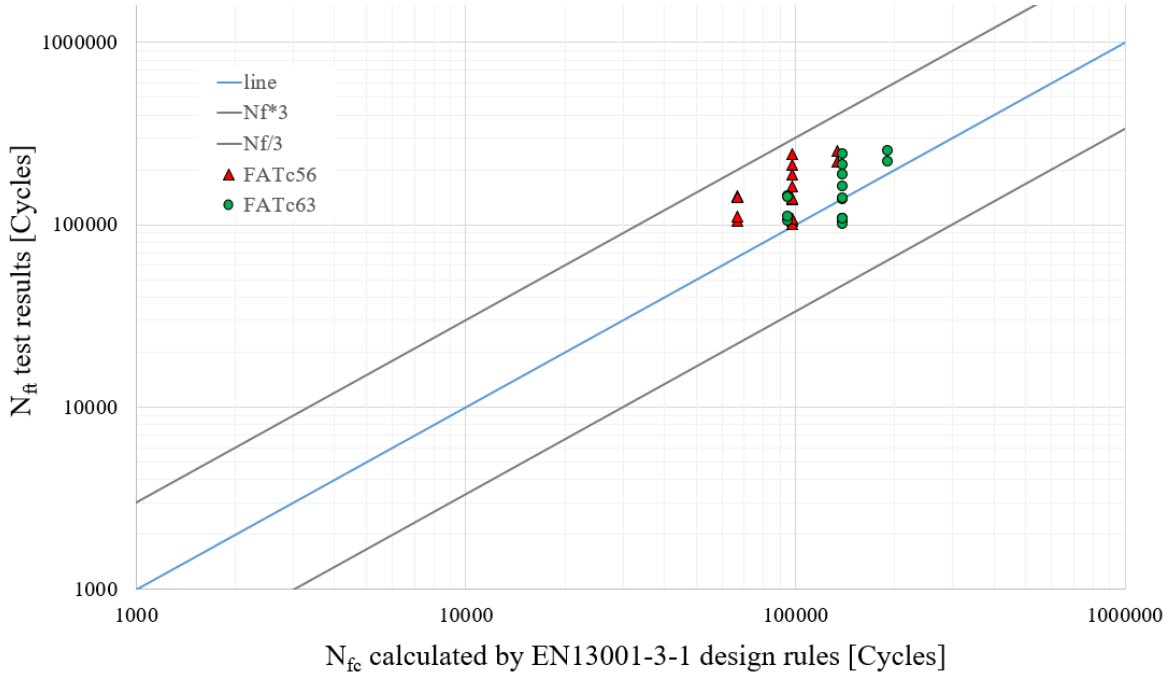

Figure 54. Top welded rail connection weld (A3) fatigue test points compared to the EN13001-3-1 design rule.

Fatigue test results of three-side welded rail connection weld are shown in Table 10.

Table 10. Test matrix of the three-side welded rail connection weld (A2) test results. The fatigue life estimation values are characteristic.

					Fatigue testing results		
Type of joint	Test piece code	Cylinder force [N]	Top flange nominal stress (FE-model) [Mpa]	Cycles to failure based on the EN13001 standard	Cycles to failure, rail weld 1	Cycles to failure, rail weld 2	Test stopped
A2							
	A2-1	60 000	-138	389 639	353 578	360 527	486 565
	A2-2	75 000	-174	193 712	264 204	270 807	270 807
	A2-3	60 000	-138	389 639	297 211	497 214	497 214
	A2-4	75 000	-174	193 712	203 441	232 174	232 174
	A2-5	75 000	-174	193 712	192 256	351 595	431 406

Fatigue test results are plotted and compared to the EN13001-3-1 standard design rules in Figure 55.

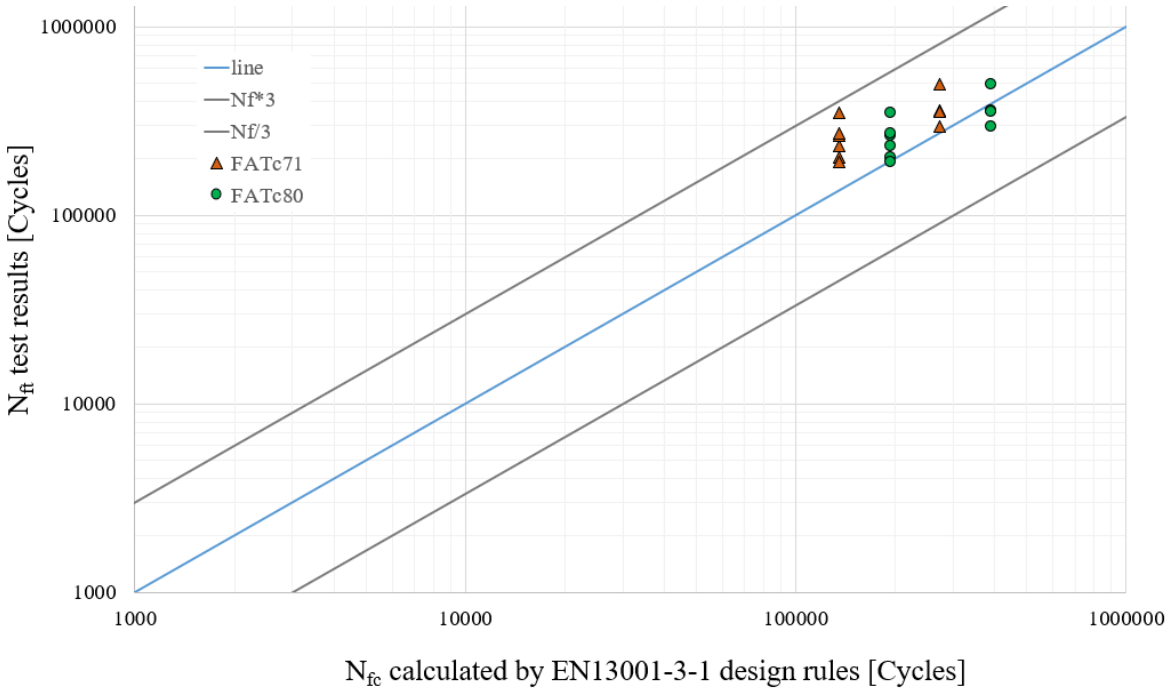

Figure 55. Three-side welded rail connection weld (A2) fatigue test points compared to the EN13001-3-1 design rule.

4.3 S-N curves and FAT_c values of the fatigue test results

For the test results, statistical evaluation is established by three different methods. Two methods are based on the IIW recommendations for the fatigue test results, and the third method is Eurocode 3 appendix D instructions.

In this chapter, FAT_c values based on the testing and S-N curves are presented. The FAT value based on the testing is also compared to the closest standard base FAT class. These S-N curves are conducted based on the IIW recommendations. There are 16 test points totally from the A3 rail connection weld and 10 test points A2 rail connection weld. For the intermittent fillet welds, there are 16 test points. The presented FAT classes are depending on how the nominal stress $\Delta\sigma$ value is defined. FAT classes derived from the test results are presented in Table 12. For the regression analysis in both cases, the S-N curve slope is fixed to be 3. In this testing, it is desired to know the derived value based on the underlying assumption that *m* value is 3. More test points are required to determine *m* value accurately from the test results. More exact values of the calculations for the regression analysis are shown in appendix VI, VII, VIII, IX, X, and XI.

S-N curve in Figure 56 $\Delta\sigma$ value is read from top flange nominal stress based on the EN13001-3-1 standard instructions. The red line is a comparison line based on the standard, and blue lines are derived from testing. The used comparison FAT_c is 56 in the S-N curve based on the EN13001-3-1 standard, and FAT_m value is created by multiplying the 56 by 1,37 factor.

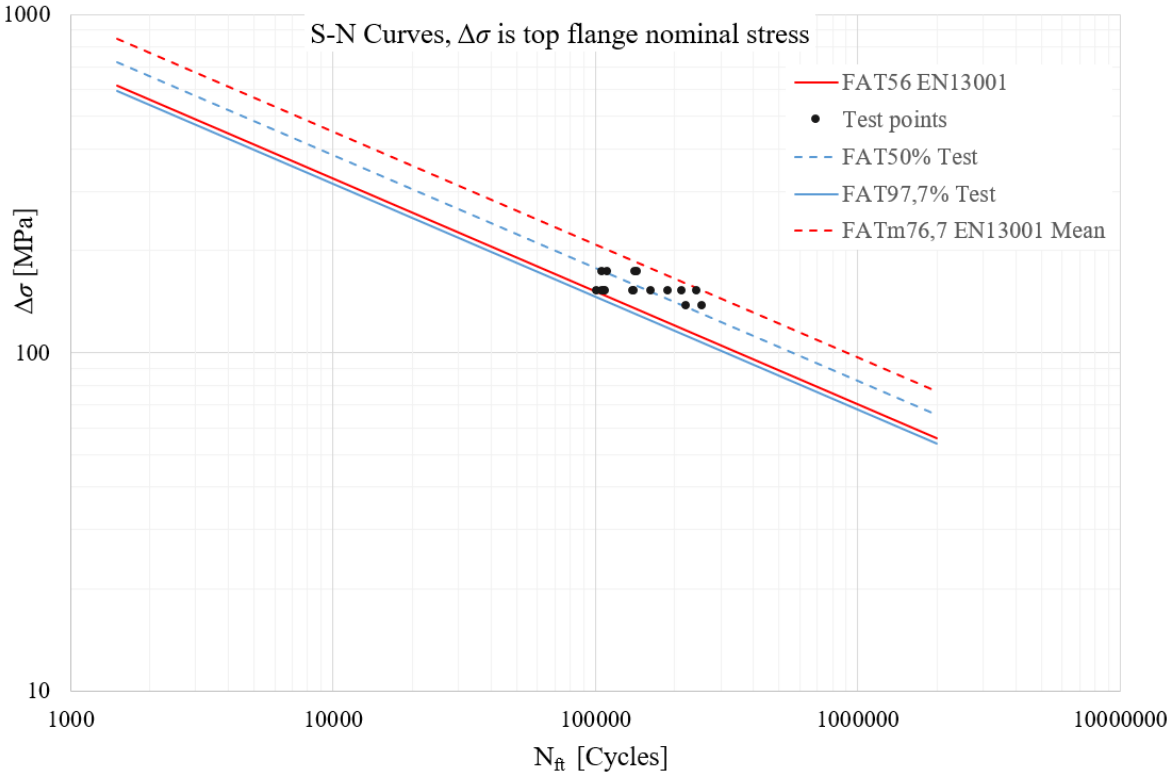

Figure 56. S-N curve based on the fatigue test results. Δσ value is top flange nominal stress as in the EN13001-3-1 standard. Top welded rail connection weld (A3).

Figure 57 Δσ is the nominal stress of rail connection weld, and it has been compared to FAT_c 36 value (red curve). The FAT_c is 36 based on the current EN1993-1-9 standard for the fatigue design rule of the weld root side, and the FAT_m value is created by multiply the 36 by 1,37 factor.

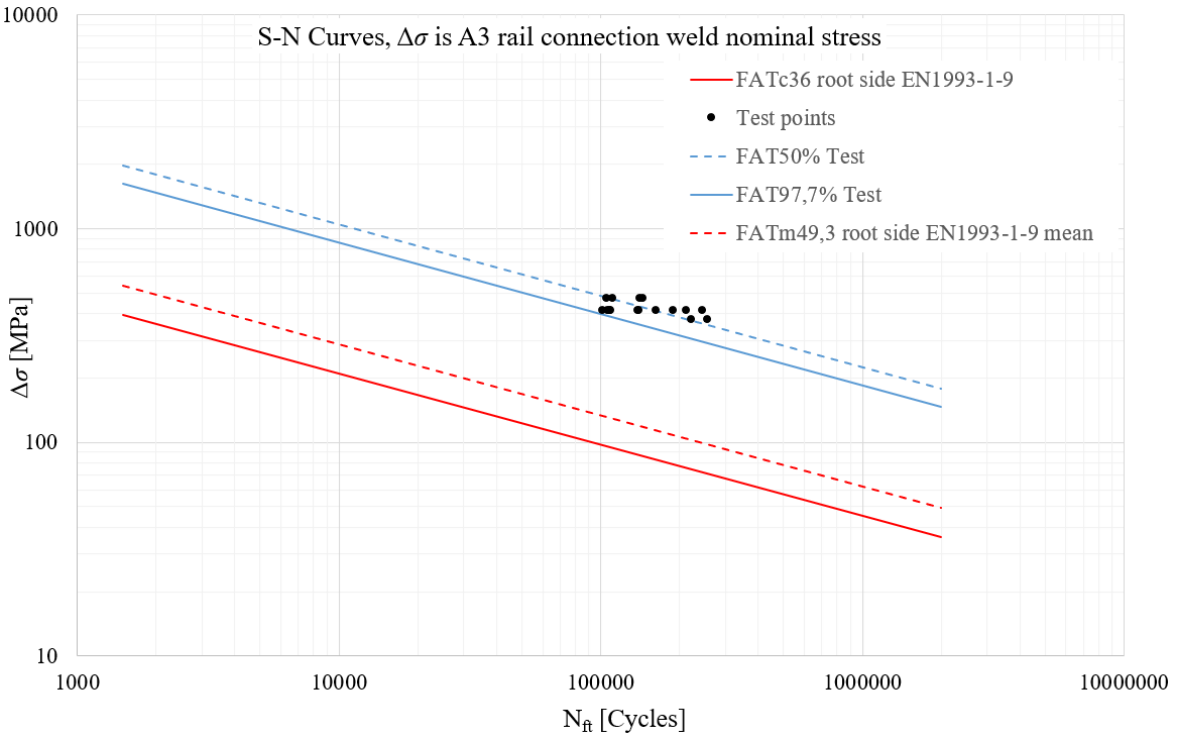

Figure 57. S-N curve based on the test results. $\Delta\sigma$ value is the nominal stress of top welded rail connection weld (A3), and comparison FAT class is taken from the EN1993-1-9 standard.

In the IIW recommendations, other regression methods can be more accurate than previously presented. The main difference between these two IIW regression analysis is how the value k is calculated. Two S-N curves are plotted based on this regression method result. S-N curves with m = 3 and m = 2.29 (based on the test results) are shown in Figure 58, and the FAT values from this regression method are presented in Table 11.

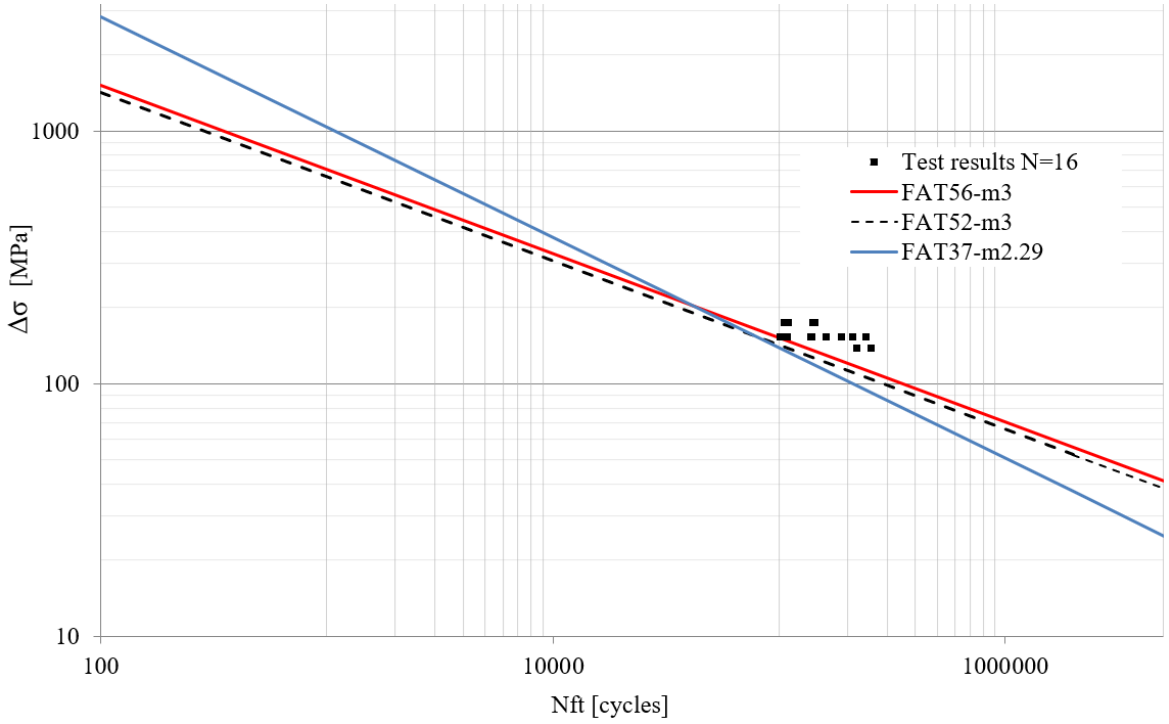

Figure 58. IIW other regression analysis method results of the top welded rail connection weld (A3).

Table 11. Results from the second IIW regression analysis.

	Top welded rail connection weld (A3)		
m	FAT_m	FAT_c	*R2*
3.00	65	52	0.25
2.29	50	37	0.28
	Three-side welded rail connection weld (A2)		
m	FAT_m	FAT_c	*R2*
3.00	84	67	0.28
1.80	55	40	0.51

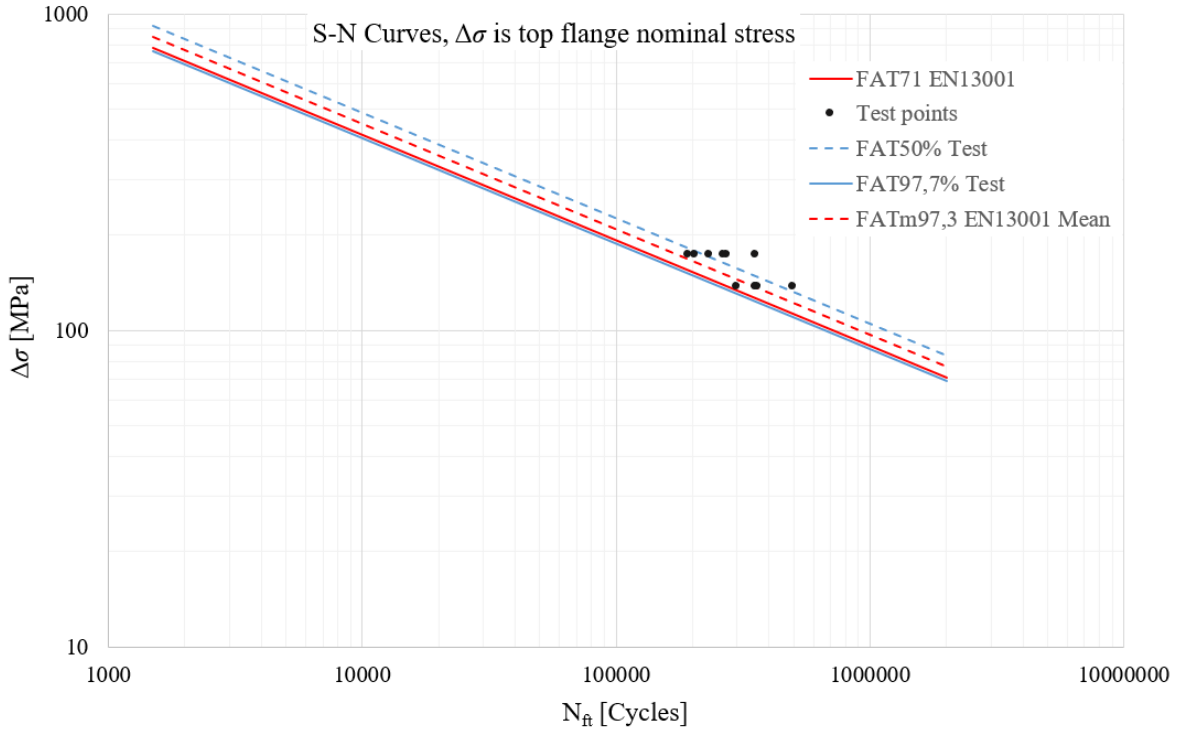

Figure 59. S-N curve based on the fatigue test results. Δσ value is read from top flange nominal stress as defined according to the EN13001-3-1 standard. Three-side welded rail connection weld (A2).

For the intermittent fillet welds, no fatigue failure has happened during the testing. Only one small crack occurred at the weld toe. Four test specimens were cut into two pieces in the intermittent fillet weld locations to see if there is a fatigue crack growing from the weld root side (Figure 60). There were not noticed any fatigue cracks at all.

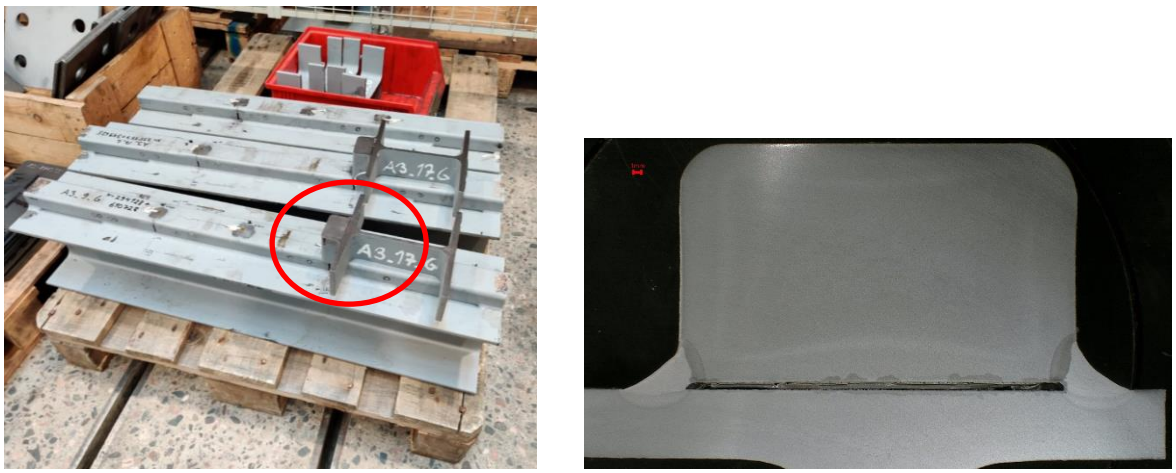

Figure 60. The weld root side of the intermittent fillet weld is inspected to see potential fatigue cracks propagated from the weld root side.

Intermittent fillet weld results are analysed using load cycles when testing is stopped. The assumption is that the fatigue failure would happen in the next load cycle. Test results with the gap between rail and the top flange are used to determine the FAT_c value because it ensures that wheel loads go through the intermittent fillet weld, and the nominal stress of the studied intermittent fillet welds is known. The run-out limit of the test specimens is set to be 500 000 cycles. The used statistical analyse is the IIW method to determine the characteristic FAT value from fatigue testing. The obtained characteristic FAT_c value is 86 in this case. In Figure 61, the S-N curve is shown and compared to the EN1993-1-9 FAT36 class.

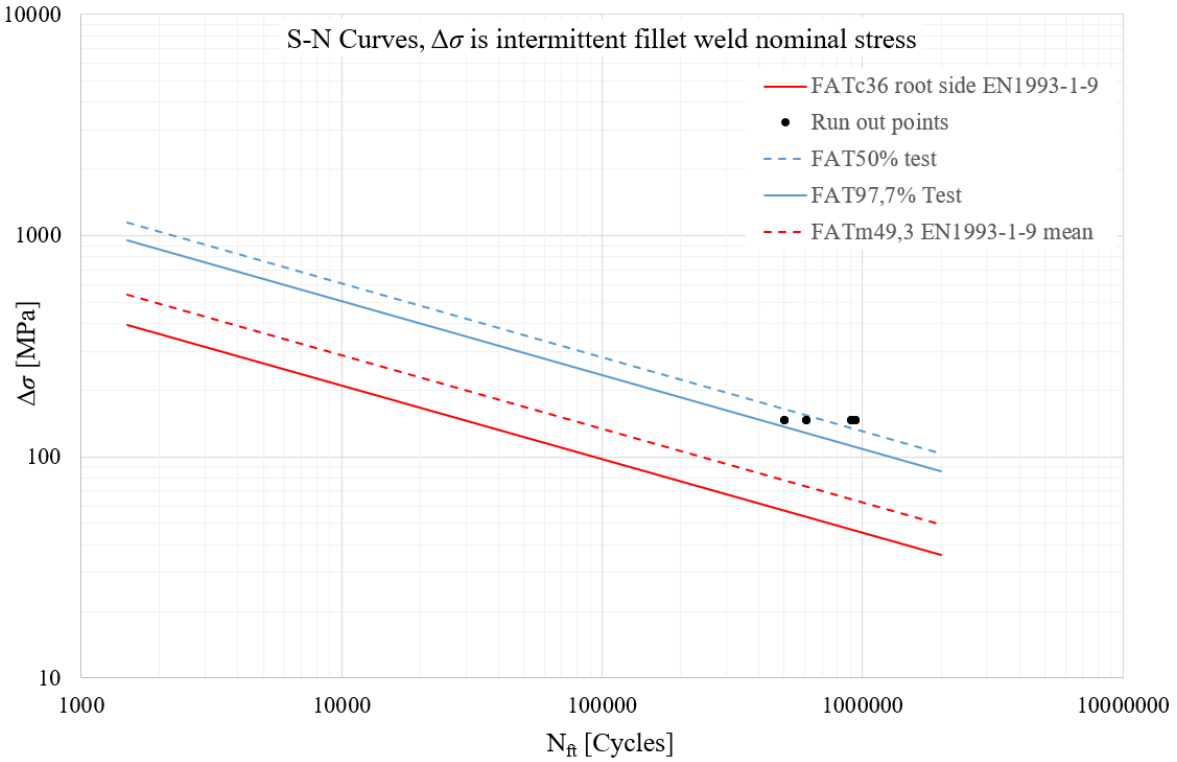

Figure 61. S-N curve of intermittent fillet weld based on the test results. The baseline FAT class is taken from the EN1993-1-9 standard.

Table 12 is a summary of the FAT_c values with different regression methods. Values are compared to the current standard values of the studied weld detail. The used values in the Eurocode regression analysis are shown in Appendix VI and X.

Table 12. Derived FAT_c values of the studied welds from the fatigue test results.

Weld detail & used statistical calculation method	FAT derived from the test results	FAT based on the standards
(A3); $\Delta\sigma$ value is nominal stress of top welded rail connection weld. IIW 97.7%	147	36 or 45
(A3); $\Delta\sigma$ value is the top flange nominal stress of the test specimen. IIW 97.7%	54	63
(A3); $\Delta\sigma$ value is top flange nominal stress of the test specimen. The second IIW regression method 97.7%	37, m = 2.29 & 52, m = 3	63
(A3); $\Delta\sigma$ value is the top flange nominal stress of the test specimen. Eurocode regression analysis	53	63
Intermittent fillet weld, $\Delta\sigma$ value is the nominal stress of the weld. IIW 97.7%	86	36 or 45
(A2); $\Delta\sigma$ value is the top flange nominal stress of the test specimen. IIW 97.7%	69	80
(A2); $\Delta\sigma$ value is the top flange nominal stress of the test specimen. The second IIW regression method 97.7%	40, m = 1.80 67, m = 3	80
(A2); $\Delta\sigma$ value is the top flange nominal stress of the test specimen. Eurocode regression analysis	67	80

4.4 Scaling test results to real-size runway application

Usually, the load-carrying beam is larger than the used one in this fatigue testing, for example, HEA340. In that case, the rail with a fixed cross-section size has a more significant impact on the overall cross-section properties when the load-carrying beam profile is small. Then, the nominal stress level change is more considerable between the rail connection weld and the top flange with smaller (HEA160) load-carrying beam compared to the large (HEA340) beam. It needs to be considered because the EN13001-3-1 standard design rules use the nominal stress of the top flange to determine the fatigue strength of rail connection

welds. That is why test results need to be scaled for the large load-carrying beam to get the correct FAT_c value. The nominal stress of rail connection weld is used as a reference value between the test specimen and large load-carrying beam in the scaling procedure, Figure 62. Finally, the top flange nominal stress of the larger beam is obtained from the FE-model. Therefore, it is conducted in order to see the difference in the top flange nominal stresses when the nominal stress of rail connection weld is fixed between different sizes of load-carrying beam profiles. This same scaling procedure can be done with the analytical equations also.

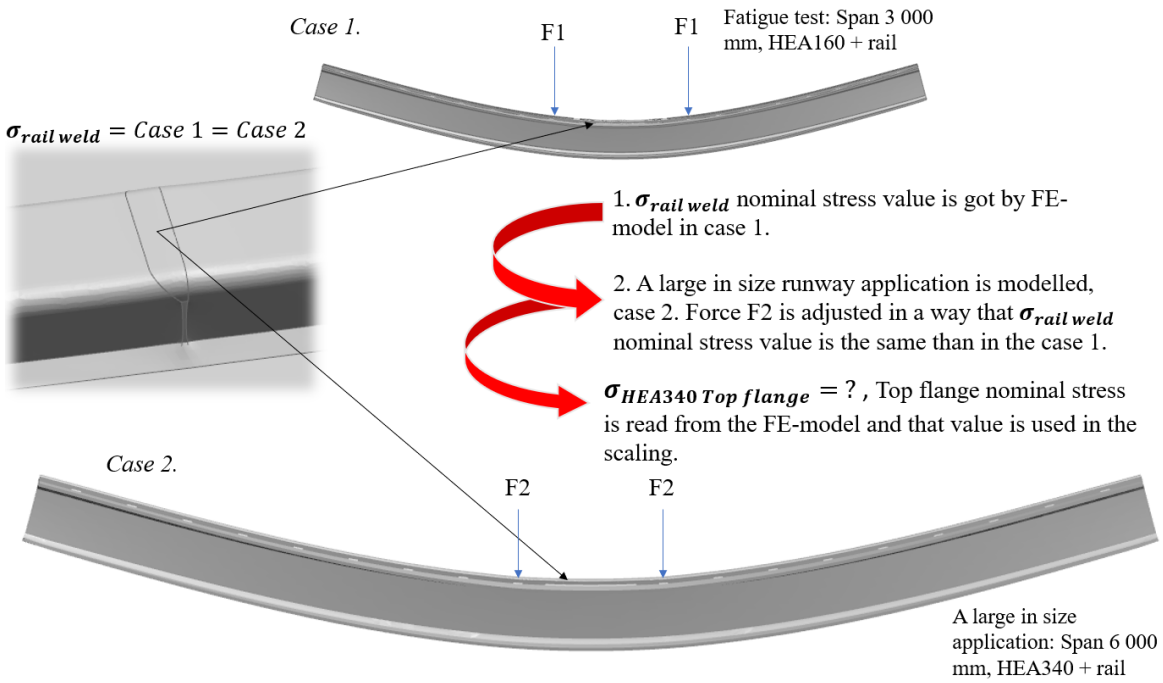

Figure 62. The main principle of the scaling procedure.

The FE-model of the larger load-carrying beam is done for the HEA340 profile, and the used rail profile size is 30 x 50 (mm). The span length is 6 000 mm, loading is 154.37 kN/cylinder, and cylinders location 800 mm away from each other. In this situation, the nominal stress is the same in the rail connection weld as in fatigue testing. From the FE-model, top flange nominal stress is drawn and based on that value, FAT_c value scaling is created. Firstly, the fatigue life is calculated by using equation 24 and characteristic FAT_c value from fatigue testing. The nominal stress of the HEA160 top flange is used. Then scaled FAT_c value is derived by equation 25 using nominal stress of the HEA340 profile top flange and fatigue life from equation 24.

$$N_f = \left(\frac{FAT_{IIW97.7test}}{\Delta\sigma_{test}}\right)^3 \cdot 2 \cdot 10^6 = \left(\frac{54}{153}\right)^3 \cdot 2 \cdot 10^6 = 87\ 735 \quad (24)$$

$$FAT_{HEA340} = \sqrt[3]{\frac{N_f}{2 \cdot 10^6}} \cdot \Delta\sigma_{HEA340\ top\ flange} = \sqrt[3]{\frac{87735}{2 \cdot 10^6}} \cdot 181\ MPa = 64 \quad (25)$$

When doing this, the FAT_c is comparable with the EN13001-3-1 standard design rules that use the nominal stress of the top flange. Table 13 shows a summary of the scaled FAT_c values. More detailed calculations are shown in Appendix V. This same procedure is also conducted with analytical equations without FE-model in Appendix XIV.

Table 13. Scaled FAT_c values of the studied welds.

Studied situation. Used nominal stress and calculation method	FAT_c derived from the test results and scaled	FAT_c based on the standard
(A3) top welded rail connection weld. Test results are scaled to large in size application by using the nominal stress of rail connection weld and IIW 97.7% value from the fatigue testing. (Nominal stress values are drawn by using FEA)	64	63
(A3) top welded rail connection weld. Test results are scaled to large in size application by using the nominal stress of rail connection weld and IIW 97.7% value from the fatigue testing. (Nominal stress values are drawn by using analytical formulas)	67	63
(A2) three-side welded rail connection weld. Test results are scaled to large in size application by using the nominal stress of rail connection weld and IIW 97.7% value from the fatigue testing.	82	80

Table 13. Scaled FAT_c values of the studied welds.

Studied weld. Used nominal stress and calculation method	FAT_c derived from the test results and scaled	FAT_c based on the standard
(A2) three-side welded rail connection weld. Test results scaled to large in size application by using the nominal stress of rail connection weld and IIW 97.7% value from the fatigue testing. (Nominal stress values are drawn by using analytical formulas)	86	80

4.5 New analytical equations based design rule for the rail connection welds

The scaled FAT_c value result shows that there is a difference in the FAT_c value depending on the load-carrying beam size. That is why a new design rule should be developed for the rail connection weld, and it should consider all the affecting variables: the load-carrying beam profile cross-section, rail cross-section, and rail connection weld cross-section. The EN13001-3-1 standard design rule does not consider these aspects. FAT class is the same for every load-carrying beam cross-sections and rail profiles.

In the new design rule for the rail connection welds, analytical equations are used. Firstly, test specimen nominal stress in the weld root $\sigma_{weld,root}$ is determined using equation 26. The moment of inertia $I_{Beam\&rail}$ includes the cross-section ($A_{profile}$) of load-carrying beam profile and rail cross-section (A_{rail}). The $e_{weld,root}$ is the distance from the neutral axel to the rail connection weld root. The principle picture of the new design rule is shown in Figure 63.

$$\sigma_{weld,root} = \frac{M}{W_y} \ , \ W_y = \frac{I_{Beam\&rail}}{e_{weld,root}} \tag{26}$$

Equation 26 is used to calculate the weld root's nominal stress for every load case in fatigue testing. This $\sigma_{weld,root}$ values are used to determine the FAT_c value from the fatigue test results for the weld root detail of rail connection weld. Based on this approach, the top welded rail connection weld FAT_c is 71, and the three-side welded rail connection weld FAT_c is 96. These FAT_c values can be used to determine the fatigue strength of rail connection weld in every runway application by using equation 27.

$$N_{\text{fc, rail connection weld}} = \left(\frac{\text{FAT}_c}{\sigma_{\text{weld,root}}}\right)^3 \cdot 2 \cdot 10^6 \quad (27)$$

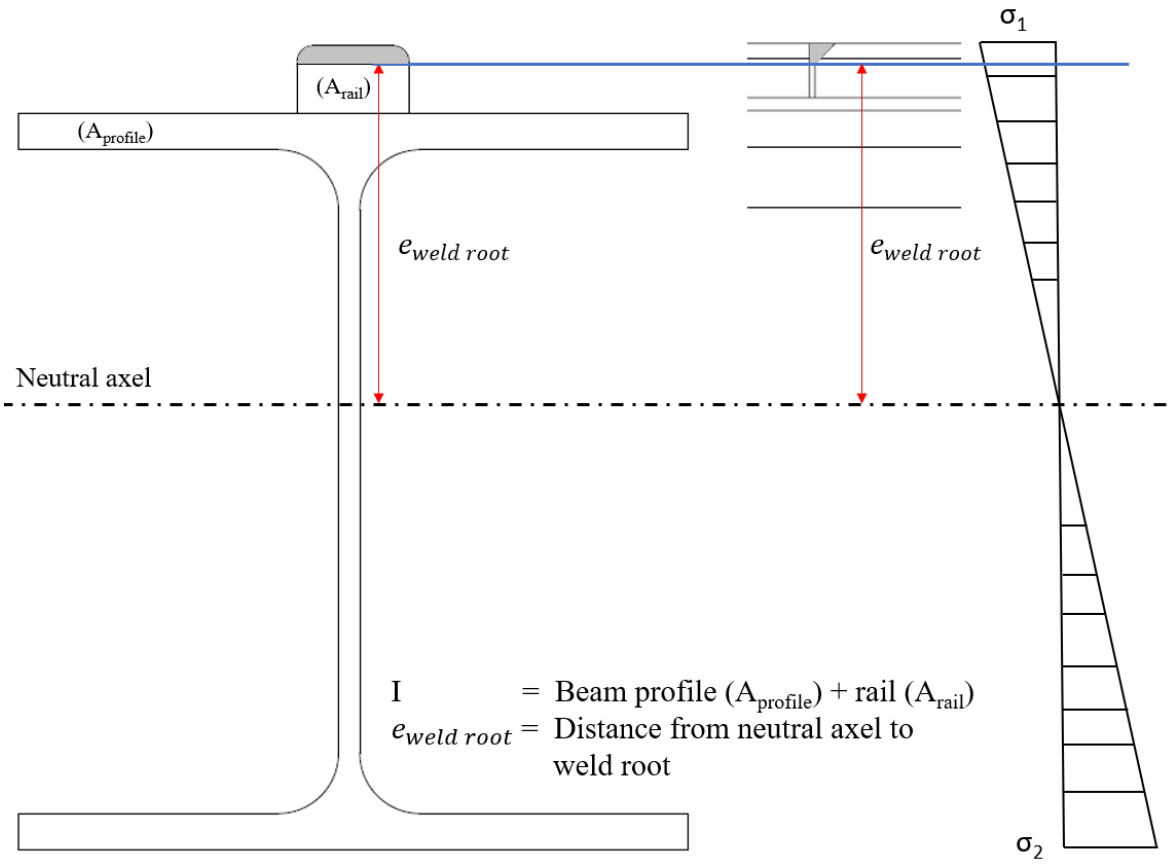

Figure 63. Principle picture of the new design rule for the rail connection welds that utilizes analytical formulas. In the figure (A3) rail connection weld detail is shown, but the same principle is used for the three-side welded rail connection weld (A2).

5 DISCUSSION

Test results show that the FAT classes of the EN13001-3-1 design rules for the rail connection welds are applicable for the bigger load-carrying beams. In addition to that, it is recommended to change the current design rule of the rail connection's weld design rule description. Based on the fatigue test results, the FAT_c value is 54 for the top welded rail connection weld, and for the three-side welded rail connection weld FAT_c value is 69. These values are based on the fatigue test results and the EN13001-3-1 design rule calculation method. IIW and Eurocode regression analysis are done to determine the FAT_c values. Figure 54 and Figure 55 show that test results of both studied rail connection welds are inside the 95% survival probability level when using current design rules from the EN13001-3-1 standard.

When using a smaller load-carrying beam, the rail cross-section starts to affect the overall cross-section properties. This effect needs to be considered when analysing the fatigue test results and comparing them to the typically used crane's runway load-carrying beams. The scaling procedure of fatigue test results related to cross-section size is presented in chapter 4.4. If the test results are scaled to the typically used runway application, the FAT_c value is 64 when the nominal stress is read from the top flange of the load-carrying beam. It complies with the FAT class 63 that is presented in the EN13001-3-1 standard for the top welded rail connection weld. For the three-side welded rail connection weld, the scaled FATc value from fatigue testing is 82, and the FAT class in the EN13001-3-1 standard is 80. These results show that EN13001-3-1 design rules work for large in size load-carrying beam profiles. For the smaller load-carrying beams, the FAT class needs to be smaller when using the EN13001-3-1 current design rule.

Characteristic FAT_c values that are derived from the fatigue test results need to be classified into the different FAT classes that are presented in the standards. Different FAT classes in the standards are shown in Figure 17. For the top welded rail connection weld, the right class is 50 or 56, and for the three-side welded rail connection weld, the FAT class should be 63 or 71. The classification depends on how much certainty is desired inside the design

value. The scaled test results FAT classes are: 63 for the top welded rail connection weld and 80 for the three-side welded rail connection weld.

Based on the fatigue test findings, a new design rule is presented in chapter 4.5. It considers all the cross-section parameters, for example, the load-carrying beam profile size and the rail cross-section and also the weld size. Analytical equations are used to calculate the fatigue life with the new design rule, and therefore, the FE-analyse is not needed. This same design rule can be used for both of the studied rail connection welds. The used FAT_c value is the only difference: FAT_c is 71 for the top welded rail connection weld, and the three-side welded FAT_c value is 96. In the standardization, the used FAT classes are 71 for the top welded rail connection weld and 90 for the three-side welded rail connection weld.

For the intermittent fillet weld, test results show that the FAT class is at least 80 under the testing condition. This value is derived from the run-out results, and it is assumed that failure would happen in the next load cycle. This result means that the currently used EN1993-1-9 design rule FAT class 36 is conservative when the loading is compressive. This finding can also be found in the fatigue test results of the top welded rail connection weld. The standardized FAT class is 140 for the top welded rail connection weld. This value is valid when the top welded rail connection weld's nominal stress is used. The weld nominal stress is drawn from the FE-model. The closest FAT class for the weld detail in the Eurocode 3 standard is FAT36, which is meant for the weld root side detail under compressive or tensile loading. Based on the test results FAT140 and FAT80 are relatively high compared to the FAT36 that is presented in the EN1993-1-9 standard. The reason for this difference between test results and standard can be that the weld root side has compressive residual stresses or slight tensile stresses that increase the fatigue strength of the welds. The EN1993-1-9 standard allows the use of the 0.6 reduction factor for the nominal stress if the loading is compressive. This factor cannot be applied for the circumstances studied here because welds are not stress-relieved. These findings highlight the importance of studying welds separately under compressive loading in comparison to tensile loading.

In the Euler & Kuhlmann's article, a similar type of fillet weld connection between rail and load-carrying beam top flange were studied. In that article, the FAT_c value has been tested for the continuous fillet weld in the rail and top flange attachment instead of intermittent

fillet weld. Testing carried out larger test specimens. Also, there was a moving wheel load situation that was studied, which differed from this project's testing principles. In that research, the proposed FAT_c value was 57 for the continuous fillet weld. The value was higher than the current FAT36 in the EN1993-1-9 standard, and it includes the shear stress change effect. (Euler & Kuhlmann, 2018) That study indicates that the fillet weld FAT class should be higher than the current FAT36 in the Eurocode 3 if the loading is only compressive. In this study, the FAT_c value is 86 for the intermittent fillet weld without the shear stress change effect. It is significantly higher than the FAT_c value 57 found in the Euler & Kuhlmann article for the continuously welded fillet weld. The FAT_c value 57 indicates that intermittent fillet weld needs to be tested under a traveling wheel load. It is an addition to stationary fatigue testing of this study, and it allows to get shear stress change effect considered in the new design rule. The difference between these two FAT_c values 57 and 86 highlights the effect of the residual stresses in the weld root side and how it affects the fatigue strength of the weld.

Test results are near one another, and the scatter of the test points is small. It creates some difficulties for the second IIW method in order to gain reliable regression analysis. It can be seen in the *R2* values that are 0.25 and 0.28, based on the test points. The target is that the *R2* value is close to 1.00, and now it is far from the targeted value. This value indicates that from a statistical point of view, test points are close to each other, and it causes variation for the regression analysis to generate accurate slope *m* value. This uncertainty affects how the final FAT_c value is going to be derived from the test results. In order to get additional accurate results of the regression analysis with this method, more testing needs to be carried out with different $\Delta\sigma$ values. These values should be significantly different from the ones tested here. It would help to get *R2* value closer to one. When the slope *m* is fixed to be three in the second IIW regression analysis, the result turns out to be close to the first IIW regression analysis result. The relatively low *R2* does not cause the problem to derivate the FAT_c values because standards recommend using fixed *m* values: three for nominal stress and five for shear stress.

Residual stresses have a significant role in the fatigue strength of the studied rail connection welds. Residual stresses are measured by X-ray in order to get more understanding of the residual stress level in the rail connection welds area. It is essential to recognize the residual

stress state in the weld root side to see if it is compressive or tensile. The residual stress measurements of the fatigue test specimens show that all around the rail connection welds, there is compressive residual stress. The main reason for the compressive residual stress is the welding order. A longitudinal assembly fillet weld is welded last. When the 500 mm fillet welds shrink after welding, it causes a force that produces the compressive residual stress in the rail connection weld. It will increase the fatigue strength of the rail connection welds. Therefore, it is recommended to have a clear description of the welding order in the design rule.

To be able to compare the residual stresses of different sizes load-carrying beam in the rail connection weld area, a large size runway load-carrying beam HEA340 is welded, and residual stresses are measured. These results are compared to the fatigue test specimens' (HEA160) residual stress results. The results of the HEA340 test specimen's residual stress measurement show that the welding order has a desirable impact. The weld root has compressive residual stress or close to zero value. Additionally, the top of the weld has tensile stress in the HEA340 test specimen. There is a compressive residual stress in the weld root side before the welding of the 500 mm assembly fillet welds. It is in line with the findings presented in the theory part of this study. These findings of the simulation results show that there are compressive residual stresses in the weld root side when multipass welding is used. Generally, it can be said that after the welding of the 500 mm assembly fillet welds, the tensile residual stress level is lowering or turning into compressive residual stress in the root side of rail connection weld. It has a positive impact on the fatigue strength of rail connection weld.

Despite the fatigue test specimens have compressive residual stresses all-around the studied rail connection welds. A failure happened in the fatigue testing from the weld root side because the weld root side has a more irregular notch shape than the grounded welds' outer surface. It causes higher local stress concentration in the weld root side, and also this explains why fatigue failure happens from the weld root side.

Hardness values are at an acceptable level in the studied welds. Typically, values under 350HV do not cause hydrogen or cold cracking in the weld area. 400HV value can be accepted if low hydrogen filler material is used. (Ovako, 2012, p. 11) Hardness values of the

heat-affected zone (HAZ) change compared to the material hardness values. It is normal, and the level of change is acceptable. The welds' and material's hardness values are close to each other. The measured values are between 160-250 HV5. Multipass welding causes the difference in the hardness value of rail connection weld between the weld root side and top area of the weld. Firstly, the previous weld is heat-treated by adjacent welding passes, and this affects the hardness values of the different areas in the rail connection weld.

Crack initiation time is much longer than the crack propagation phase in the fatigue life of rail connection weld. Based on the Franc2D results, the FAT_c value is 16 for the top welded (A3) rail connection weld, and FAT_c value is 24 for the intermittent fillet weld. These values are relatively low compared to the fatigue test results. Crack initiation and propagation phase can be seen in the strain gauge values of the fatigue test specimens. During the testing, strain gauge values stay stable for a specific time. Then crack propagation occurs, and it causes fatigue failure to happen in the rail connection weld. Figure 52 shows how the strain gauge values start to change during fatigue testing. The strain gauge is located top of the rail connection weld. It indicates if any changes are about to happen in the weld and what the failure stage is. Strain gauge values indicate that the crack propagation time is only one small fraction of the total fatigue life of the weld. The crack initiation phase is dominant. That is why the linear elastic fracture mechanics does not give an accurate fatigue life estimation of the studied welds. Franc2D analysis takes into account the crack propagation phase but not at all the crack initiation phase.

Fatigue life estimations vary quite much, depending on the used method. For example, the nominal stress method based on the EN13001-3-1 standard design rule gives 98 066 cycles with FAT56, and 139 630 cycles with FAT63 for the top welded rail connection weld in 66 kN force per cylinder loading situation. The ENS method gives only a 3 979 cycle fatigue life estimation. Fatigue test results were between 105 000 – 242 000 cycles, and the average amount of cycles to cause fatigue failure with ten test points is 150 393. The ENS method considers the compressive stress to be as effective as tensile stress. The difference between the ENS method and the fatigue test results show that there is a need to create a more accurate calculation method for the weld. These methods should take into consideration the residual stress and compressive load effective part.

The 4R method is entirely accurate as a fatigue strength assessment method for the studied welds, even though it is created to assess the fatigue strength of the weld toe. In this study, the R_{local} is used in the rail connection weld root. The 4R method predicts 83 000 load cycle fatigue life for the top welded rail connection weld when the test force is 66 kN/cylinder. It is a characteristic value, and the fatigue test results are matching with this fatigue life estimation. Summary of the results and accuracy of the different methods concerning the fatigue test results are shown in Figure 64. Also, the excellent fatigue life of the intermittent fillet welds indicates that the total compressive linear $\Delta\sigma$ stress range is not entirely effective.

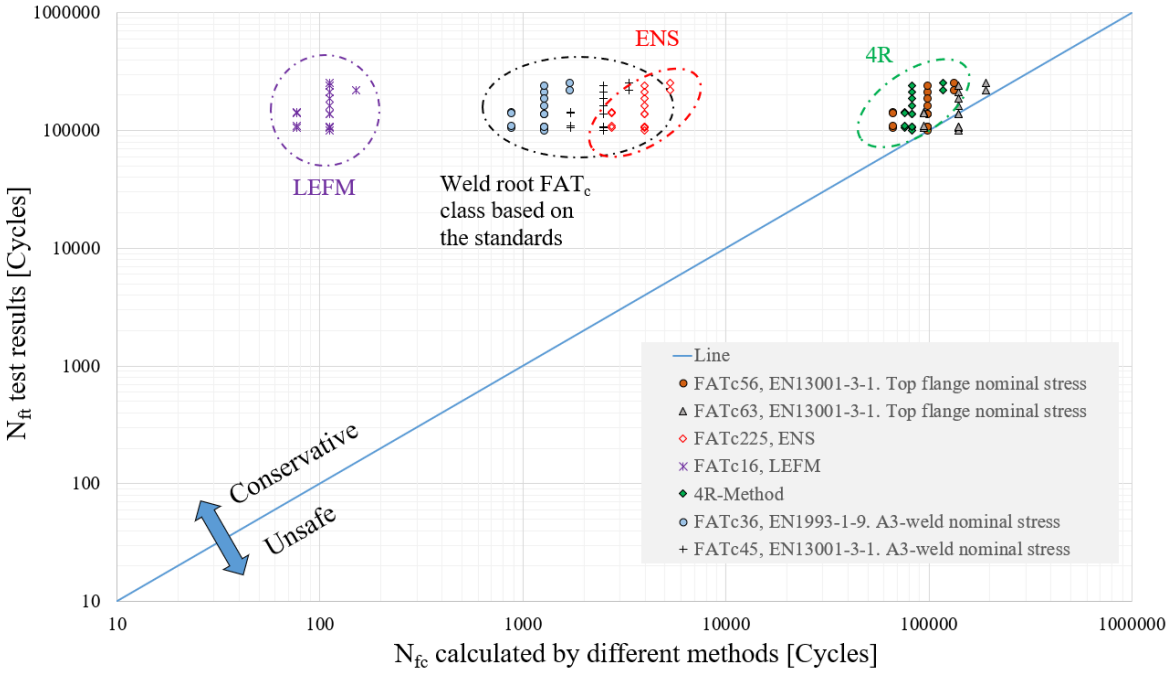

Figure 64. Top welded rail connection weld (A3) fatigue life estimations by different fatigue strength assessment methods compared to the fatigue test results. The fatigue life estimation values are characteristic.

In the fatigue testing, when the loading is increased to 75 kN/cylinder, test specimens fatigue life stays almost the same as the lower 66 kN/cylinder load case. It shows that the local stress ratio influences the fatigue life of the welds. In the testing, the stress ratio is zero for external loading. The used forces and test frequency are constant. Test results indicate that the experiences stress ratio $\Delta\sigma_2$ of weld detail is different from the assumed $\Delta\sigma$ situation. Residual stresses have a role in this situation, and they will affect the local stress ratio R_{local} that the weld is experiencing. It is different from the external load stress ratio R. Compressive

residual stress reduces the tensile stress part in the weld and increases the fatigue strength of the studied welds.

The effective notch stress method can be utilized to estimate effective $\Delta\sigma_2$ value. The mean value of the fatigue test results is used. By using different mean values, the $\Delta\sigma_2$ is solved with the ENS method equation 28 with $FAT_{ENS,mean}$ value. This procedure was done for the top welded rail connection weld and intermittent fillet weld.

$$\left(\frac{FAT_{ENS,mean}}{ENS_{factor} \cdot \Delta\sigma_2}\right)^3 \cdot 2 \cdot 10^6 = N_{ft,\ \text{average test}} \tag{28}$$

Finally, $\Delta\sigma_2$ value is compared to the nominal stress range of the studied weld in equation 29.

$$\frac{\Delta\sigma_2}{\Delta\sigma} \cdot 100\% = \text{Effective stress (\%)} \tag{29}$$

Effective stress (%) values are shown in Table 14. For the intermittent fillet weld, run-out and maximum testing results are used in N_{ft} value.

Table 14. Estimation of the effective stress range of the total stress range in the studied welds. ENS method results are utilized.

Top welded rail connection weld A3, N_{ft} = 150 393 cycles	Intermittent fillet weld (a_w = 4 mm), N_{ft} = 500 000 cycles	Intermittent fillet weld (a_w = 4 mm), N_{ft} = 938 440 cycles
41%	70%	57%

Values seen in Table 14, show that the total compressive loading is not entirely effective. Finally, it is seen that the values 41% and 57% are relatively small because the EN1993-1-9 standard indicates that 60% of the compressive loading is effective for the stress relived and non-welded components.

While conducting fatigue testing, the failure happened differently depending on the studied rail connection weld. In the fatigue testing, the failure of top welded rail connection weld

happened firstly in the longitudinal assembly fillet welds before the rail connection weld had a fatigue failure. It is due to the fact that the weld root shape of the longitudinal assembly fillet weld is not desirable from the fatigue point of view. The clearance between the rail parts allows the weld to *fall* inside the clearance, and the unfavorable root side shape is created. It will increase the local stress concentration and causes earlier fatigue failure. However, the clearance size is needed to make sure that the desired residual stress state in the rail connection welds is achieved due to the force caused by shrinkage after welding the longitudinal assembly fillet welds. If there is no clearance size, the contact between the rail parts resists the deformation of the rail parts. The contact between the rail parts has a negative impact on the formation of the desired residual stress state in the rail connection weld. The fatigue failure of a three-side welded rail connection weld happened in the rail connection weld area. Firstly, fatigue cracks occurred around the weld, and then fatigue cracks merged, and fatigue failure happened.

5.1 Further studies

Many research topics can be studied further based on this study. In this study, the intermittent fillet weld was tested under compressive loading. High FAT class FAT80 indicates that there are compressive or slight tensile residual stresses in the weld root side. That is why tensile loading should be tested to see the fatigue strength in that loading situation.

The residual stress state in the weld consists of many variables. Therefore, welding order and the gap between rail and top flange need to be studied more to see how those factors affect the final residual stress state in the welds. There can be a possibility that the gap between rail and top flange produces better residual stress state in the weld root than without the gap. The effect of this detail to the final residual stress state needs to be verified. The effect of welding order can be studied with FEA simulation and laboratory testing to see how it affects the final residual stress state in the welds in different locations.

6 CONCLUSION

Based on the test results and the statistical evaluations, it can be stated that the EN13001-3-1 design rules for the rail connection welds apply if the load-carrying beam is large. Smaller load-carrying beams need to have a different FAT class if the EN13001-3-1 standard design rule calculation procedure is used. It is coming from the fact that the current design rules do not take into consideration the distance between the neutral axis of the load-carrying beam and the rail from the weld. Both IIW and Eurocode regression analysis are utilized in order to gain the characteristic FAT_c values from the fatigue test results. These methods give the same level results and are in line with the EN13001-3-1 standard design rule if the load-carrying beam is large. Based on this research, these results can be harmonized with the new upcoming Eurocode 3 version if this notification is considered. In addition to the EN13001-3-1 standard description, it is recommended to have an instruction of the right welding order, Figure 65. The right welding order improves the residual stress state in the weld root and increases weld fatigue strength capacity. As previously presented, this design rule is valid for large in size load-carrying beams.

3.15	*m* = 3	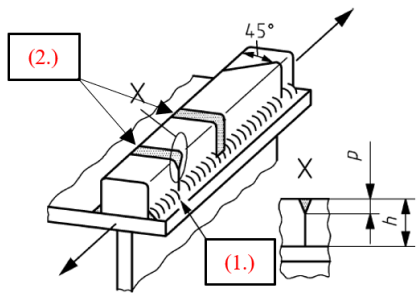 Plate with a rail welded on it, rail joints without butt weld or with partial penetration butt weld, design stress is that calculated in the plate	Basic conditions: — all welds quality level C or better Special conditions: — continuous welds (1) over the joint on both sides of the rail with at least a length of 3 times *h* +1 NC - Welding order needs to be followed to utilize special conditions Welding order: 1. Rail connection weld (2) must be welded first 2. Continuous welds (1) over the joint are welded last
	45	rail joint cut perpendicular or at any other angle, e.g. 45°, *p* = 0,	
	56	single weld on top of the rail, $h > p \geq 0{,}3 \times h$	
	71	welds on top and on the two sides of the rail, $h > p \geq 0{,}2 \times h$	

Figure 65. The proposed addition to the EN13001-3-1 standard detail category description of the rail connection weld.

A new design rule is presented in Figure 66. It takes into account the profile of the beam, the rail cross-section, and the weld size. The design rule has been created to give accurate fatigue life estimation for every runaway application and also for smaller load-carrying beams. This design rule is valid when special conditions are applied from Figure 65.

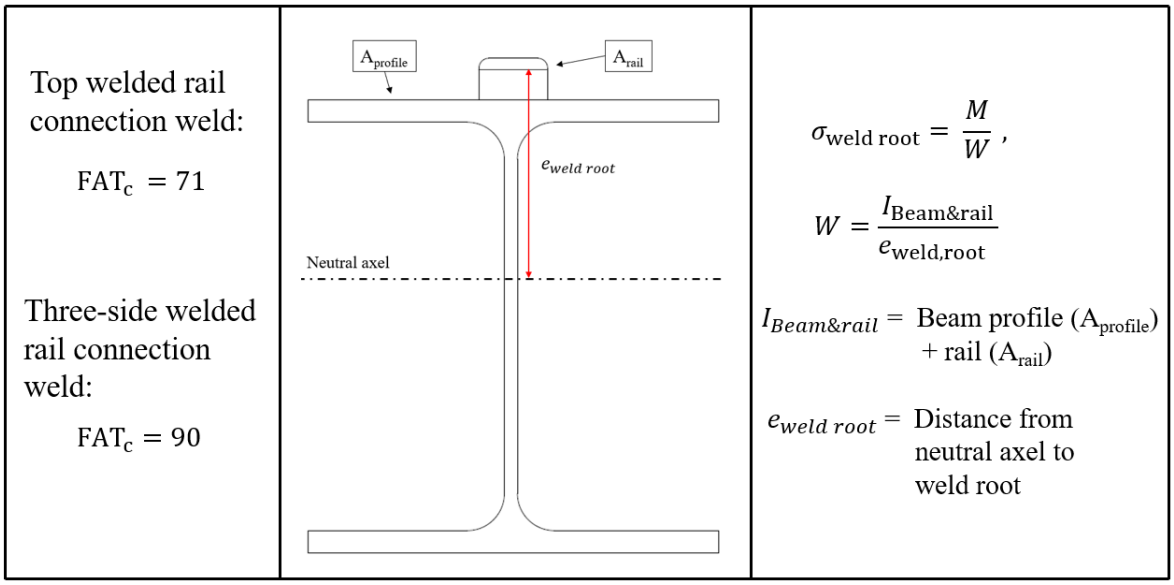

Figure 66. A new proposed design rules for the rail connection welds.

Intermittent fillet weld needs more testing in order to determine an accurate design rule for the weld detail. At this moment, it can be said that intermittent fillet weld FAT class should be higher than FAT36 in the current EN1993-1-9 standard if the intermittent fillet weld is under compressive loading. This study results show that the stress state and residual stresses of the intermittent fillet weld root side have a significant role in fatigue strength. Also, it is recommended to test the intermittent fillet weld by a traveling wheel and, in which case, the shear stress change effect is considered. This way, it is possible to give definite design rules for the intermittent fillet weld detail.

With the right welding order, it is possible to affect the residual stresses of the weld. A competent steel structure designer takes this into account and increases the fatigue strength of the welds by utilizing the right welding order and clearance size. It is possible to do for the rail connection welds in this study. Residual stress measurement results show that by using the right welding order, it is possible to achieve desirable residual stresses in the welds to increase fatigue strength. The clearance size needs to be taken into account to get the

desired residual stress state. At the same time, the clearance will generate poor quality to the root side of the assembly fillet weld. It is essential to find a compromise between these two aspects to achieving the best result in the design.

This study's fatigue testing shows that the welds under compressive loading have a better FAT class than if the loading is tensile. The current Eurocode 3 standard assumes that compressive loading is as effective for the weld than tensile loading if the weld is not stress-relieved. That is why it is essential to study welds under compressive loading more in order to get a specific reduction factor for the compression stress part and avoid designing over conservative steel structure designs.

LIST OF REFERENCES

Bertil, J. & Dobmann G., H. A. K. M. M. G., 2016. *IIW Guidelines on Weld Quality in Relationship to Fatigue Strength.* s.l.:Springer Nature.

Björk, T., Ahola, A. & Skriko, T., 2018. 4R Method for consideration of the fatigue performance of welded joints - Background and applications. *Proceedings of the ninth international conference on Advances in Steel Structures*, -(-), p. 10.

Dowling, N. E., 2013. *Mechanical Behavior of Materials - Engineering Methods for Deformation, Fracture, and Fatigue.* 4th ed. Essex: Pearson.

EN13001-3-1, 2018. *Cranes. General Design. Part 3-1: Limit States and proof competence of steel structure.* 1st ed. Helsinki: Finnish Standards Association.

EN1990, 2006. *Eurocode - Basis of structural design.* Helsinki: Finnish Standards Association (SFS).

EN1993-1-9, 2005. *Eurocode 3: Design of steel structures - Part 1-9: Fatigue.* Brussels: European committee for standardization.

EN6507-1, 2018. *Metallic materials. Vickers hardness test. Part 1: Test method.* 2nd ed. Helsinki: Mechanical Engineering and Metals Industry Standardization in Finland.

EN9015-1, 2011. *Destructive tests on welds in metallic materials. Hardness testing.*. 1st ed. Helsinki: Mechanical Engineering and Metals Industry Standardization.

Euler, M. & Kuhlmann, U., 2018. Aufgeschweißte Flach- und Vierkantschienen, Ermüdungsnachweis für Schweißnähte zur Schienenbefestigung. *Stahlbau*, Volume 87, p. 20.

Fricke, W., 2013. IIW guideline for the assessment of weld root fatigue. *Welding in the World,* 57(6), pp. 753-791.

Gulvanessian, H., Calgaro, J.-A. & Holicky, M., 2002. *Designers' Guide to Eurocode: Basis of Structural Design.* 2nd ed. s.l.:ICE Institution of Civil Engineers.

Hobbacher, A., 2014. *Recommendations for fatigue design of welded joints and components.* 2nd ed. Wilhelmshaven: Springer.

Kouhi, J., 2015. *Eurocode 3 Käsikirja EN1993-1-2 ja EN1993-1-9.* 1st ed. Helsinki: Teräsrakenneyhdistys ry.

Nussbaumer, A., Borges, L. & Davaine, L., 2018. *Fatigue Design of Steel and Composite Structures.* 2nd ed. Berlin: ECCS - European Convention for Constructional Steelwork.

Ongelin, P. & Valkonen, I., 2010. *Hitsatut profiilit EN 1993 -käsikirja.* 3th ed. Keuruu: Rautaruukki Oyj.

Ovako, 2012. *Ovakon terästen hitsaus.* 1st ed. Imatra: s.n.

Poutiainen, I., 2006. *A Modified Structural stress method for fatigue assessment of welded structures.* Lappeenranta: Lappeenrannan teknillinen yliopiston Digipaino.

Rabb, R., 2013. *Todennäköisyysteoriaan pohjautuva väsymisanalyysi.* 1st ed. Vaasa: Bod - Books on Demand, Helsinki.

Radaj D, S. C. F. W., 2006. *Fatigue assessment of welded joints by local approaches.* 2nd ed. Cambridge: Abington Publishing.

APPENDIX I

Main dimensions of the test set up at LUT University.

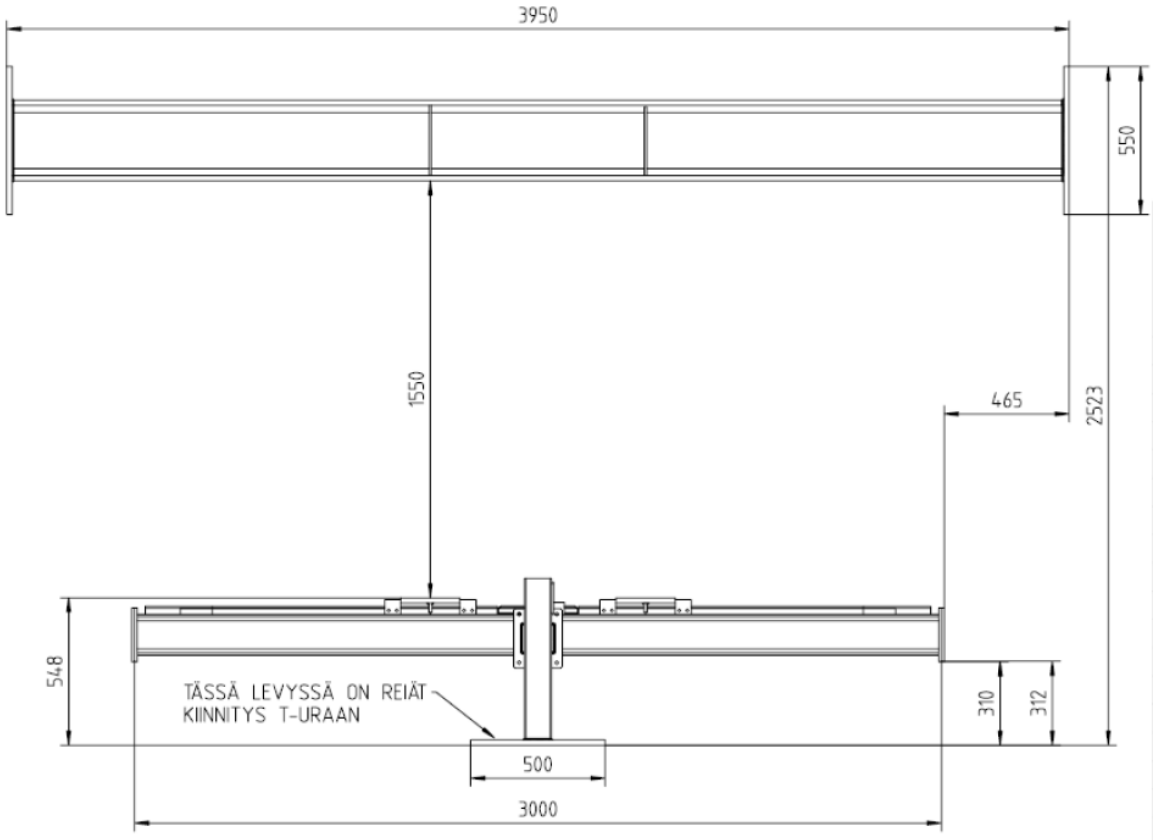

ENS-method effective notch radius locations in the studied welds.

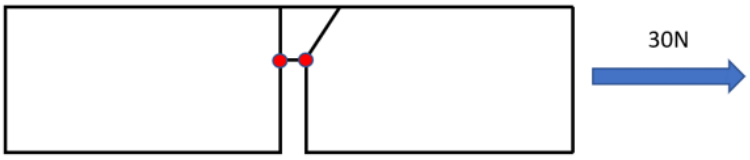

ENS value from the FE-model = 14.26 = ENS radius location

real ENS = 4.28 , weld height / rail height * ENS from model

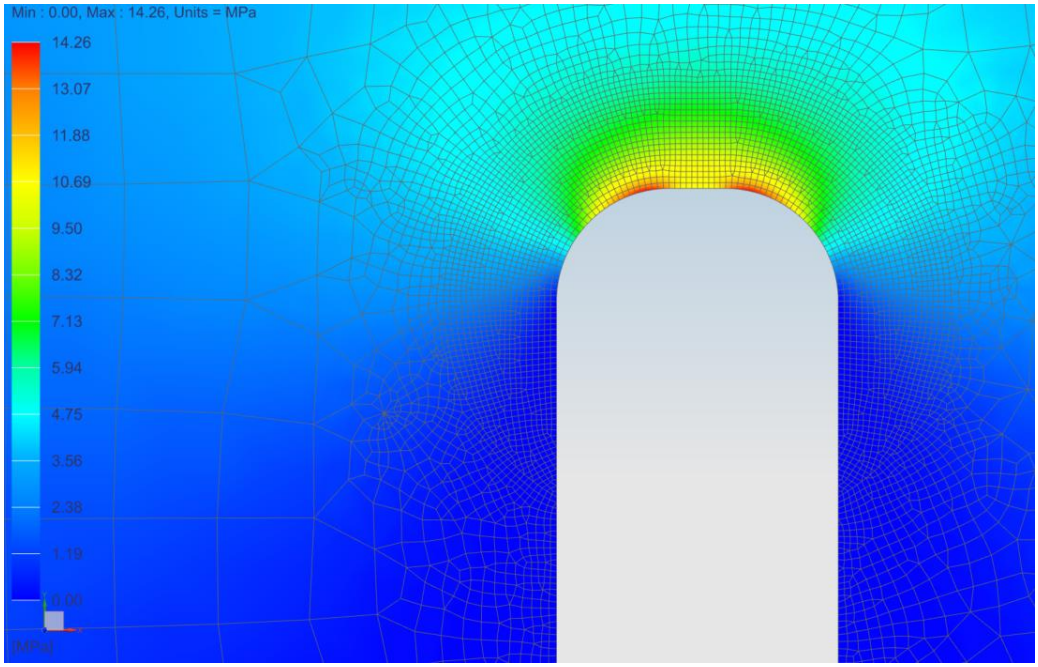

ENS-method effective notch radius locations in the studied welds.

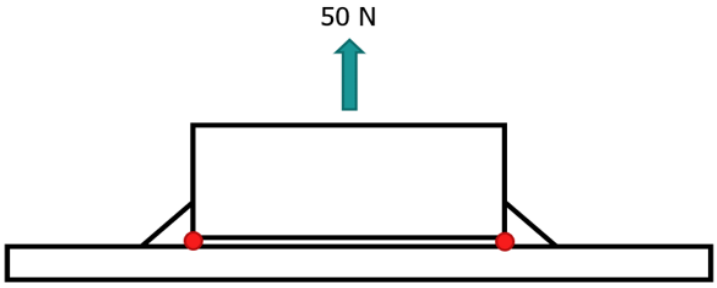

● = ENS radius location

ENS value from the FE-model = 26.42

real ENS, when a_w is 4 mm = 4.23 , throat thickness * 2 / rail width * ENS from model

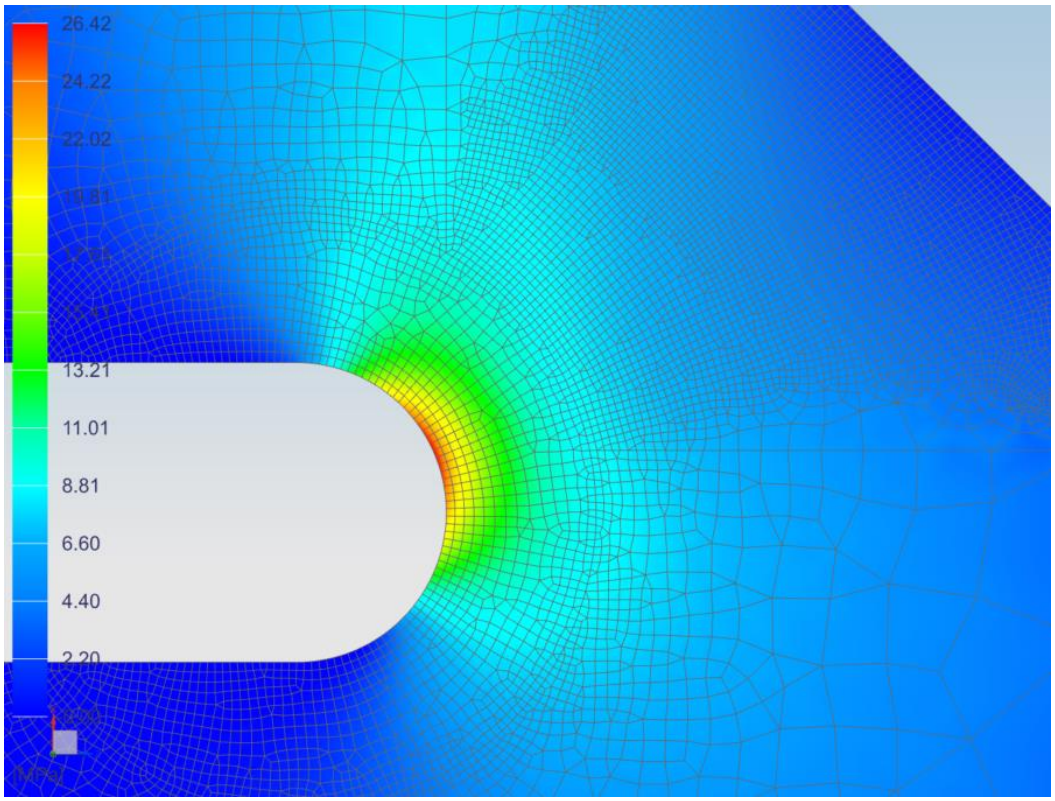

APPENDIX III

Linear elastic fracture mechanics theoretical calculations and comparison to Franc2D analysis result.

First K1 value is calculated by hand to see that Franc 2D model is working like it should be.

$a_i := 21$ $w := 30$ $\Delta\sigma := 100$

$n := \frac{a_i}{w} = 0.7$ Because the ratio is big Y value needs to be calculated and used in the K1 calculation.

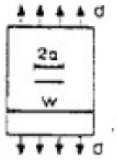

$$K_1 = \sigma\sqrt{\pi a}\left(\sec\frac{\pi a}{W}\right)^{1/2}$$

$$K_1 := \Delta\sigma\cdot\sqrt{\pi\cdot a_i}\cdot\left(\frac{\pi\cdot a_i}{w}\right)^{\left(\frac{1}{2}\right)} = 1205$$

KI value is in the Franc2D analysis 1156.2 in the first step.

APPENDIX IV

4R method calculation procedure.

$n := 0.15$ $E := 207000$

$H := 1.65 \cdot 520 = 858$ $\sigma_{res} := 200$ $\sigma_{weldnominal} := 418$

$K_t := 4.89$

$$\frac{\sigma_{min}}{E} + \left(\frac{\sigma_{min}}{H}\right)^{\frac{1}{n}} - \left[\frac{\left(K_t \cdot \sigma_{weldnominal} + \sigma_{res}\right)^2}{\sigma_{min} \cdot E}\right] \text{solve}, \sigma_{min} \rightarrow 534.97965599202098995 = 534.98$$

$\sigma_{min} := -534.98$

$$\frac{\Delta\sigma}{E} + \left[2\left(\frac{\Delta\sigma}{2H}\right)^{\frac{1}{n}}\right] - \left[\frac{\left(K_t \cdot \sigma_{weldnominal}\right)^2}{\Delta\sigma \cdot E}\right] \text{solve}, \Delta\sigma \rightarrow 856.33475275292075896 = 856.335$$

$\Delta\sigma := 856.335$

$\sigma_{max} := \sigma_{min} + \Delta\sigma = 321.355$

$$R_{local} := \frac{\sigma_{min}}{\sigma_{max}} = -1.665$$

$m_{ref} := 5.85$ $C_{ref} := 10^{20.83}$

$$N_{fc4R} := \frac{\left(\sqrt{1 - R_{local}}\right)^{m_{ref}} \cdot C_{ref}}{\Delta\sigma^{m_{ref}}} = 83001$$

$$N_{fcENS} := \frac{225^3 \cdot 2 \cdot 10^6}{\left(K_t \cdot \sigma_{weldnominal}\right)^3} = 2668$$

FAT$_c$ value scaling procedure to the typically used crane's runway application profile size.

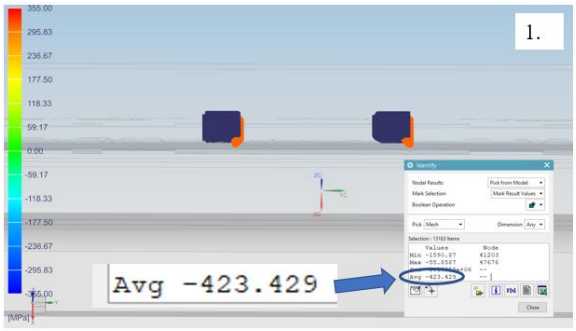

1. HEA340 is modelled in a way that there is same nominal stress in the rail connection weld than in the testing (66kN/cylinder force)

2. HEA340 top flange nominal stress is read from the model and used in the scaling

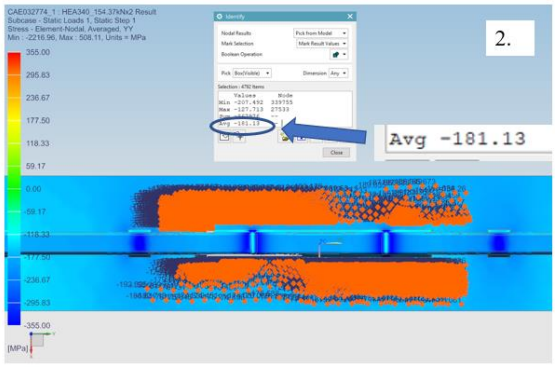

$FAT_{IIW97.7} := 53.96$ $\Delta\sigma := 153$ $\Delta\sigma_{topflangeHEA340} := 181.1$

This nominal stress value is taken from top flange by using FE-model. Span is choosed to be 6 000mm and used profile is HEA340. Cylinder distance is 800mm between each other.

In this situation the rail connection weld nominal stress is the same than in the testing. Therefore it is possible to make scaling between testing and a real size load-carrying beam.

$$N_f := \left(\frac{FAT_{IIW97.7}}{\Delta\sigma}\right)^3 \cdot 2 \cdot 10^6 = 87735$$

$$FAT_{realHEA340} := \left(\frac{N_f}{2 \cdot 10^6}\right)^{\frac{1}{3}} \cdot \Delta\sigma_{topflangeHEA340} = 63.87$$

Eurocode 3 regression analysis result. The used values of the rail connection weld A3. Nominal stress of the top flange is used.

D.7.2 Assessment via the characteristic value

Number of test points: 16

VX unknown (10 points), kn=	1.92	, It is assumed that Vx is unknown
γm =	1	
nd	1	
mx =	65.40	, FAT50% value from IIW result is used
sx =	1.318	, Standard deviation from IIW result is used. Calculation method is the same than EC3
Vx = sx/mx (D.3) clause		
Vx calculated =	0.020	, D.3
Vx =	0.100	, This value is the minium allowed based on the EN1990 standard instructions and it is used

$$X_d = \eta_d \frac{X_{k(n)}}{\gamma_m} = \frac{\eta_d}{\gamma_m} m_X \{1 - k_n V_X\} \qquad (D.1)$$

Xd = 52.8 , D.1

IIW recommendations regression analysis and used values of the rail connection weld A3. Nominal stress of the top flange is used.

n, testpoints= 16

Force/cylinder	Δσ in top flange [Mpa]	m	k1
66kN	153	3	2.06
75kN	174.5	3	2.06
60kN	138	3	2.06

Test piece code	Test piece number	Cycles to failure, Nf	Δσ in connection weld [Mpa]	y=log(Nf)	x=log(Δσ)	xy	x^2	log(Cmean)	log(Ci)	(log(Cmean)-Log(Ci))^2
A3-9 G	3	138482	153	5.14	2.18	11.23	4.77	11.75	11.70	0.0027
A3-9 G	3	161552	153	5.21	2.18	11.38	4.77	11.75	11.76	0.0002
A3-18 G	5	108301	153	5.03	2.18	11.00	4.77	11.75	11.59	0.0253
A3-17 G	4	138907	153	5.14	2.18	11.24	4.77	11.75	11.70	0.0026
A3-16 G	2	100856	153	5.00	2.18	10.93	4.77	11.75	11.56	0.0361
A3-16 G	2	188278	153	5.27	2.18	11.52	4.77	11.75	11.83	0.0066
A3-17 G	4	105357	153	5.02	2.18	10.97	4.77	11.75	11.58	0.0292
A3-18 G	5	107686	153	5.03	2.18	10.99	4.77	11.75	11.59	0.0261
A3-7	6	211865	153	5.33	2.18	11.64	4.77	11.75	11.88	0.0175
A3-7	6	242648	153	5.38	2.18	11.76	4.77	11.75	11.94	0.0366
A3-6	7	143769	174.2	5.16	2.24	11.56	5.02	11.75	11.88	0.0177
A3-6	7	140596	174.2	5.15	2.24	11.54	5.02	11.75	11.87	0.0152
A3-11	8	104901	174.2	5.02	2.24	11.25	5.02	11.75	11.74	0.0000
A3-11	8	110357	174.2	5.04	2.24	11.30	5.02	11.75	11.77	0.0003
A3-2	1	221194	138	5.34	2.14	11.44	4.58	11.75	11.76	0.0003
A3-2	1	254110	138	5.41	2.14	11.57	4.58	11.75	11.82	0.0059

SUM values	
x	35.09
y	82.69
xy	181.32
x^2	76.98
(log(Cmean-Log(Ci))^2	0.22
k=	-3.00
b=	11.75
FAT, 50%=	**65.40**
Stdv	0.12
LOGCchar	11.50
FAT, 97.7%	**53.96**

IIW recommendations regression analysis and used values of the rail connection weld A3. Nominal stress of the A3 rail connection weld is used.

n, testpoints=	16													
Force/cylinder	Δσ in top flange [Mpa]	m	k1											
66kN	153	3	2.06											
75kN	174.5	3	2.06											
60kN	138	3	2.06											
	Test piece code	Test piece number	Cycles to failure, Nf	Δσ in connection weld [Mpa]	y=log(Nf)	x=log(Δσ)	xy	x^2	log(Cmean)	log(Ci)	(log(Cmean)-Log(Ci))^2		SUM values	
	A3-9 G	3	138482	417.5	5.14	2.62	13.47	6.87	13.06	13.00	0.0028		x	42.07
	A3-9 G	3	161552	417.5	5.21	2.62	13.65	6.87	13.06	13.07	0.0002		y	82.69
	A3-18 G	5	108301	417.5	5.03	2.62	13.19	6.87	13.06	12.90	0.0255		xy	217.39
	A3-17 G	4	138907	417.5	5.14	2.62	13.48	6.87	13.06	13.00	0.0027		x^2	110.63
	A3-16 G	2	100856	417.5	5.00	2.62	13.11	6.87	13.06	12.87	0.0363		(log(Cmean-Log(Ci))^2	0.22
	A3-16 G	2	188278	417.5	5.27	2.62	13.82	6.87	13.06	13.14	0.0065		k=	-3.00
	A3-17 G	4	105357	417.5	5.02	2.62	13.16	6.87	13.06	12.88	0.0294		b=	13.06
	A3-18 G	5	107686	417.5	5.03	2.62	13.19	6.87	13.06	12.89	0.0263		**FAT, 50%=**	**178.53**
	A3-7	6	211865	417.5	5.33	2.62	13.96	6.87	13.06	13.19	0.0174		Stdv	0.12
	A3-7	6	242648	417.5	5.38	2.62	14.11	6.87	13.06	13.25	0.0364		LOGCchar	12.81
	A3-6	7	143769	474.4	5.16	2.68	13.80	7.16	13.06	13.19	0.0169		**FAT, 97.7%**	**147.27**
	A3-6	7	140596	474.4	5.15	2.68	13.78	7.16	13.06	13.18	0.0145			
	A3-11	8	104901	474.4	5.02	2.68	13.44	7.16	13.06	13.05	0.0000			
	A3-11	8	110357	474.4	5.04	2.68	13.50	7.16	13.06	13.07	0.0002			
	A3-2	1	221194	379.5	5.34	2.58	13.79	6.65	13.06	13.08	0.0007			
	A3-2	1	254110	379.5	5.41	2.58	13.94	6.65	13.06	13.14	0.0075			

IIW recommendations regression analysis and used values of the intermittent fillet weld. Nominal stress of intermittent fillet weld is used.

n, testpoints=	16													SUM values	
Force/cylinder 66kN	Δσ	m	k1											x	34.66
	146.67	3	2.06											y	93.64
				Δσ intermittent fillet weld [Mpa]	**y=log(Nf)**	**x=log(Δσ)**	**xy**	**x^2**	**log(Cmean)**	**log(Ci)**	**(log(Cmean)-Log(Ci))^2**			xy	202.85
	Test piece code	**Test piece number**	**Cycles to failure, Nf**											x^2	75.09
														(log(Cmean-Log(Ci))^2	0.22
	A3-9 G	3	904856	146.67	5.96	2.17	12.90	4.69	12.35	12.46	0.0108			k=	-3.00
	A3-9 G	3	904856	146.67	5.96	2.17	12.90	4.69	12.35	12.46	0.0108			b=	12.35
	A3-9 G	3	904856	146.67	5.96	2.17	12.90	4.69	12.35	12.46	0.0108			**FAT, 50%=**	**103.95**
	A3-9 G	3	904856	146.67	5.96	2.17	12.90	4.69	12.35	12.46	0.0108				
	A3-18 G	5	500008	146.67	5.70	2.17	12.35	4.69	12.35	12.20	0.0236			**Stdv**	**0.12**
	A3-17 G	4	605182	146.67	5.78	2.17	12.53	4.69	12.35	12.28	0.0050			LOGCchar	12.11
	A3-16 G	2	938440	146.67	5.97	2.17	12.94	4.69	12.35	12.47	0.0144			**FAT, 97.7%**	**86.05**
	A3-16 G	2	938440	146.67	5.97	2.17	12.94	4.69	12.35	12.47	0.0144				
	A3-17 G	4	605182	146.67	5.78	2.17	12.53	4.69	12.35	12.28	0.0050				
	A3-18 G	5	500008	146.67	5.70	2.17	12.35	4.69	12.35	12.20	0.0236				
	A3-18 G	5	500008	146.67	5.70	2.17	12.35	4.69	12.35	12.20	0.0236				
	A3-18 G	5	500008	146.67	5.70	2.17	12.35	4.69	12.35	12.20	0.0236				
	A3-17 G	4	605182	146.67	5.78	2.17	12.53	4.69	12.35	12.28	0.0050				
	A3-17 G	4	605182	146.67	5.78	2.17	12.53	4.69	12.35	12.28	0.0050				
	A3-16 G	2	938440	146.67	5.97	2.17	12.94	4.69	12.35	12.47	0.0144				
	A3-16 G	2	938440	146.67	5.97	2.17	12.94	4.69	12.35	12.47	0.0144				

Eurocode 3 regression analysis result. The used values of the three-side welded rail connection weld A2. Nominal stress of the top flange is used.

D.7.2 Assessment via the characteristic value

Number of test points:	10	
VX unknown (10 points)	1.92	, It is assumed that Vx is unknown
γm =	1	
nd	1	
mx =	83.44	, FAT50% value from IIW result is used

$$V_x = s_x / m_x \qquad \text{(D.3)}$$

sx =	1.288	, Standard deviation from IIW result is used. Calculation method is the same than EC3
Vx calculated=	0.015	, D.3
Vx =	0.100	, This is the minium allowed value based on the EN1990 standard instructions and it is used

$$X_d = \eta_d \frac{X_{k(n)}}{\gamma_m} = \frac{\eta_d}{\gamma_m} m_X \{1 - k_n V_X\} \qquad \text{(D.1)}$$

Xd =	**67.420**	, D.1

IIW recommendations regression analysis and used values of the three-side welded rail connection weld A2. Nominal stress of the top flange is used.

n, testpoints=	10												
Force/cylinder	Δσ in top flange [Mpa]	m	k1	Test piece code	Cycles to failure, Nf	Δσ in connection weld [Mpa]	y=log(Nf)	x=log(Δσ)	xy	x^2	log(Cmean)	log(Ci)	(log(Cmean)-Log(Ci))^2	SUM values	
75kN	174.2	3	2.17											x	22.01
60kN	138	3	2.17											y	54.63
				A2-1	353578	138	5.55	2.14	11.87	4.58	12.07	11.97	0.0094	xy	120.18
				A2-1	360527	138	5.56	2.14	11.89	4.58	12.07	11.98	0.0078	x^2	48.45
				A2-2	264204	174.2	5.42	2.24	12.15	5.02	12.07	12.15	0.0064	(log(Cmean-Log(Ci))^2	0.11
				A2-2	270807	174.2	5.43	2.24	12.17	5.02	12.07	12.16	0.0082	k=	-3.00
				A2-3	297211	138	5.47	2.14	11.71	4.58	12.07	11.89	0.0297	b=	12.07
				A2-3	497214	138	5.70	2.14	12.19	4.58	12.07	12.12	0.0026	**FAT, 50%=**	**83.44**
				A2-4	203441	174.2	5.31	2.24	11.90	5.02	12.07	12.03	0.0011		
				A2-4	232174	174.2	5.37	2.24	12.03	5.02	12.07	12.09	0.0006	LOG(Stdv)	0.11
				A2-5	192256	174.2	5.28	2.24	11.84	5.02	12.07	12.01	0.0034	LOGCchar	11.82
				A2-5	351595	174.2	5.55	2.24	12.43	5.02	12.07	12.27	0.0416	**FAT, 97.7%**	**69.38**

Material certificates.

A10 **Sales Agent:**
ArcelorMittal Commercial
Long Finland OY
Topeliuksenkatu 15
FI-00250 HELSINKI

A01 **Plant:**
ArcelorMittal Belval & Differdange
Site de Belval
L-4008 Esch/Alzette

A04
ArcelorMittal Belval & Differdange
Service Gestion Qualité
66, rue de Luxembourg
L-4009 Esch/Alzette
A06

Certificate Nr X4017111

Delivery note number 4017111 from 20 June 2019 A03

A08 Our reference : 1100570324
A07 Your reference : 1112978
04.06.2019
OY KONTINO AB

OY KONTINO AB
PO Box 27
FI-01301 VANTAA
A05

S355J2+M ACCORDING TO EN 10025-2/2004 CEV=0,43%MAX,14 CHEM EL, SUITABLE FOR GALVANISATION
B02

Inspection certificate according to EN 10204:2004 / 3.1
A02

Ord.item	B01 Product	Length	B13 Weight	B07 Heat nr	Weight	Bund.	B05 Bars
000002	HE 160 A	12.100 mm	16,553 to	84887	11,035 to		30
				84891	4,414 to		12
				84892	1,104 to		3
000003	HE 160 A	15.100 mm	10,557 to	84891	10,557 to		23

Heat nr B07	Heat analysis (%) C	Mn	P	S	Si	N	Al	Cu	Ni	Cr	V	Nb	Mo	Ti	CEV
Min					0,14										
Max	0,20	1,60	0,030	0,030	0,25			0,55				0,060			0,43
84887	0,08	1,14	0,029	0,019	0,17	0,009	0,002	0,37	0,14	0,12	0,006	0,035	0,030	0,022	0,34
84891	0,08	1,14	0,024	0,021	0,17	0,010	0,001	0,41	0,17	0,13	0,006	0,036	0,050	0,022	0,35
84892	0,08	1,13	0,026	0,025	0,17	0,009	0,002	0,41	0,16	0,12	0,006	0,036	0,060	0,023	0,34

Heat nr	Tensile test			Charpy impact test						
	N/mm2	N/mm2	5,65VS	C40 KV		UNAGED			J	
	ReH	Rm	A(%)	Position	mm	°C	1	2	3	M
B07	C11	C12	C13	C01	C02	C41	C03	C42		C43
Min	355	470	22,00	FL.1/3	L		-20	14		20
Max		630								
84887	405	503	30,92	FL.1/3	L	7,5	-20	116	110	155	127
84891	416	518	30,62	FL.1/3	L	7,5	-20	133	149	132	138
84892	422	522	28,42	FL.1/3	L	7,5	-20	145	119	142	135

Z05
Hot rolled products of structural steels according to EN10025-1:2004
Intended uses : Building constructions or civil engineering
Durability : No performance determined
Regulated substance : No performance determined
Weldability : according to EN 1011-2
EAF-Steel

Klecker Roberto
Porteur de signature spéciale
Z03

Z04
CE
0769
06

Code of the product type: 1.0577 / DOP: AMEB-2/09-CPR-13-1

EN 10168:2004

Material certificates.

RIVA ACCIAIO S.P.A.
STABILIMENTO DI CERVENO
Loc. Nisole
25040 Cerveno(BS) ITALIA
Tel. 0364-627211 Fax. 0364-433986

Sede legale e amministrativa: Viale Certosa, 249 - 20151 Milano
telefono 02 30700 - telefax 032 38000346 - 38003147 - 38002974
codice fiscale, partita iva e numero iscrizione Registro Imprese Milano 08521290158

INSPECTION CERTIFICATE

A03 Certificate number: 48427
Certificate date: 27/11/2018

WE CERTIFY THAT THE PRODUCT CONCERNING THIS DOCUMENT IS IN ACCORDANCE WITH THE ORDER REQUIREMENTS

B14 Standard Reference: UNI EN 10204/2005
B15 Type: 3.1

B02 Steel Grade: S355J2 EN10025-2 profi
B07 Year/Heat number: 18/39918
A06 Customer Data: EMMECI S.R.L. VIA BRERA, 16 20121 MILANO

B01 Shape: FLAT
B09 Dim. 1 X Dim. 2: 50.00 X 30.00

B04 Delivery Condition: 10025
B09 Length: 12.000
C70 Process: EAF MELTING SUBMERGED CC 160

A07 Client Order: 34/2018
A08 Confirmation: 07 UN156 001
C14 Reduction Rate: 17.07

CHEMICAL ANALYSIS - CAST ANALYSIS

C71 C	C72 Mn	C73 Si	C74 P	C75 S	C76 Cr	C77 Ni	C78 Mo	C79 Cu	C80 Sn	C85 Al	C91 Ti
0.190	1.290	0.210	0.010	0.008	0.170	0.070	0.030	0.130	0.005	0.022	0.011

C87 V	C88 Nb	C89 B	C92 Ca				C83 N	C94 $O_{2[ppm]}$	C95 $H_{2[ppm]}$		C96 CEV
0.002	0.001	0.0000					0.0095				0.46

MECHANICAL PROPERTIES

C01 Test: L - Rolled
C03 Heat Treatment: SPECIMEN AS ROLLED

TENSILE TEST

C08 Sample Dim.	C10 Test Dim.	C12 R_{eH} [MPa]	C17 R_{eL} [MPa]	C13 $A5_{\%}$	C15 $Z_{\%}$	C22 HB
	10	572	380	28.8		

IMPACT TEST

C07 Test Dim.	C40 Type	C42 $K_{1/3}$	C42 $K_{2/3}$	C42 $K_{3/3}$	C43 $K_{1/3}$	C44 Temp
10x10	KV	110.0	113.0	116.0	113.0	-20°C

JOMINY TEST

C03 Normalizing / Hardening

C61 mm																		C45 DI
C60 HRC																		

C65 Austenitic Grain Size: MAC QUAID - EHN 6
C62 Micro Inclusion Rating:
C05 Banded Structure:
C31 Hardness: +AR | +A | +FP

ADDITIONAL INFORMATION

B03
RETTILINEITA' 1.5 MM/M MAX
FIXED L. > 10 TONS

127286

Kontino Oy Ab

D51 Remarks:

ELECTRONIC DOC VALID WITHOUT SIGNATURE

A10 DDT Data
N° 13600

Z04
CE
RIVA ACCIAIO S.P.A. STABILIMENTO DI CERVENO
25040 Loc. Nisole Cerveno(BS)
06
1608-CPR-P053
EN 10025-1
Steel S355J2 EN 10025-2

Z01 Q.C. Manager: G.B. Vaira

Z02

Material certificates.

RIVA ACCIAIO S.P.A.
STABILIMENTO DI CERVENO
Loc. Nisole
25040 Cerveno(BS) ITALIA
Tel. 0364-627211 Fax. 0364-433986

Sede legale e amministrativa: Viale Certosa, 249 - 20151 Milano
telefono 02 30700 - telefax 032 38000346 - 38003147 - 38002974
codice fiscale, partita iva e numero iscrizione Registro Imprese Milano 08521290158

INSPECTION CERTIFICATE

A03 Certificate number: 84922
Certificate date: 03/05/2019

WE CERTIFY THAT THE PRODUCT CONCERNING THIS DOCUMENT IS IN ACCORDANCE WITH THE ORDER REQUIREMENTS

B14 Standard Reference: UNI EN 10204/2005
B15 Type: 3.1

B02 Steel Grade: S355J2 EN10025-2 profi
B07 Year/Heat number: 19/41054
A06 Customer Data: EMMECI S.R.L.
VIA BRERA, 16
20121 MILANO

B01 Shape: FLAT
B09 Dim. 1 X Dim. 2: 50,00 X 30,00

B04 Delivery Condition: 10025
B09 Length: 12,000
C70 Process: EAF MELTING
SUBMERGED CC 160

A07 Client Order: 56/2018
A08 Confirmation: 07 UT432 001
C14 Reduction Rate: 17,07

CHEMICAL ANALYSIS - CAST ANALYSIS

C71 C	C72 Mn	C73 Si	C74 P	C75 S	C76 Cr	C77 Ni	C78 Mo	C79 Cu	C80 Sn	C86 Al	C91 Ti
0,170	1,310	0,250	0,017	0,010	0,120	0,050	0,010	0,120	0,008	0,028	0,013

C87 V	C88 Nb	C89 B	C92 Ca				C93 N	C94 $O_{2(ppm)}$	C95 $H_{2(ppm)}$		C96 CEV
		0,0000					0,0103				0,43

MECHANICAL PROPERTIES

C01 Test: L
C03 Heat Treatment: SPECIMEN AS ROLLED

TENSILE TEST

C09 Sample Dim.	C10 Test Dim.	C12 R_{m} [MPa]	C11 R_{e} [MPa]	C13 $A5_{\%}$	C18 $Z_{\%}$	
	10	592	385	27,9		

IMPACT TEST

C41 Test Dim.	C40 Type	C42 $K_{1[J]}$	C42 $K_{2[J]}$	C42 $K_{3[J]}$	C42 $K_{v[J]}$	C44 Temp.
10x10	KV	111,0	116,0	118,0	115,0	-20°C

C22 HB

JOMINY TEST

C03 Normalizing / Hardening

C01 mm																				C45 DI
C03 HRC																				

C65 Austenitic Grain Size: MAC QUAID - EHN 6
C62 Micro Inclusion Rating:

C05 Banded Structure:
C31 Hardness: +AR | +A | +FP

ADDITIONAL INFORMATION

B03
RETTILINEITA' 1.5 MM/M MAX
FIXED L. > 10 TONS

D51 Remarks:

ELECTRONIC DOC VALID WITHOUT SIGNATURE

A10 DDT Data
Nº 4975

Z04 CE
RIVA ACCIAIO S.P.A. STABILIMENTO DI CERVENO
25040 Loc. Nisole Cerveno(BS)
06
1608-CPR-P053
EN 10025-1
Hot rolled structural steel products
Intended uses: Building construction or civil engineering
Tolerances on dimensions and shape:
Elongation
Tensile strength
Yield strength
Impact strength
Weldability
Durability: No performance determined
Regulated substance: No performance determined
Steel
S355J2
EN 10025-2

Z01 Q.C. Manager: G.B. Vaira
Z02

APPENDIX XIII

HEA160 and HEA340 dimensions.

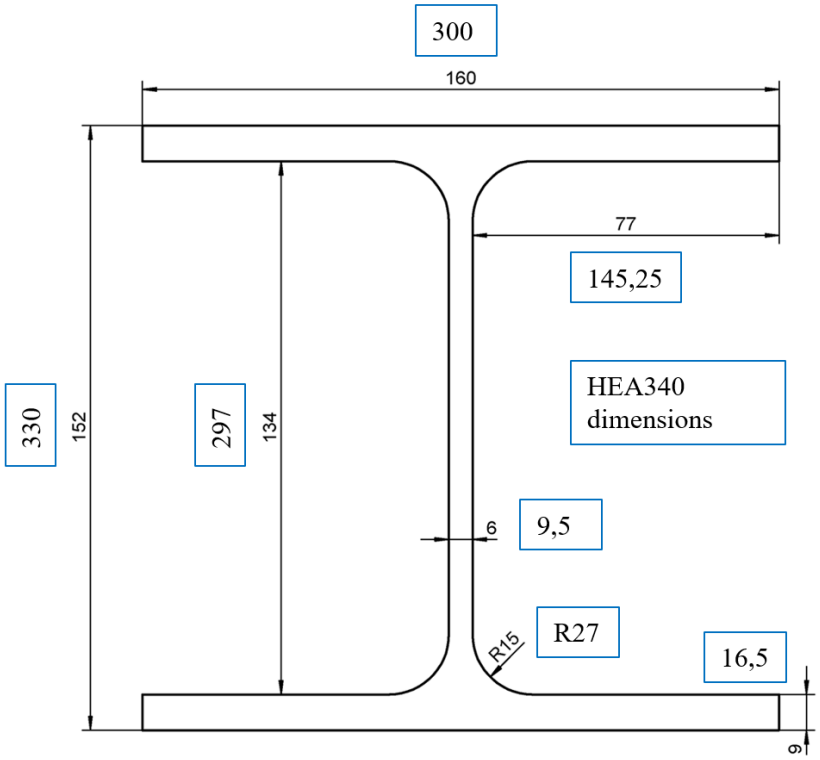

Test result FAT_c value scaled to the real size application by using analytical equations. The example is the top welded rail connection weld.

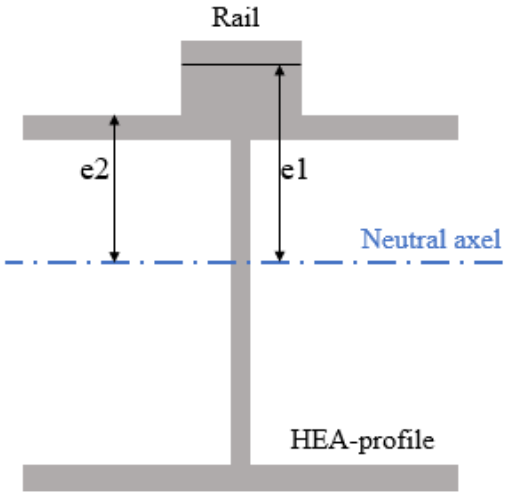

$I_{HEA160rail} := 24885588$ $I_{HEA340rail} := 307799774.6$

$neutralaxel_{HEA160rail} := 102.3$ $neutralaxel_{HEA340rail} := 184.0$

Height of HEA160 = 152 Height of HEA340 = 330

Rail connection weld (A3) root location from top flange = 21

$e1_{weldrootHEA160} := 152 + 21 - neutralaxel_{HEA160rail} = 70.7$

$e2_{TopflangeHEA160} := 152 - neutralaxel_{HEA160rail} = 49.7$

$e1_{weldrootHEA340} := 330 + 21 - neutralaxel_{HEA340rail} = 167$

$e2_{TopflangeHEA340} := 330 - neutralaxel_{HEA340rail} = 146$

$$W_{HEA160weldroot} := \frac{I_{HEA160rail}}{e1_{weldrootHEA160}} = 3.52 \times 10^5$$

$$W_{HEA160topflange} := \frac{I_{HEA160rail}}{e2_{TopflangeHEA160}} = 5.007 \times 10^5$$

$$W_{HEA340weldroot} := \frac{I_{HEA340rail}}{e1_{weldrootHEA340}} = 1.843 \times 10^6$$

$$W_{HEA340topflange} := \frac{I_{HEA340rail}}{e2_{TopflangeHEA340}} = 2.108 \times 10^6$$

Test result FATc value scaled to the real size application by using analytical equations.

The studied test situation is 66kN/cylinder force:

$$M_{test66kN} := \frac{(3000 - 800)}{2} \cdot 75000 = 8.25 \times 10^{7}$$

$$\sigma_{HEA160weldroot} := \frac{M_{test66kN}}{W_{HEA160weldroot}} = 234.383$$

$$\sigma_{HEA160Topflange} := \frac{M_{test66kN}}{W_{HEA160topflange}} = 164.764$$

Then Mscaled value needs to be calculated to get correct moment value to get same stress level in the rail connection weld in HEA340 beam than in the testing with HEA160 beam.

$$M_{scaled} := \sigma_{HEA160weldroot} \cdot W_{HEA340weldroot} = 4.32 \times 10^{8}$$

Now the nominal stresses are calculated in the HEA340 beam runway application:

$$\sigma_{HEA340weldroot} := \frac{M_{scaled}}{W_{HEA340weldroot}} = 234.383$$

$$\sigma_{HEA340Topflange} := \frac{M_{scaled}}{W_{HEA340topflange}} = 204.909$$

Finally characteristic FAT class based on fatigue test results is scaled to real size runway application situation by using top flange nominal stress like in the EN13001 standard:

$$FAT_{IIW97.7tests} := 53.96$$

$$\Delta\sigma_{HEA160Topflange} := 183.66 \qquad \Delta\sigma_{HEA340Topflange} := 228.41$$

$$N_f := \left(\frac{FAT_{IIW97.7tests}}{\Delta\sigma_{HEA160Topflange}}\right)^{3} \cdot 2 \cdot 10^{6} = 50723$$

$$FAT_{realHEA340} := \left(\frac{N_f}{2 \cdot 10^{6}}\right)^{\frac{1}{3}} \cdot \Delta\sigma_{HEA340Topflange} = 67.108$$

Hardness test (HV5) results.

	Intermittent fillet weld, weld root			**Intermittent fillet weld, weld top**	
Measuring point	Distance from the starting point of measurement	HV5 Hardness	Measuring point	Distance from the starting point of measurement	HV5 Hardness
1	0,000	157	1	0,000	157
2	1,000	160	2	1,000	161
3	2,000	174	3	2,000	175
4	2,500	252	4	2,500	232
5	3,000	365	5	3,000	287
6	3,500	342	6	3,500	387
7	4,000	244	7	4,000	404
8	5,000	252	8	4,500	262
9	6,000	255	9	5,500	250
10	6,500	258	10	6,500	251
11	7,000	262	11	7,500	252
12	7,500	265	12	8,500	258
13	8,000	242	13	9,500	258
14	8,500	234	14	10,500	255
15	9,000	220	15	11,000	259
16	9,500	206	16	11,500	255
17	10,000	198	17	12,000	216
18	10,500	193	18	12,500	197
19	11,500	184	19	13,500	180
20	12,500	182	20	14,500	169
21	13,500	174	21	15,500	170

Hardness test (HV5) results.

	A3 rail connection weld, weld root			**A3 rail connection weld, weld top**	
Measuring point	Distance from the starting point of measurement	HV5 Hardness	Measuring point	Distance from the starting point of measurement	HV5 Hardness
1	0,000	181	1	0,000	178
2	1,000	180	2	1,000	181
3	2,000	181	3	2,000	247
4	3,000	183	4	2,500	276
5	4,000	184	5	3,000	332
6	5,000	204	6	3,500	353
7	5,500	220	7	4,000	330
8	6,000	239	8	4,500	243
9	6,500	258	9	5,000	226
10	7,000	281	10	5,500	234
11	7,500	287	11	6,500	240
12	8,000	257	12	8,000	231
13	8,500	238	13	9,500	234
14	9,500	232	14	11,000	229
15	10,500	232	15	12,500	224
16	11,500	210	16	14,000	229
17	12,000	321	17	15,000	248
18	12,500	277	18	16,000	314
19	13,000	229	19	16,500	377
20	13,500	196	20	17,000	374
21	14,500	188	21	17,500	349
22	15,500	172	22	18,000	285
23	16,500	173	23	18,500	258
			24	19,000	206
			25	19,500	189
			26	20,500	186
			27	21,500	187
			28	22,500	181

Hardness test (HV5) results.

Vertical weld of A2 rail connection weld, middle of the weld

Measuring point	Distance from the starting point of measurement	HV5 Hardness
1	0,000	163
2	1,000	164
3	2,000	186
4	2,500	200
5	3,000	219
6	3,500	222
7	4,000	231
8	4,500	243
9	5,000	257
10	5,500	273
11	6,000	297
12	6,500	297
13	7,000	308
14	7,500	320
15	8,000	220
16	8,500	219
17	9,500	219
18	10,500	221
19	11,500	225
20	12,500	220
21	13,500	228
22	14,500	225
23	15,500	222
24	16,000	244
25	16,500	296
26	17,000	281
27	17,500	273
28	18,000	267
29	18,500	239
30	19,000	226
31	19,500	222
32	20,000	215
33	20,500	215
34	21,000	204
35	21,500	194
36	22,500	166
37	23,500	163
38	24,500	161

Relevant strain gauges data of the fatigue test specimens.

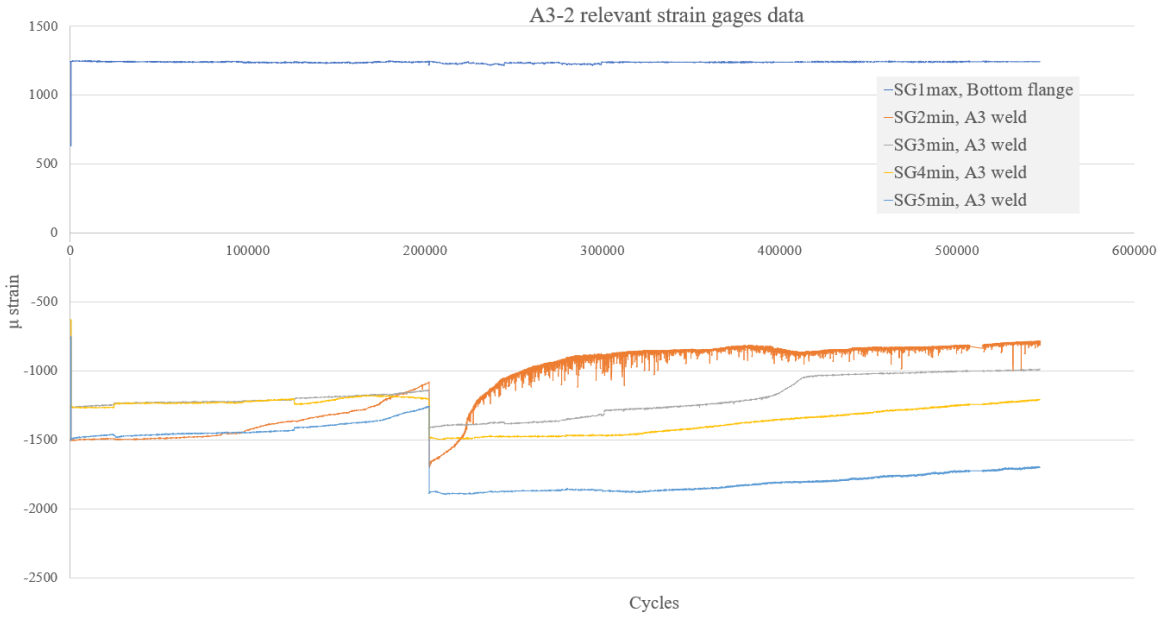

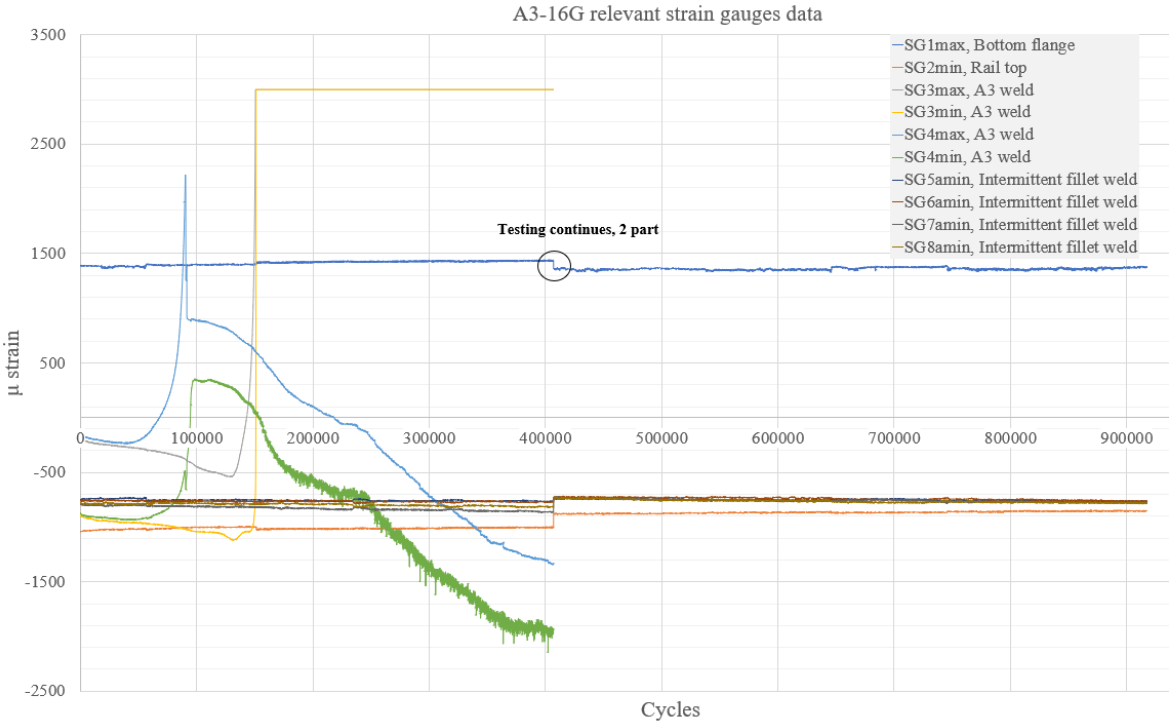

Relevant strain gauges data of the fatigue test specimens.

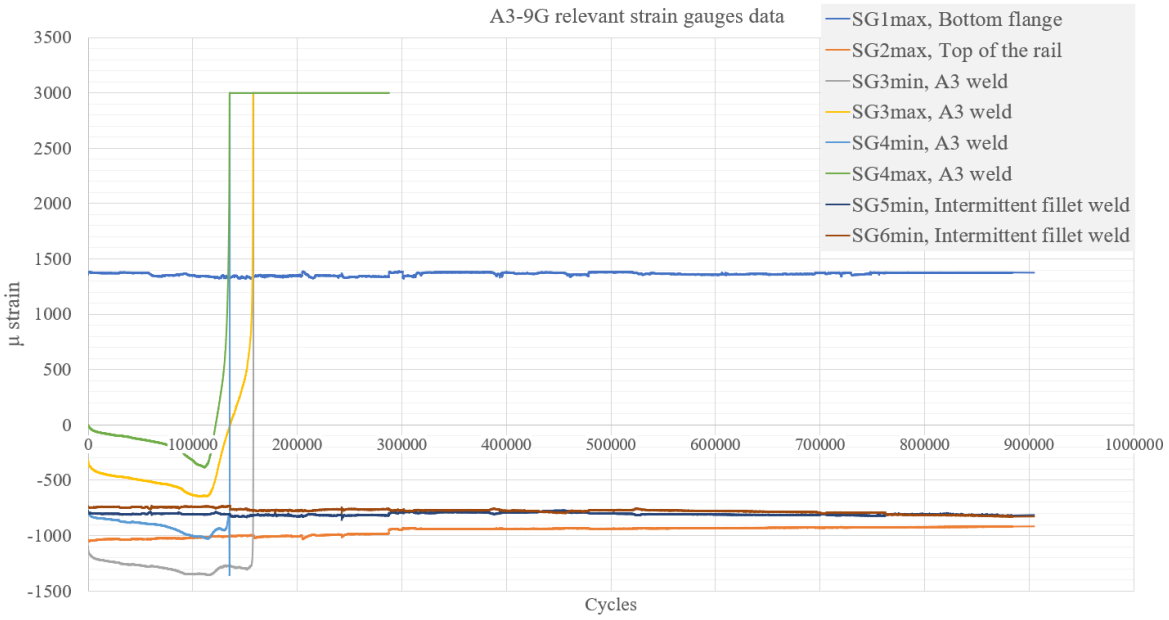

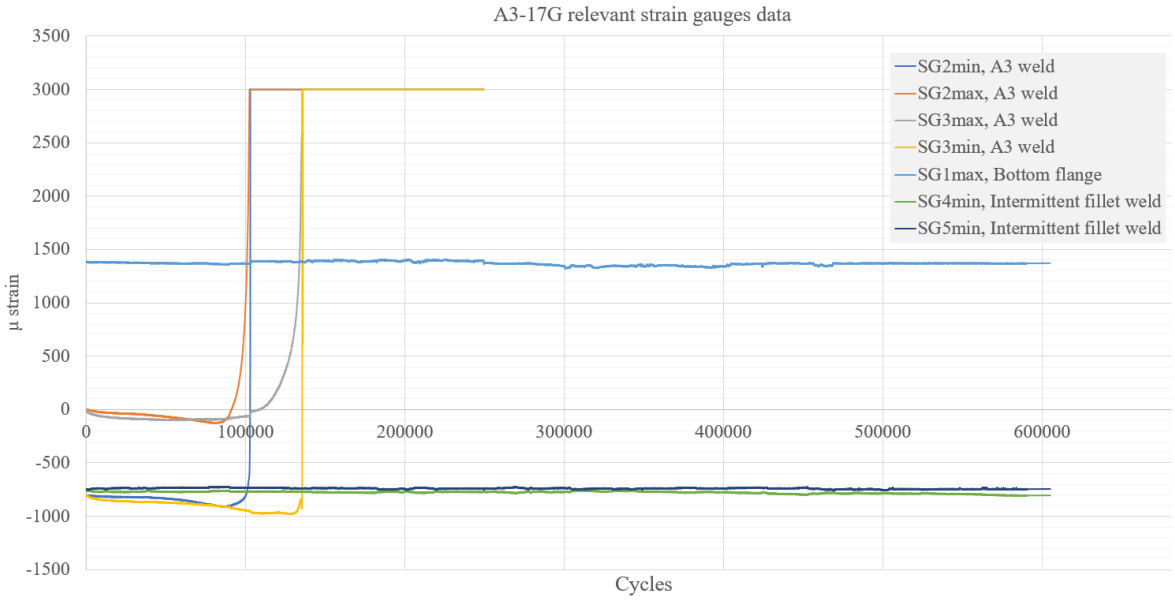

Relevant strain gauges data of the fatigue test specimens.

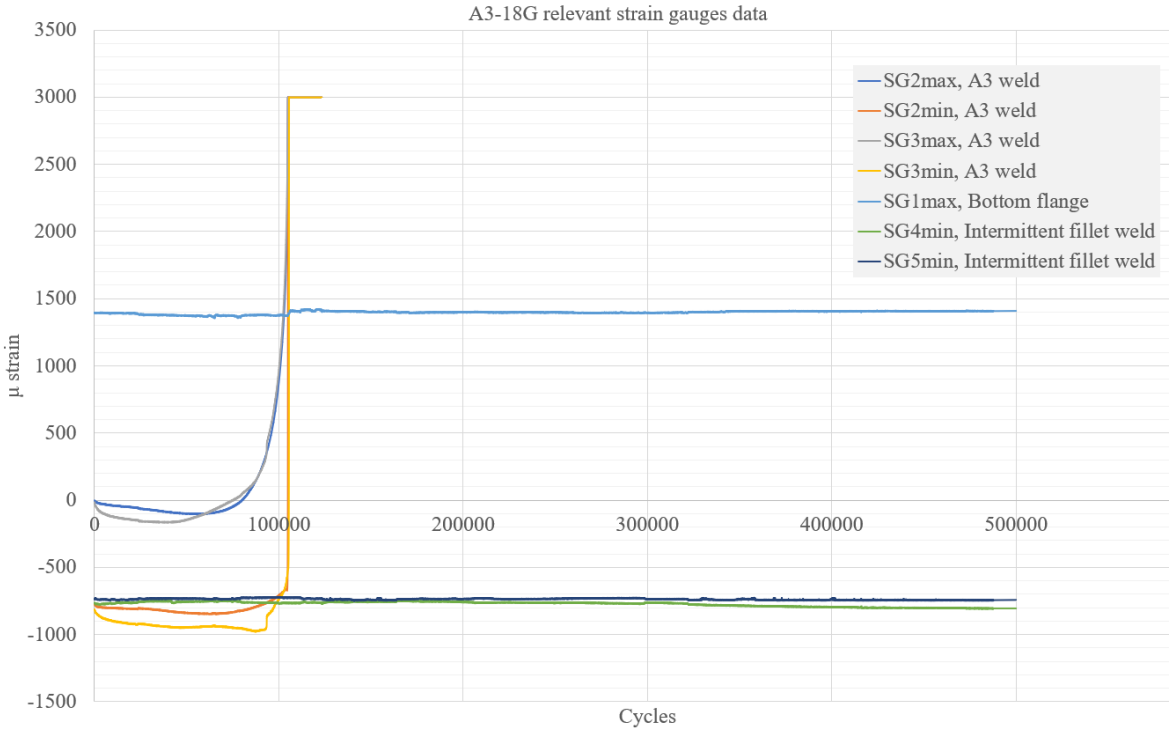

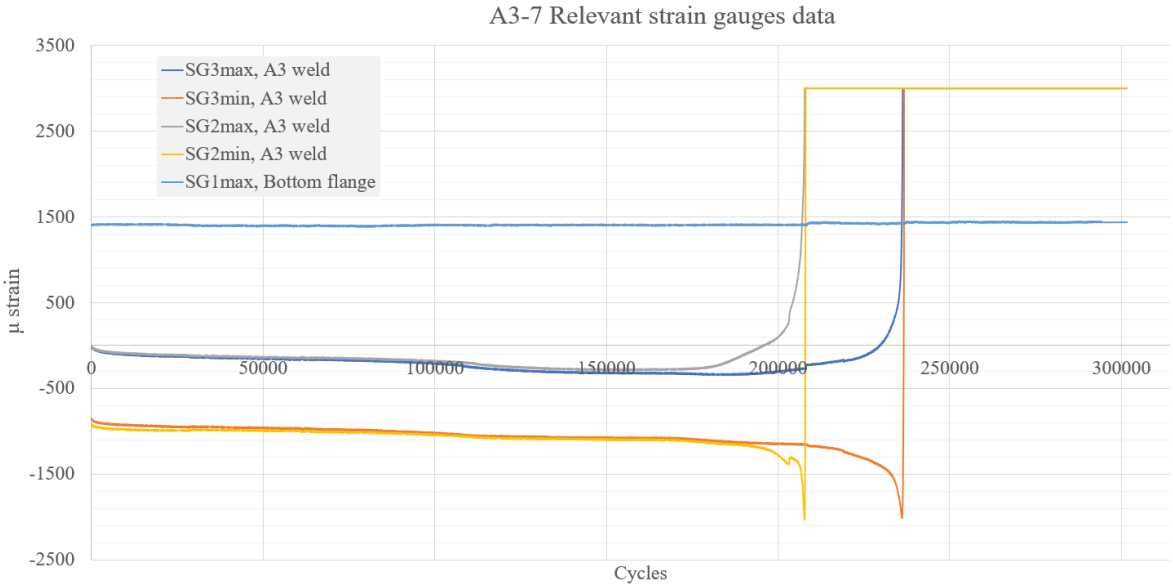

Relevant strain gauges data of the fatigue test specimens.

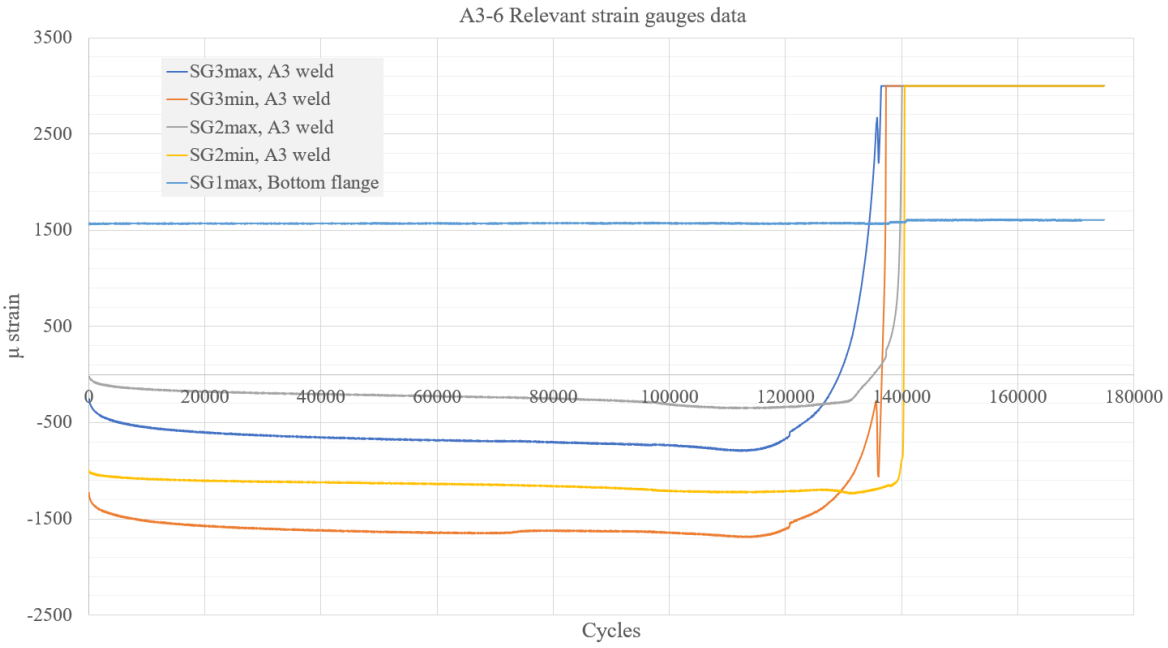

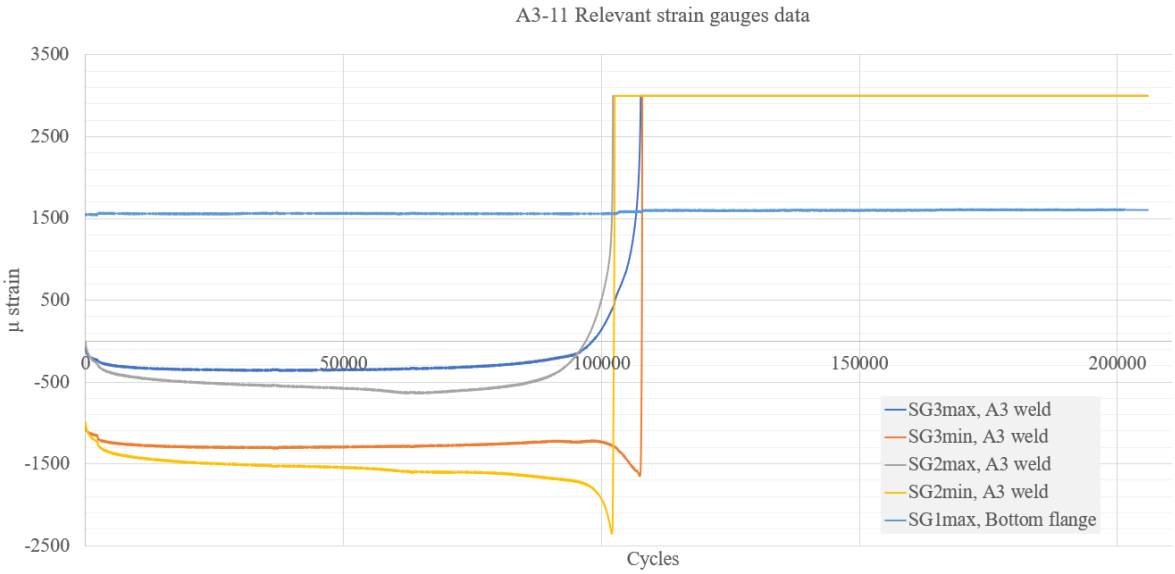

Relevant strain gauges data of the fatigue test specimens.

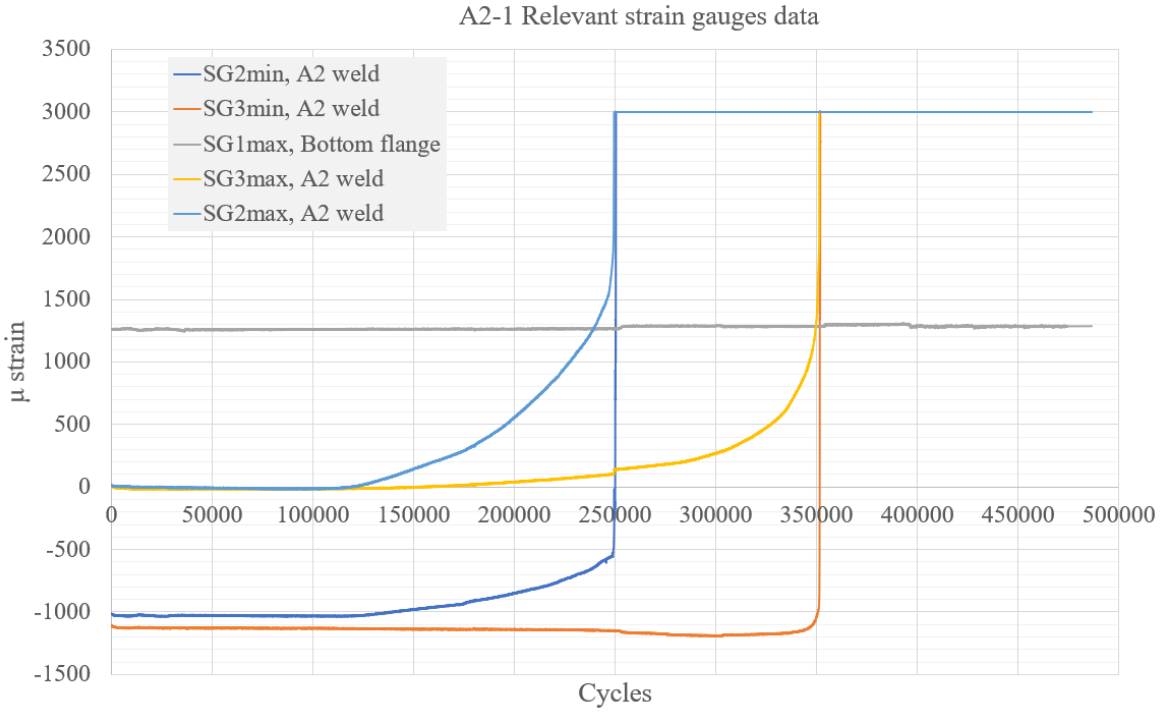

Fatigue failures have happened in 353 578 cycles and 360 527 cycles. Laboratory staff observations have been used.

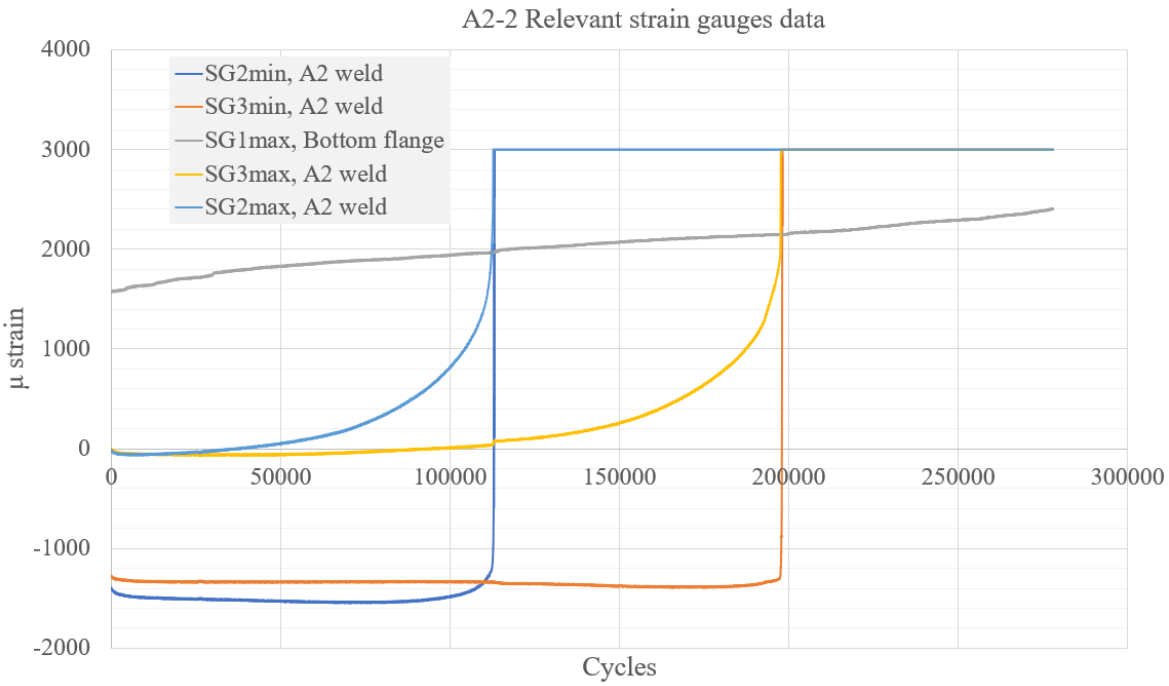

Fatigue failures have happened in 264 204 cycles and 270 807 cycles. Laboratory staff observations have been used. SG1 strain gauge has damaged during fatigue testing.

Relevant strain gauges data of the fatigue test specimens.

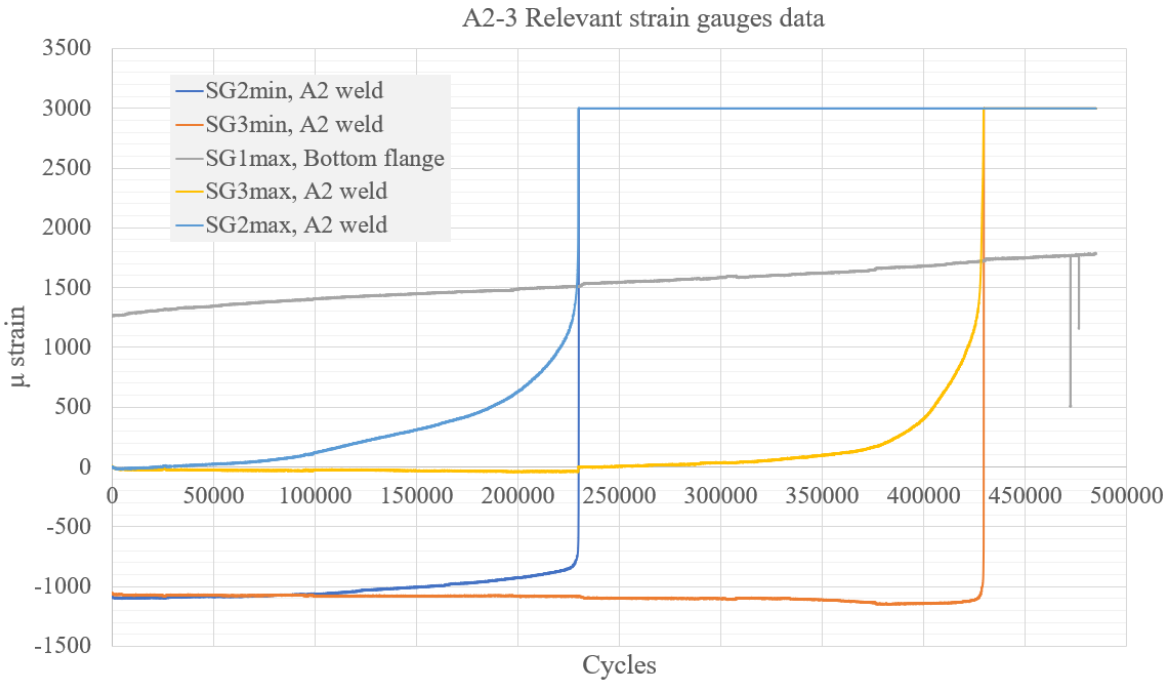

Fatigue failures have happened in 297 211 cycles and 497 214 cycles. Laboratory staff observations have been used.

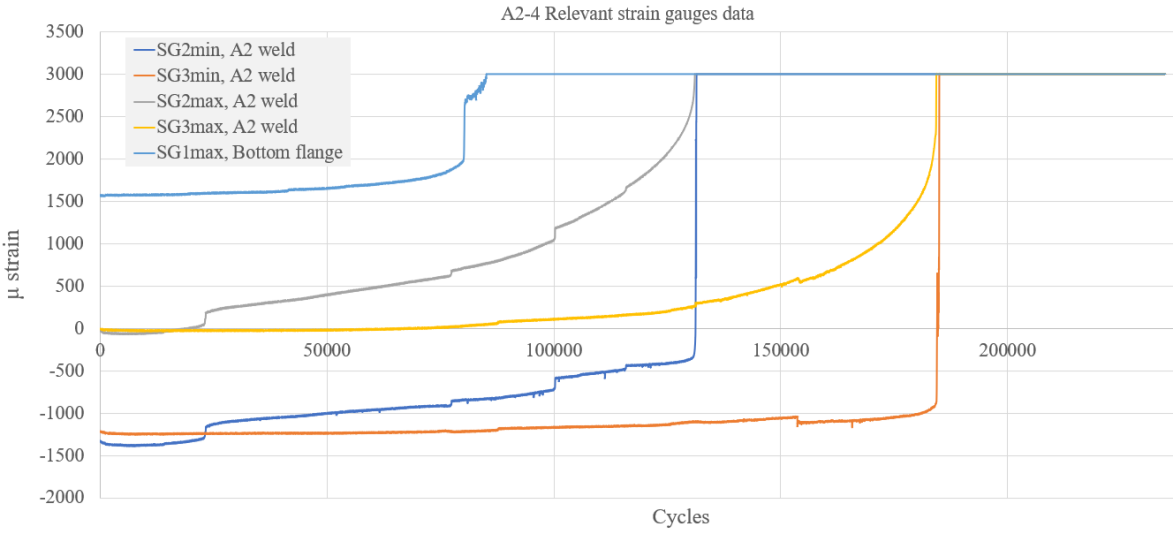

Fatigue failures have happened in 203 441 cycles and 232 174 cycles. Laboratory staff observations have been used. The problem in the strain gauges measurements machine and the strain gauges data is defective after 20 000 cycles.

Relevant strain gauges data of the fatigue test specimens.

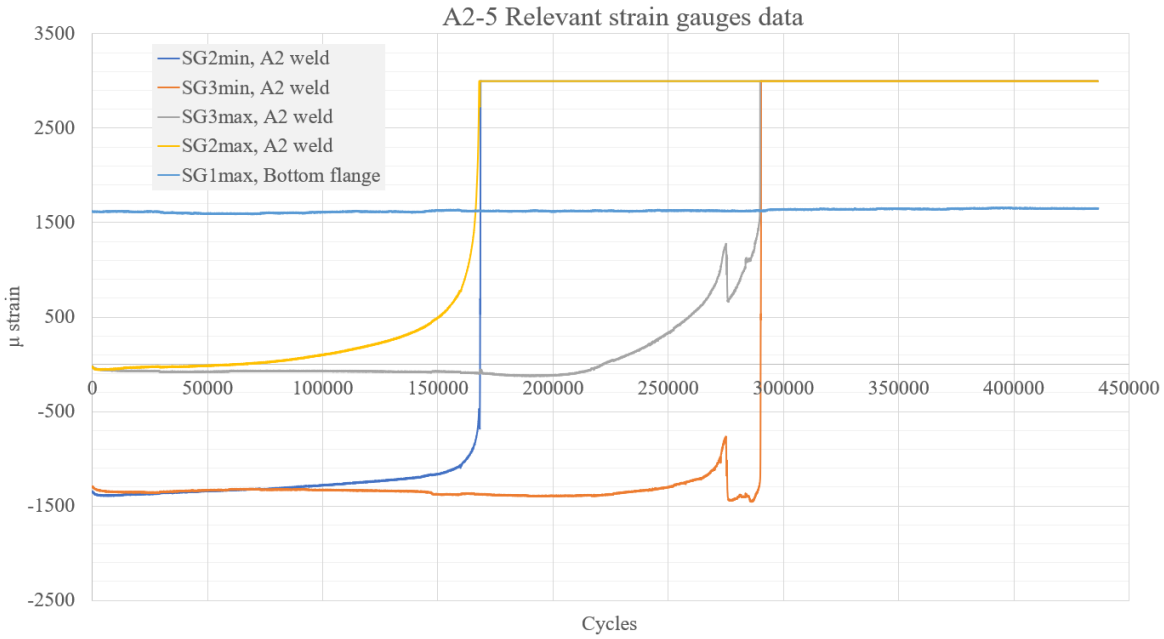

Fatigue failures have happened in 192 256 cycles and 351 595 cycles. Laboratory staff observations have been used.